THE DYNAMIC RESPONSE OF GRID FRAMEWORKS

by

C.W. AUSTIN

A thesis submitted to the University of Edinburgh for the degree of Doctor of Philosophy.

August 1970.

TABLE OF CONTENTS

SUMMARY

The grids considered in this study consist of plane rectangular frameworks of interconnected beams, simply supported on two opposite sides and freely vibrating at right angles to their plane. Several existing methods of predicting natural frequencies and modes of vibration are reviewed briefly and a new method of analysis is described. The results of this analysis are presented in the form of design curves, and the accuracy of the method is demonstrated by comparison with the results of laboratory model tests.

A field test of a particular highway bridge, constructed with universal beams and a concrete slab with composite action, is reported, and it is concluded that the proposed design method can be used to predict several resonant frequencies of this type of structure. Recordings of the vibrations of the bridge under normal traffic conditions are used in an attempt to correlate its response with the speed and axle spacings of individual vehicles. The importance of considering modes of vibration higher than the fundamental is demonstrated.

A C K N O W L E D G E M E N T S

I am grateful to Professors A.W. Hendry and L.G. Jaeger and Dr A.D.S. Barr for their supervision of this research project; to the technical staffs of the Departments of Mechanical, Civil and Electrical Engineering for their practical assistance; to Dr W. Henderson and his staff in the Scottish Development Department for their encouragement and help with the organisation of the bridge test; to Messrs. Keith and Fraser of Stirling County Council for their permission to use the Touch Burn Bridge; to Mr George Reid and his staff at the Kincardine Bridge for erecting the access staging and fitting the vibrator to the Touch Burn Bridge; to Mr Bob Brown and his men at Drem airfield for helping to test and modify the vibrator; to my wife and friends for help with the preparation of this thesis; and to Mrs Marace Dareau for typing the manuscript.

NOTATION

Principal notation is listed below although symbols of a more local nature are introduced as required.

a	amplitude
A	constant
B	constant
C	constant
D	constant
EI	stiffness
h	bay width of grid (see fig.2 page 5)
i	integer
j	integer
L	length of grid, also as a subscript indicating longitudinal direction
m	mass per unit length
n	integer
N	number of transverse beams
P	load
S	shear force
t	time
T	a function of time alone, also as a subscript indicating transverse direction
x	displacement in the longitudinal direction (see fig. 2, page 5)
X	a function of x alone
y	deflection (see fig. 2, page 5)

z	displacement in the transverse direction (see fig. 2, page 5)
Z	a function of z alone
α	grid stiffness parameter (see section 2.2)
K	grid frequency parameter (see section 2.2)
λ	grid weight parameter (see section 2.2)
ψ	grid eigenvalue (see section 2.2)
ω	circular frequency

CHAPTER 1

Chapter 1.

Introduction

1.1 Dynamics of structures

Most civil engineering structures are likely to have to withstand dynamic loads. Some common causes are:

1. Shockwaves; as a result of earthquakes, explosions, etc.
2. Moving loads; for example, heavy vehicles crossing highway bridges, and in the past particularly, the 'hammer-blow' effect associated with the balancing system employed on steam locomotives.
3. Unbalanced machinery; particularly dangerous if the speed of the machinery ever approaches the natural frequency of any part of the supporting structure.

While a dynamic load can sometimes be eliminated or its severity reduced by improved mechanical engineering design, the problem of designing a structure to withstand the dynamic load lies in the realm of the civil engineer.

In problems of dynamics, the inertia of accelerating masses must be taken into consideration. Basically, it is this inertia force which distinguishes the field of dynamics as a special branch of mechanics. Rogers (1) gives an introduction and bibliography to

the subject of dynamic disturbances and the consequent response of structures.

A single mass, free to move only vertically and supported on a spring has just one natural frequency and mode of vibration. This is a one-degree-of-freedom system. In general, a system has as many frequencies and modes as degrees of freedom. Civil engineering structures have distributed mass and stiffness and consequently an infinite number of natural frequencies and modes of vibration.

When the frequency of the disturbing force coincides with one of these natural frequencies, resonance exists and the amplitude of the vibration greatly increases, resisted only by the damping in the structure.

1.2. Field of study

It has been the purpose of this study to investigate a method of predicting natural frequencies and modes of a rectangular gridwork of interconnected beams, simply supported on two opposite sides and freely vibrating at right angles to its plane. Several existing methods are reviewed briefly in section 1.3 and a new analysis is presented in chapter 2. Design curves are given which enable the structural engineer to predict several resonant frequencies of a grid very easily using the well-known 'alpha'

parameter used by Hendry and Jaeger in their static design method for grillages (2). The accuracy of the method is demonstrated by comparison with the results from laboratory model tests, in chapter 3.

The relationship between the resonant frequencies of a highway bridge and its dynamic response to traffic is discussed and the application of the proposed design method to certain highway bridges is considered in chapter 4. A field test to find the resonant frequencies and modes of vibration of a particular highway bridge and to observe its behaviour under normal traffic conditions is reported.

1.3 Review of methods of analysis

1.3.1 Inglis' method

C.E. Inglis was a great exponent of harmonic analysis and wrote very eloquently of its application to vibrations in railway bridges (3). The bridges consisted of two main trusses connected by transverse members and Inglis treated them as simple beams. He considered only two modes of vibration and dealt with the 'anti-phased' mode (fig. 1) by assuming that the transverse members were pin jointed to the main trusses. Thus the natural frequencies of the two modes were obtained by adding one half and one sixth of the mass of the transverse members respectively,

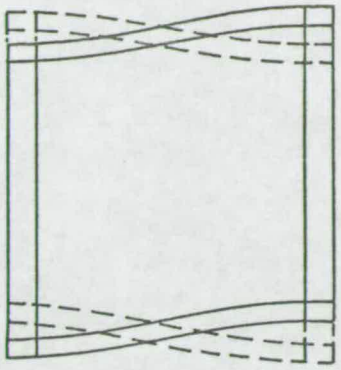

Fig. 1. Cross section through a railway bridge showing the 'anti-phased' mode of vibration.

into the mass of the main trusses, and then using the simple beam theory.

Inglis used harmonic analysis to predict the response of these simple beam type of bridges to moving vehicles and his method of doing this has been widely applied (1, 5, 19). His method of calculating resonant frequencies is restricted to only two modes of vibration and is of little use for grids with more than two longitudinal girders.

1.3.2 Formal method

Solutions to the partial differential equations describing the motion of the beams in each direction are sought, and use is made of boundary conditions and compatibility conditions at the joints to derive a frequency equation for the grid.

Commonly occuring grids consist of fairly light beams running in one direction, the transverse direction, supported on a few relatively stiff and heavy beams running in the other, the longitudinal direction (fig. 2).

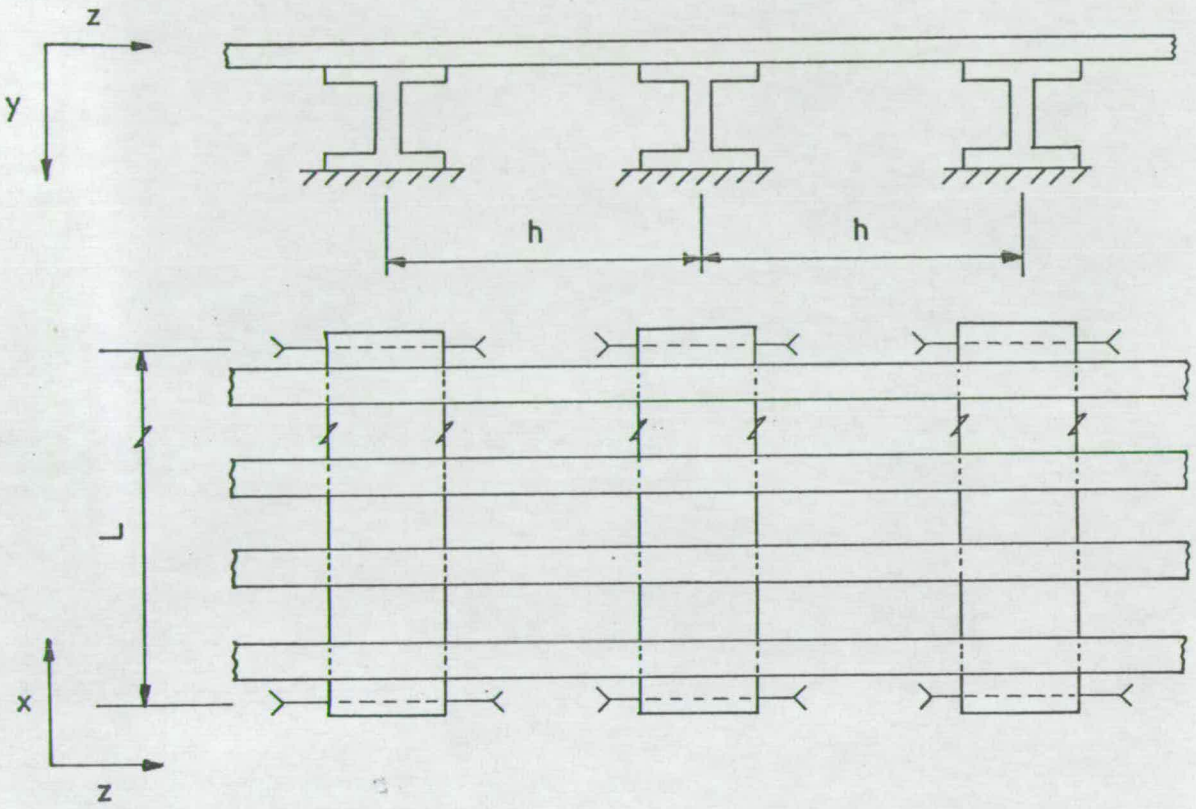

Fig. 2. A structure of the type considered here as a grid framework

The inertia force due to the acceleration of an element of a transverse beam is in equilibrium with the shear forces on the element (fig. 3). Thus:

$$m_T dz \frac{\partial^2 y}{\partial t^2} + \frac{\partial S}{\partial z} dz = 0$$

If we neglect damping and other secondary effects, the equation of equilibrium of a transverse beam between

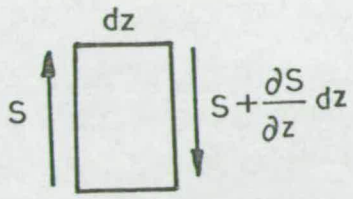

Fig. 3. An element of a transverse beam.

longitudinals becomes:

$$EI_T \frac{\partial^4 y}{\partial z^4} + m_T \frac{\partial^2 y}{\partial t^2} = 0$$

The longitudinal beams additionally carry point loads along their lengths from the transverse beams. If the transverse beams are all the same and are evenly spaced, they may be treated as a spread medium and the point loads replaced by a distributed load P(x, t). The equilibrium equation of a longitudinal beam becomes:

$$EI_L \frac{\partial^4 y}{\partial x^4} + m_L \frac{\partial^2 y}{\partial t^2} = P(x, t)$$

The distributed load P(x, t) is equated to the shear force in the transverse medium at the connections and the equations are solved subject to the appropriate boundary conditions. A solution is given by Rogers for a simple grid with only one longitudinal beam.

1.3.3 Lumped mass method

The grid framework is reduced to a few points of concentrated mass connected together by weightless elements possessing stiffness. The new system has a finite number of degrees of freedom (and modes of vibration), and can be described by a set of ordinary differential equations.

The flexibility of the connecting elements is given in the form of 'flexibility coefficients' or 'displacement influence coefficients' viz: d_{ij} is the displacement of mass point i per unit load at mass point j. These coefficients can be obtained from a static analysis, such as that of Hendry and Jaeger or by experiment. If the system consists of n masses, the deflection y_i of the i'th mass M_i is given by:

$$y_i + \sum_{j=1..n} M_j \frac{d^2 y_j}{dt^2} d_{ij} = 0$$

and if we investigate solutions of the form:

$$y_i = a_i \sin \omega t$$

the problem reduces to a set of homogeneous linear equations involving the eigenvalue ω.

This well-known technique has been described in general elsewhere (1,8) and has been successfully applied to grid frameworks by Hendry (4), Zeidan (5)

and the present author (6).

The accuracy of the method depends on the judicious choice of position for the lumped masses, and on the care with which the distribution coefficients are estimated. A further disadvantage is that no general solution in parametric form is obtained.

1.3.4 Finite elements

The grid framework is divided into elements with distributed mass and stiffness. An approximate deflection function for each element is chosen with as many arbitrary constants as independent displacements of the element. The arbitrary constants are found in terms of the independant displacements and equilibrium equations are obtained for each element. Compatibility conditions between elements reduce the equations to an eigenvalue problem.

A typical procedure uses simple beam elements (fig. 4), with four independent displacements.

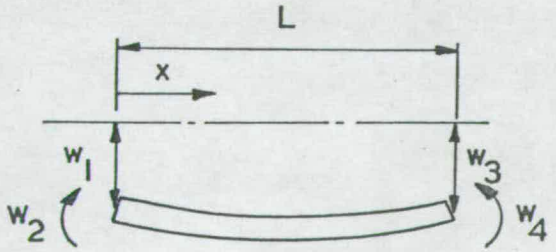

Fig. 4. A typical element for finite element analysis

A suitable displacement function could be:

$$y = A + Bx + Cx^2 + Dx^3$$

and in terms of the displacements:

$$y = (1 - 3(\frac{x}{L})^2 + 2(\frac{x}{L})^3)W_1 + (3(\frac{x}{L})^2 - 2(\frac{x}{L})^3)W_3$$

$$+ (- x + \frac{2x^2}{L} - \frac{x^3}{L^2})W_2 + (- \frac{x^2}{L} + \frac{x^3}{L^2})W_4$$

The potential and kinetic energies of the element can be calculated and the principle of virtual work used to obtain the forces required to deform the element and to overcome its inertia. The total set of forces $\underline{F}$ on the element is given by the matrix equation:

$$\underline{F} = (S_E - \omega^2 M_E)\underline{W}$$

where S_E and M_E are the stiffness and mass matrices of the element respectively. Equilibrium conditions at the joints yield the eigenvalue problem:

$$(S - \omega^2 M)\underline{W} = 0$$

where S and M are the stiffness and mass matrices of the whole grid respectively.

Leckie and Lindberg (28) have used this method to analyse vibrating beams with various end conditions, and have compared its accuracy with other lumped-parameter methods. They conclude that reliable results can be obtained, even when only a small number of

elements are used, and that the error in the frequency parameter always varies inversely as the fourth power of the number of elements.

1.3.5 Harmonic analysis

This method is based on a suggestion of Jaeger and has been successfully applied to the symmetric modes of three and four girder grids by Hendry (4), Zeidan (5) and the present author (6). The use of Harmonic Analysis itself has been described by Inglis (3,7).

The transverse beams are treated as a spread medium, and compatible solutions are sought for the partial differential equations describing the equilibrium of the longitudinals and this medium respectively. However, when writing the equation of equilibrium of the transverse medium the entire width of the grid is considered, and the point loads from the longitudinals are distributed into their harmonic components. The first harmonic only is considered and a sinusoidal shape function assumed for the deflection of the transverse medium.

This method has the advantage that a general solution in terms of only two grid parameters can be obtained for any particular type of grid. One of these parameters is the 'alpha' parameter from the Hendry and Jaeger static design method. Zeidan has given design curves. The method has limited application because

only two symmetrical modes of vibration have been considered.

1.3.6. Slab theory

The stiffness and mass of the beams in each direction are spread and use is made of the well-known plate deflection equation (9). If the spacing of the beams in a given direction is e, and if the torsion of the beams is neglected, the equation of the equivalent slab becomes:

$$\frac{EI_L}{m_L e_L}\frac{\partial^4 y}{\partial x^4} + \frac{EI_T}{m_T e_T}\frac{\partial^4 y}{\partial z^4} + \frac{\partial^2 y}{\partial t^2} = 0$$

By assuming a solution of the form:

$$y = X(x).Z(z).T(t)$$

an uncoupled set of three easily soluble differential equations is obtained. Application of boundary conditions to the solutions yields a frequency equation.

The method has been described elsewhere (1, 8) and is well established for the analysis of closely spaced grids of beams. However, the present work is mainly concerned with grids consisting of transverse beams resting on a few relatively stiff and heavy longitudinal beams, and the assumption of a spread medium in both directions is consequently open to doubt.

1.3.7 Complementary systems

This method, developed by Bleich (10), relies on the reduction of the grid frame to a number of simpler systems, the natural frequencies of which can be easily found. Bleich's theorem states that the deflection of any point of the original system is equal to the sum of the deflections of the complementary systems under the same load. The deflection of the grid framework is expressed as the sum of the 'normal modes' of the complementary systems and use is made of the orthogonality property of the 'normal modes' to obtain a frequency equation.

'Normal modes' are dealt with in standard textbooks (1,8,11) and Rogers has applied Bleich's method to a simple floor system using only two complementary systems. Zeidan (5) has successfully used the method to analyse a three-girder grid. His calculations which involve four complementary systems are tedious and do not yield a general solution in parametric form.

CHAPTER 2

Chapter 2.

Proposed design method

2.1 Introduction

With the exception of Inglis' method and harmonic analysis, all the above methods suffer the disadvantage of not yielding general solutions in parametric form. Consequently, they are of little interest to designers. Inglis' method is not applicable to multi-girder grids and the method of harmonic analysis is presently restricted to only two symmetric modes by the shape which is assumed for the deflected form of the transverse medium.

The following analysis is based on formal methods and a suggestion by Jaeger. It enables all the natural frequencies of grids of any size to be predicted. Design curves can be constructed in terms of only two dimensionless parameters.

2.2 Analysis

In this analysis the torsion of beams is neglected and the transverse beams are treated as a spread medium. The justification for this is discussed in chapter five. The longitudinal beams each carry a distributed load P(x,t) from the transverse medium in addition to their own inertia force, and the equation of their undamped vibration is:

$$EI_L \frac{\partial^4 y}{\partial x^4} + m_L \frac{\partial^2 y}{\partial t^2} = P(x,t)$$

The form of the force P(x,t) is unknown and it is convenient to split it into harmonic components, thus:

$$P(x,t) = \sum_{n=1..\infty} (P_n \sin \frac{n\pi x}{L}).\sin\omega t$$

where ω is the frequency of the grid, and referring to figure 2 (section 1.3.2).

The general solution to the above partial differential equation is the sum of the homogeneous solution and a particular solution. The homogeneous solution would represent the free vibration of a longitudinal beam at one of its own natural frequencies. The particular solution represents the forced vibration at the grid frequency. As the longitudinal beams are constrained to move with the rest of the grid, they cannot vibrate freely and so only the particular solution need be considered.

For free vibrations of the grid, the particular solution will be:

$$y(x,t) = \sum_{n=1,2..\infty} (a_n \sin \frac{n\pi x}{L}).\sin\omega t$$

where a_n is the amplitude of the n'th deflection harmonic. This solution is the sum of the 'normal functions' of the longitudinal beam and satisfies the

conditions that the ends are simply supported, i.e.

$$y = \frac{d^2y}{dx^2} = 0 \quad \text{at both ends.}$$

The unknown amplitudes a_n can be found in terms of the forces by substituting in the differential equation. Thus:

$$EI_L \sum_n \left(\frac{n\pi}{L}\right)^4 a_n \sin\frac{n\pi x}{L}.\sin\omega t - m_L\omega^2 \sum_n a_n \sin\frac{n\pi x}{L}\sin\omega t$$

$$= \sum_n P_n \sin\frac{n\pi x}{L}.\sin\omega t$$

Equating coefficients of $\sin\frac{n\pi x}{L}$:

$$EI_L\left(\frac{n\pi}{L}\right)^4 a_n - m_L\omega^2 a_n = P_n$$

$$a_n = \frac{P_n}{EI_L\left(\frac{n\pi}{L}\right)^4 + m_L\omega^2}$$

The solution becomes:

$$y = \sum_n \frac{P_n}{EI_L\left(\frac{n\pi}{L}\right)^4 - m_L\omega^2} \sin\frac{n\pi x}{L} . \sin\omega t$$

Thus each harmonic of load from the transverse medium produces a similar proportional deflection harmonic. The combination of harmonics which occurs in practice depends on the excitation. For the study

of free vibrations, each harmonic is treated separately. Thus:

$$P_n = \left[\frac{EI_L}{m_L}\left(\frac{n\pi}{L}\right)^4 - \omega^2\right] m_L a_n$$

$$= \left[(\omega_L)_n^2 - \omega^2\right] m_L a_n$$

where $(\omega_L)_n$ is the frequency of the n'th mode of a simply supported longitudinal girder vibrating on its own.

If there are N transverse beams in the grid, then, the equation of equilibrium of an element of the equivalent transverse medium is:

$$\frac{NEI_T}{L}\frac{\partial^4 y}{\partial z^2} + \frac{Nm_T}{L}\frac{\partial^2 y}{\partial t^2} = 0$$

Substitution of a solution of the form:

$$y(z,t) = Z(z).\sin\omega t$$

gives:

$$EI_T \frac{d^4 Z}{dz^4} + m_T\omega^2 Z = 0$$

The general solution of this equation is:

$$Z = A\sin\mu_T z + B\cos\mu_T z + C\sinh\mu_T z + D\cosh\mu_T z$$

where $\mu_T = \sqrt[4]{\frac{m_T\omega^2}{EI_T}}$

Thus the deflection of each span of the transverse

medium is expressed in terms of the frequency and four constants, which depend on boundary conditions. Successive differentiation yields the slope, bending moment and shear respectively in the same terms.

Consider now the connection between the transverse medium and a longitudinal beam (fig. 5).

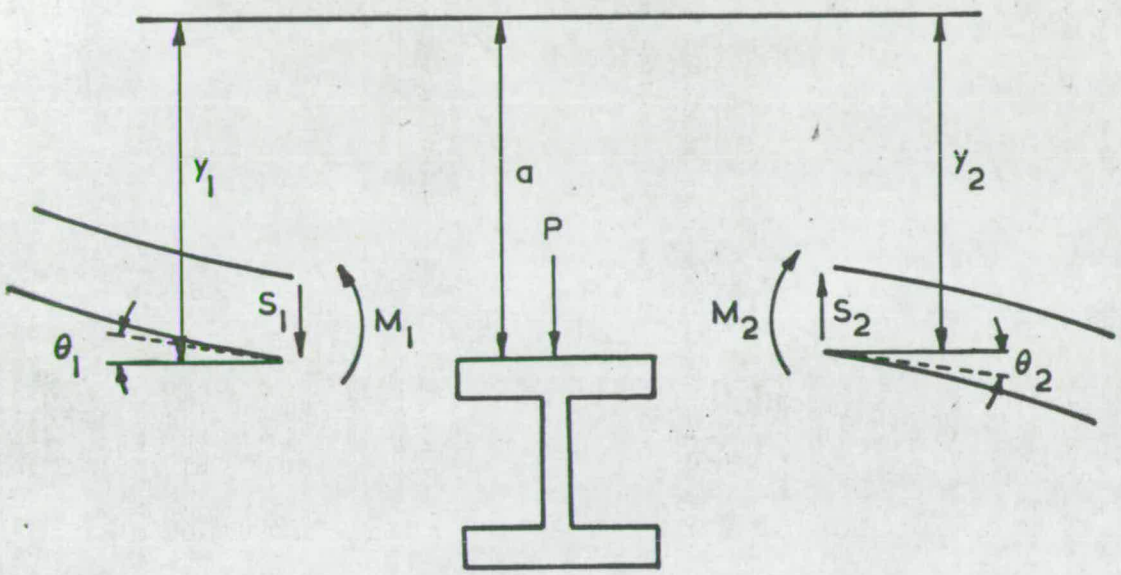

Fig. 5. Connection between the transverse medium and a longitudinal beam at mid-span.

If the transverse medium is continuous and if the torsional stiffness of the longitudinal beam is neglected, the compatibility conditions are:

$$S_2 - S_1 = P = \left[\omega_L^2 - \omega^2\right] m_L a$$

$$M_1 = M_2$$

$$y_1 = y_2 = a$$

$$\varphi_1 = \varphi_2$$

If these conditions are applied to each connection of

a grid with n longitudinal girders, we have a set of 5n-4 homogeneous equations in terms of the arbitrary constants, the unknown amplitudes of the longitudinals and the frequency of vibration. For the simplest case, a grid with only two longitudinal girders, the matrix equation is:

$$\begin{bmatrix} \eta & 0 & -1 & 0 & 1 & 0 \\ 0 & 0 & 0 & -1 & 0 & 1 \\ 0 & \eta & \cos\phi & -\sin\phi & -\cosh\phi & -\sinh\phi \\ 0 & 0 & -\sin\phi & -\cos\phi & \sinh\phi & \cosh\phi \\ -1 & 0 & 0 & 1 & 0 & 1 \\ 0 & -1 & \sin\phi & \cos\phi & \sinh\phi & \cosh\phi \end{bmatrix} \begin{bmatrix} a_1 \\ a_2 \\ A \\ B \\ C \\ D \end{bmatrix} = 0$$

where $\eta = (\omega_L^2 - \omega^2) \dfrac{m_L \quad L}{\mu_T^3 \; NEI_T}$ and $\phi = \mu_T h$

This is an eigenvalue problem and a frequency equation could be obtained by setting the determinant of the coefficient matrix to zero in the normal way.

The parameters of the problem can be simplified:

$$\phi = \mu_T h = 4\sqrt{\frac{m_T \omega^2}{EI_T}}.h = \pi.\sqrt{\frac{\omega}{\omega_T}}$$

and

$$\eta = \left[\omega_L^2 - \omega^2\right] \frac{m_L \quad L}{\mu_T^3 \; NEI_T}$$

$$= \frac{Lm_L}{Nm_T h} \left(\frac{\omega_L^2}{\omega^2} - 1\right) \pi \sqrt{\frac{\omega}{\omega_T}}$$

where ω_T is the fundamental frequency at which a simply supported transverse beam would vibrate on its own. The problem can now be presented in terms of just two dimensionless parameters, namely:

$$\lambda = \frac{Nm_T h}{Lm_L}$$

$$= \frac{\text{mass of a unit strip of the transverse medium}}{\text{mass of longitudinal beam per unit length}}$$

$$K = \frac{\omega_L}{\omega_T}$$

$$= \frac{\text{freq. of a simply supported longitudinal beam vibrating on its own}}{\text{freq. of a simply supported transverse beam vibrating on its own}}$$

and the eigenvalue is:

$$\psi = \frac{\omega}{\omega_L}$$

$$= \frac{\text{freq. of the grid}}{\text{freq. of a simply supported longitudinal beam}}$$

These parameters are convenient for most purposes, although structural engineers may prefer to replace K by the alpha parameter used by Hendry and Jaeger in their static design method for similar structures (2).

In that case:

$$K = \frac{\omega_L}{\omega_T} = \left(\frac{h}{L}\right)^2 \sqrt{\frac{EI_L m_T}{EI_T m_L}} = \sqrt{\frac{12}{\pi^4}\frac{\lambda}{\alpha}}$$

where: $\alpha = \frac{12}{\pi^4}\left(\frac{L}{h}\right)^3 \frac{NEI_T}{EI_L}$

When a longitudinal harmonic higher than the first is considered, ω_L must be replaced by the frequency of a simply supported longitudinal vibrating on its own in that mode. When considering the n'th harmonic, K may be replaced by n^2K or alternatively, α replaced by α/n^4.

2.3 Solution of the eigenvalue problem

The frequency of vibration of the grid appears in the coefficient matrix as part of the argument of trigonometric and hyperbolic functions. Consequently, the solution of the equation obtained by setting the determinant to zero becomes intractible and an alternative method of solution has to be sought. Osborne (12) has given an iterative method for solving problems in which the eigenvalue occurs non-linearly. If the matrix equation is expressed as:

$$M(\psi).V = 0$$

the iterative process is:

$$\left.\begin{aligned} M(\psi_i).V_{i+1} &= \frac{dM(\psi_i)}{d\psi}.\frac{V_i}{(V_i)_{pi}} \\ \psi_{i+1} &= \psi_i - \frac{1}{(V_{i+1})_{pi}} \end{aligned}\right\}$$

where pi is the index of the element of the vector V_i having maximum modulus. The initial estimate of the eigenvalue is chosen so that the determinant is approximately zero. Arbitrary values are assigned to the elements of the first eigenvector.

Since there is an infinite number of solutions, it is important to ensure that the iteration produces only those required. The criterion used to check which solution has been found, is based on the zero-crossing property of normal modes. This property is described elsewhere (13,14) and implies that for each mode of vibration of the grid, the transverse medium taken as a whole, has a unique number of nodes. This is confirmed by experiment. The first mode has no nodes, the second one, the third two and so on. Typical mode shapes are shown in figure 10 (section 2.4).

The complete procedure is thus:

1. Construct a matrix for the given grid.
2. Evaluate the determinant for a range of trial values of the eigenvalue.
3. When the sign of the determinant changes, try to iterate.

4. If an eigenvalue is found, check that it is the correct one, by counting nodes of the mode shape.
5. If it is not, repeat the procedure from step two, using a range with smaller intervals.
6. Continue to look for the next eigenvalue from step two.

Fortunately, this procedure is well suited to digital computation. Three main subroutines have been written and certain 'formal parameters' are used in each. When a call is made in the programme for a subroutine, the 'formal parameters' are 'called by value', that is, new identifiers are automatically declared for them, and given the values of the 'actual parameters' in the call. In this way, a subroutine can be called by an instruction within its own body, and the identifiers at each level are not confused. This is a 'recursive' technique and a similar process is used here.

The three subroutines are:

1. Assemble matrices: formal parameter: r

This subroutine constructs the coefficient matrix and its derivative with respect to the eigenvalue, using the value of r in place of the eigenvalue.

2. Test determinant: formal parameters: u_1, du, u_2

The determinant of the coefficient matrix is evaluated for a series of trial values of the eigenvalue from u_1 in steps of du up to u_2. When the sign of the

determinant changes, the iterative subroutine is called. A simplified flow chart is given in figure 6. Actual parameters are given in brackets after the call.

3. Iterate: formal parameter : p

The Osborne iterative procedure is carried out using p as an initial approximation to the eigenvalue. The set of linear equations involved in the iteration are solved by triangular factorization of the coefficient matrix with row interchanges using a library subroutine. The iteration is continued until an eigenvalue is found to the required accuracy. The eigenvalue is checked and if it is the one required, the results are printed out, and control is returned to previous subroutine.

If the iteration produces the wrong eigenvalue or if it does not converge at all, the 'test determinant' subroutine is called to look for a change of sign of the determinant over a smaller range with closer intervals. A check is made to ensure that the recursion is not continued 'ad infinitum'. A simplified flow-chart is given in figure 7.

The parameters required by the programme are the two grid parameters and the range and interval for the first application of the 'test determinant' routine. The intervals must be chosen so that not more than one eigenvalue occurs in each. A simplified flow-chart is given in figure 8.

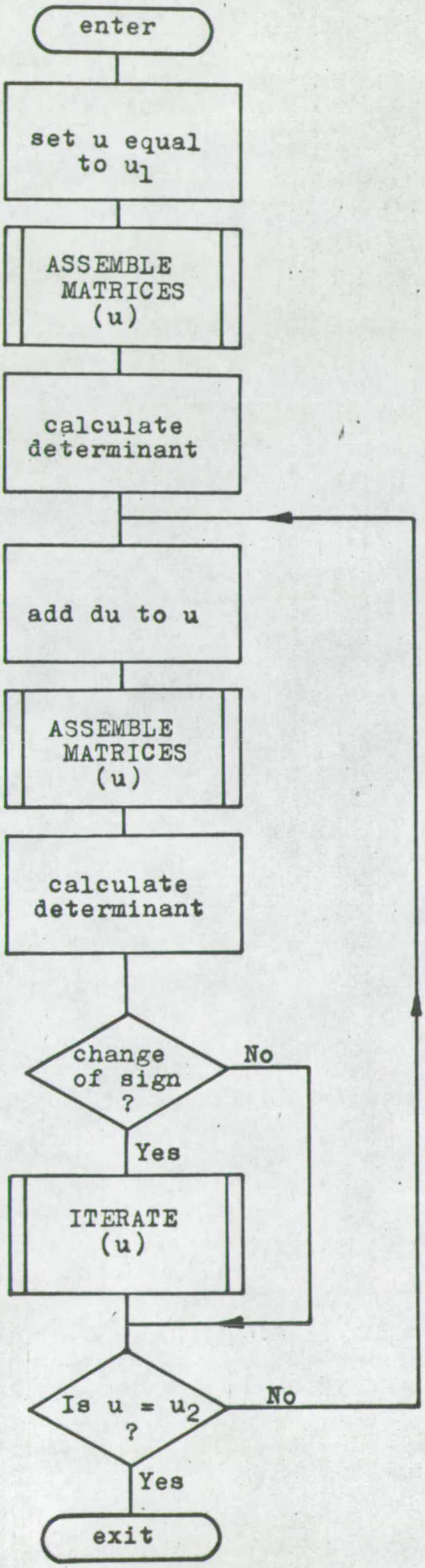

Fig. 6. Routine: 'TEST DETERMINANT' (formal parameters: u_1, du, u_2)

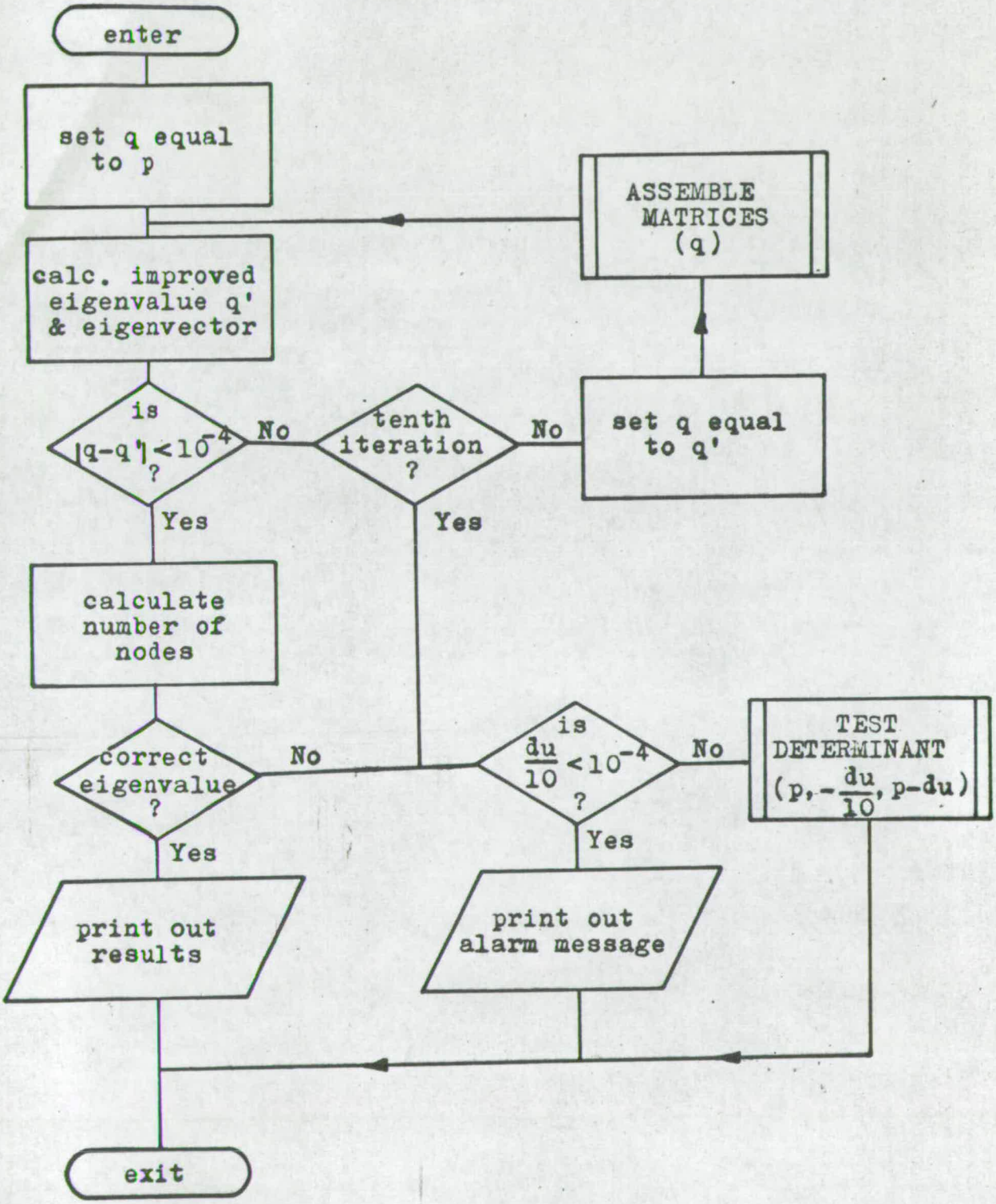

Fig. 7. Routine: 'ITERATE' (formal parameter p).

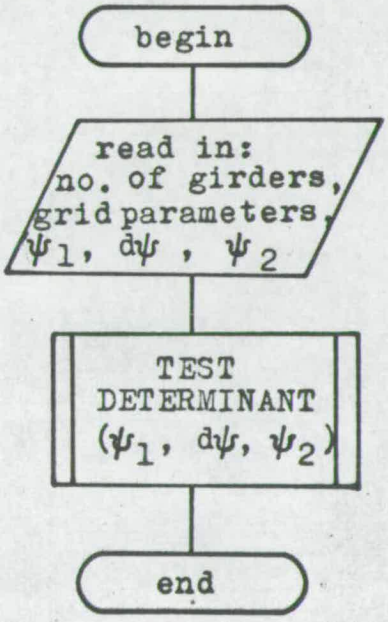

Fig. 8. Program to solve the eigenvalue problem.

2.4 Theoretical results

A special print-out from the computer is shown in figure 9 and illustrates the recursive technique in action. A change of sign of the determinant of the coefficient matrix is detected as the trial eigenvalue changes from 0.8 to 1.0, and the iterative procedure is entered in an attempt to calculate the exact eigenvalue. In this case however, the count of nodes of the transverse mode shape, calculated from the eigenvector, indicates that the iteration has produced the wrong eigenvalue and so the process is repeated using smaller intervals of the trial eigenvalue. After converging on the correct eigenvalue, the eigenvector is used to calculate the transverse mode shape, bending moments and energy.

Figure 10 shows the first six transverse mode shapes of a typical four girder grid. Henceforward, modes will be identified by two integers; the number of the longitudinal harmonic first, followed by the number of the transverse mode.

In order to provide the design curves, the programs were rewritten to instruct the computer to cycle through a range of the grid parameters. Each mode of vibration was treated separately, so that each eigenvalue could be used as the initial approximation for the iteration for the next, slightly different grid. The design curves for the first three transverse modes of vibration (modes 1-1, 1-2, and 1-3) of two, three and

Fig. 9. A special computer print-out showing the recursive technique

```
MODES OF A   2  GIRDER GRID
==========================

LAMDA =  0.459        KAPPA =  0.432        LONGITUDINAL MODE NO  2
    6.0000000000E -1    8.0000000000E -1    1.0000000000E  0          2          3          4.    1.0000000000E  0
9.8000E -1    9.6000000000E -1    9.4000000000E -1

MODE NUMBER   1
  5 FINAL EIGENVALUE (PHI) =  0.9571       PSI =  2.2155
    FINAL EIGENVECTOR =  1.00000E  0    1.00000E  0    1.46748E  1    5.00000E -1    -4.55785E -1    5.00000E -1


MODE SHAPE


BAY NUMBER   1

  Z       DEFLECTION     MOMENT                 Z       DEFLECTION     MOMENT

 0.0     1.0000E  0    -4.7877E-11             0.1     5.2976E  0    4.3401E  0
 0.2     9.1709E  0     8.2045E  0             0.3     1.2241E  1    1.1246E  1
 0.4     1.4211E  1     1.3189E  1             0.5     1.4889E  1    1.3857E  1
 0.6     1.4211E  1     1.3189E  1             0.7     1.2241E  1    1.1246E  1
 0.8     9.1709E  0     8.2045E  0             0.9     5.2976E  0    4.3401E  0
 1.0     1.0000E  0    -1.5495E-10


ENERGY CONSTANT FOR THIS MODE =  5.027187E  1
```

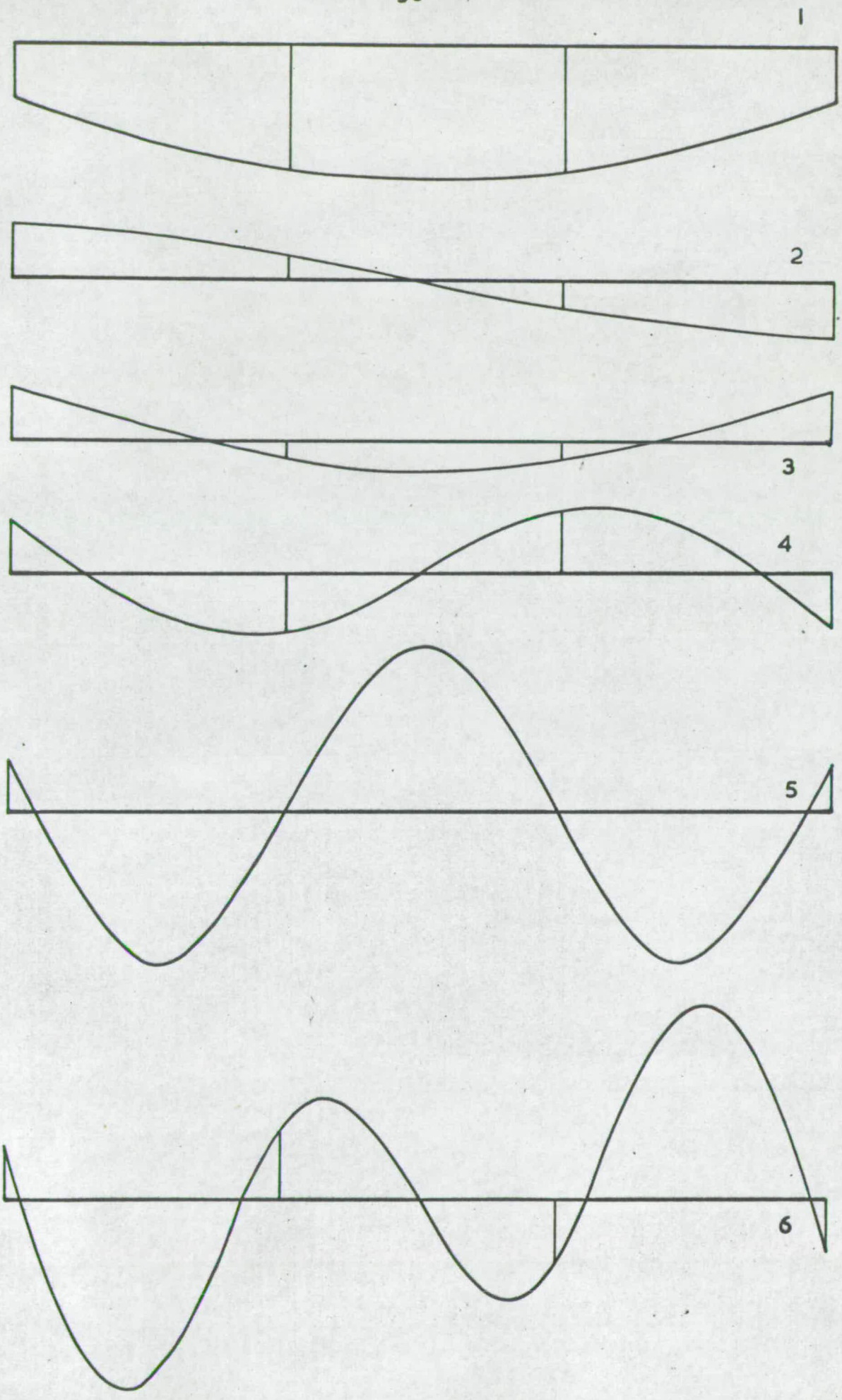

Fig. 10. Transverse mode shapes of a four-girder grid.

four girder grids are given in terms of the parameter K in figures 28-36 and in terms of α in figures 37-45.

A further modification to the program was carried out to enable the results of the laboratory tests to be compared with the theory. A series of results were obtained for a range of values of the λ parameter, all else remaining constant. The curves are shown in figures 46-50.

CHAPTER 3

Chapter 3.

Laboratory tests

3.1 Experimental set-up

3.1.1 Model grid and supports

In order to test the theory with the assumption of no torsion, a torsionless grid was designed and constructed. The longitudinal girders consisted of 3" x 2" R.S.J. sections supported at one end by a ball race on a steel pin, and at the other by bolting to the middle of a vertical strip of spring steel to reduce axial tension. The design of the supports is illustrated in figures 11 and 12. The transversals were made of 1 1/16" diameter hollow steel tubes with thin longitudinal splits to reduce their torsional rigidity. They were fitted with brass bushes and connected to the longitudinals by a steel pin bolted to the web as shown in figures 13 and 14.

To vary the parameters of the grid, extra mass was added to the transverse beams, in the form of 1" x 1" x 1½" lead blocks attached with Terry clips. These are evident in figure 14. The consequent problems of damping and rotatory inertia caused by these eccentric masses are discussed in section 3.2.3.

The grid was vibrated with electro-mechanical vibrators and suitable bases for these instruments were designed and constructed. The grid supports and vibrators were bolted to a heavy concrete 'strong floor'

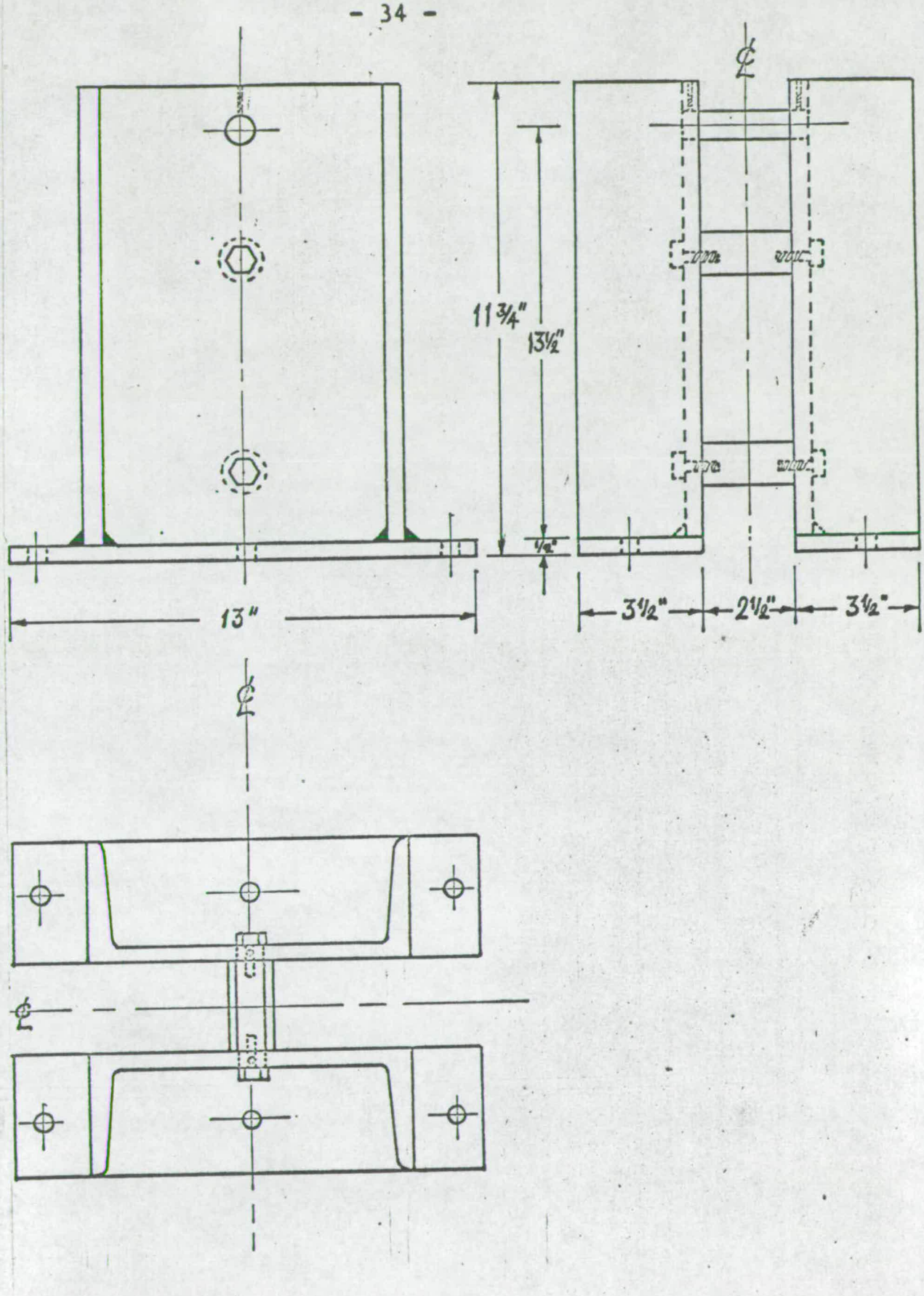

Fig. 11. Pinned support - scale 1" = 4"
Channel: 9" x 3½" x 22 lb.
Suspension: 3/4" diam. steel pin held by two grub screws.

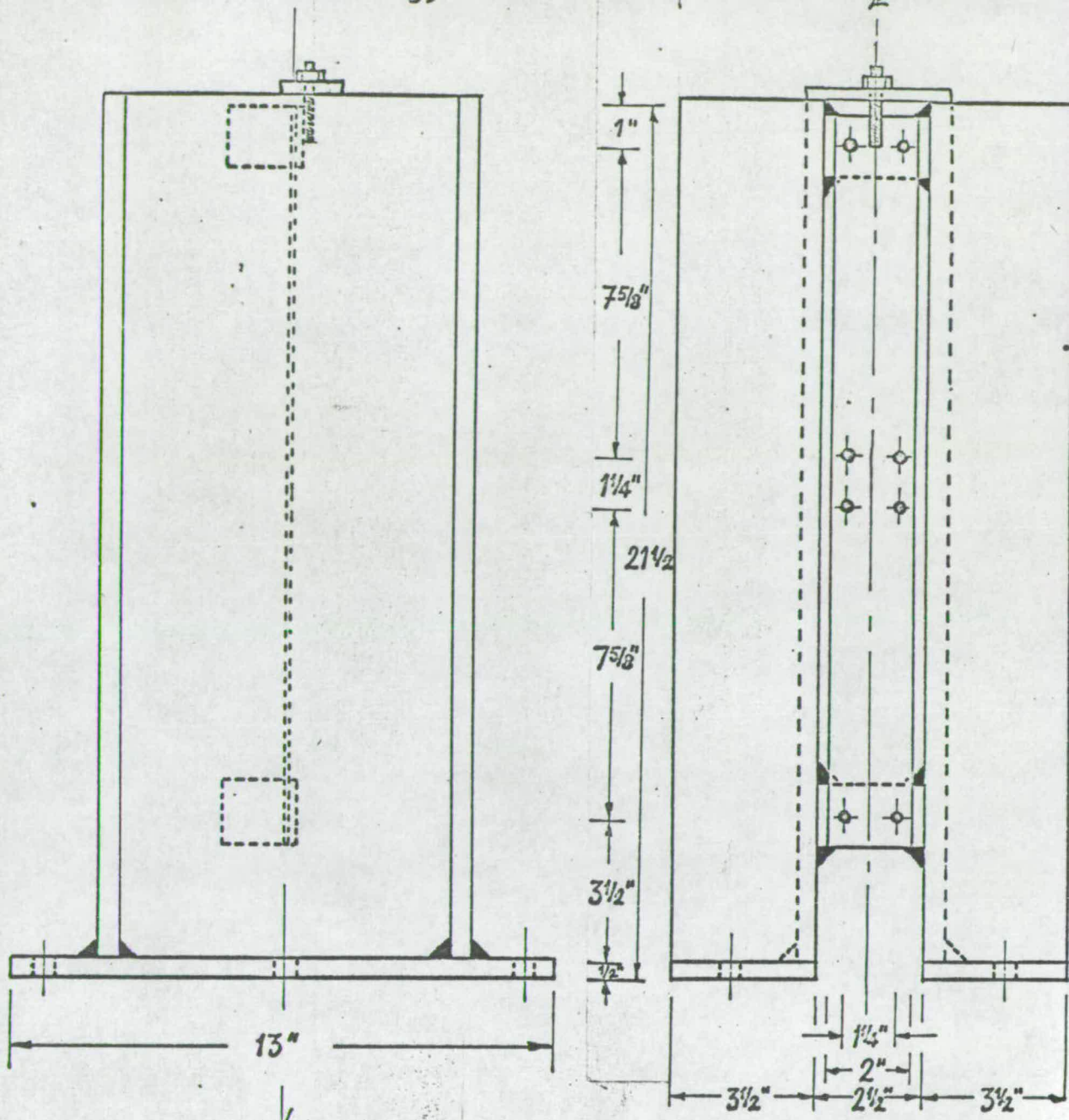

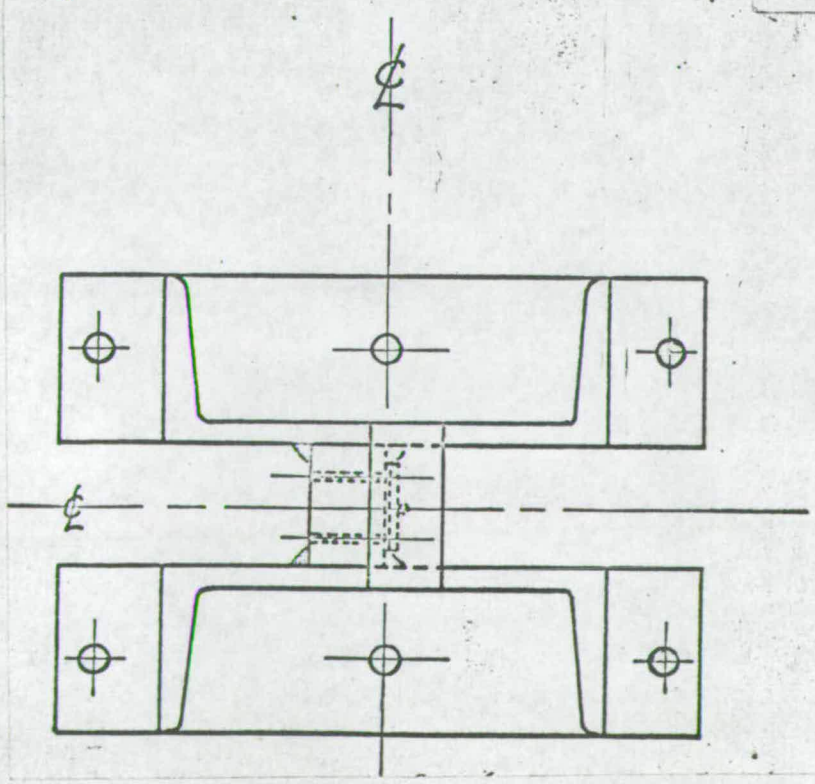

Fig. 12. Spring steel support - scale 1" = 4"
Channel: 9" x 3½" x 22lb
Suspension: 10 thou." spring steel strip with 1/8" thick plate soldered on each end and bolted to 1½" square steel section. Screw tightening device fitted to the top plate.

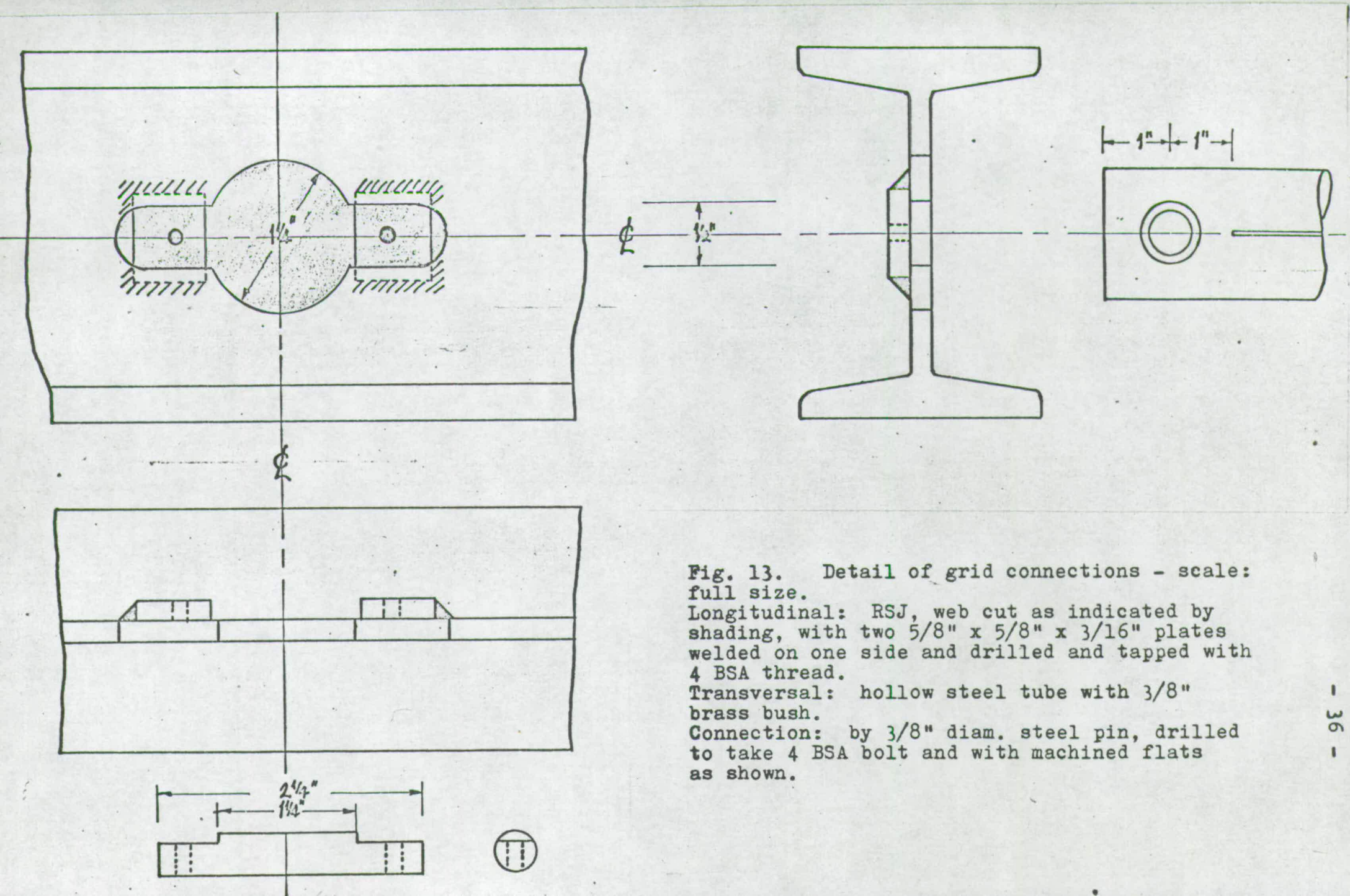

Fig. 13. Detail of grid connections - scale: full size.
Longitudinal: RSJ, web cut as indicated by shading, with two 5/8" x 5/8" x 3/16" plates welded on one side and drilled and tapped with 4 BSA thread.
Transversal: hollow steel tube with 3/8" brass bush.
Connection: by 3/8" diam. steel pin, drilled to take 4 BSA bolt and with machined flats as shown.

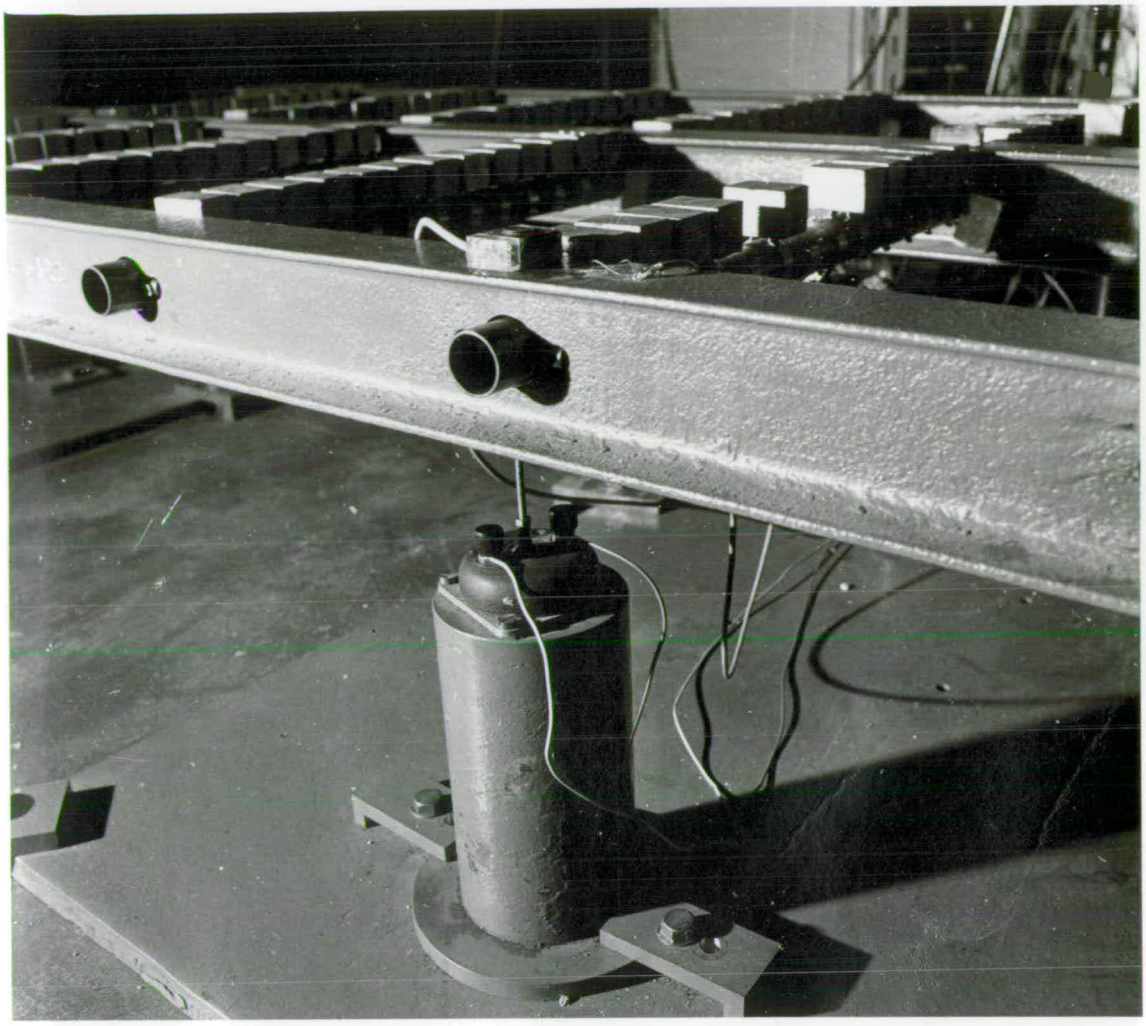

Fig. 14. Detail of the model grid showing the pinned connection between the transverse tubes and the longitudinal girders. Also shown are an electro-mechanical vibrator, an accelerometer and a strain gauge attached to the flange of the longitudinal girder.

and the complete set-up is illustrated in figure 15.

3.1.2 Instrumentation

The instrumentation used to detect the vibrations and strains of the grids is illustrated diagrammatically in figure 16, and can be seen in figure 15.

Strain gauges were attached at the quarter points on the top of the centre transverse tube and also at the mid-points of the top flanges of the outer longitudinal girders. Each gauge required a 120 ohm resistance to provide the second arm of the bridge circuit.

The miniature accelerometers were of the inductive type, giving a linear response when energized by a ten volt three kc/s supply. Positive and negative accelerations produced voltages which were 180° out of phase with each other and were distinguished by the phase sensitive detector in the demodulator. The demodulated signals from the accelerometers and the strain gauges were adjusted by the multi-channel carrier amplifier/attenuator stage and could be applied to several instruments. An oscilloscope was used for general observations,

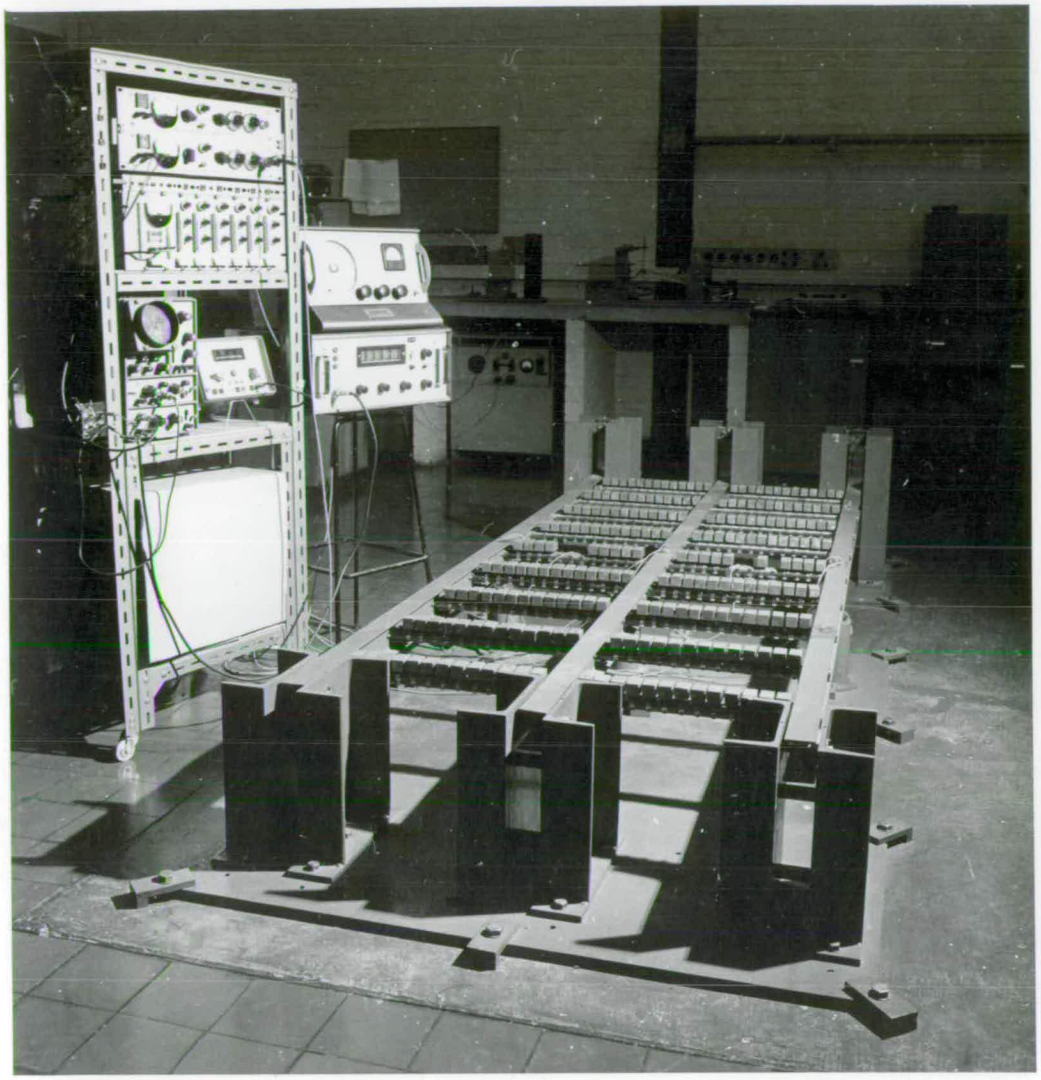

Fig. 15. General view of the three-girder model grid and instrumentation.

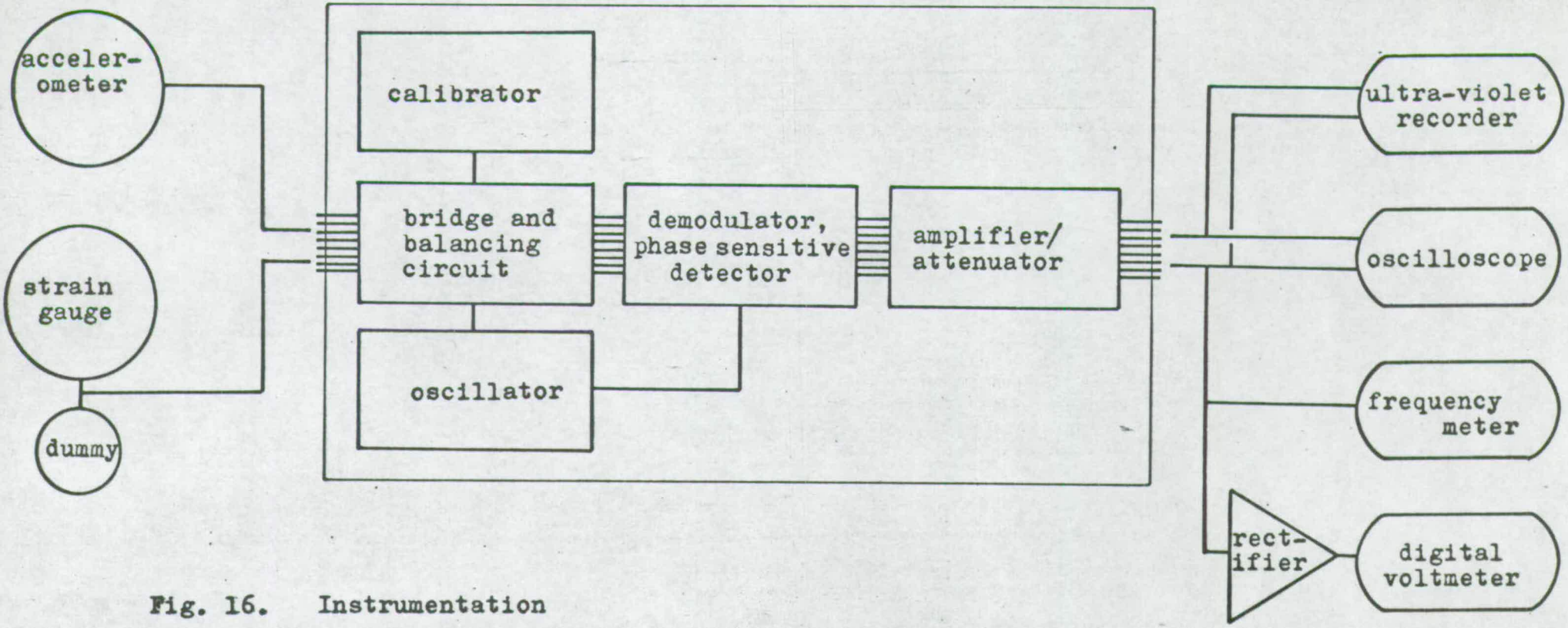

Fig. 16. Instrumentation

and an ultra violet recorder for permanent records. The frequency and voltage of the signals were measured with a frequency meter and a digital voltmeter. A power oscillator was used to excite the vibrators.

3.2 Experimental Procedure

3.2.1 Instrument Linearity Check

The linearity of the system as a whole was checked by comparison with another electrodynamic vibration pick-up and vibration meter which were already calibrated. The accelerometers were placed beside the second pick-up on a vibrating surface while the amplitude of the vibration was varied. This check was repeated under different conditions to investigate the effect of frequency and attenuation. The results obtained are plotted in figure 51 and show that the response is linear for a large range of acceleration. The linearity is not affected by frequency or attenuation.

Calibration of the system was not necessary because only relative measurements were required to detect

resonance and describe mode shapes.

3.2.2 Spring steel support check

Spring steel supports were used to reduce axial tension in the longitudinal girders. The tightening devices on the spring steel strips were adjusted carefully until the strips were uniformly taut. A check was made to ensure that the supports behaved as simple supports.

A single beam was set up between one pin and one spring steel support and vibrated at one of its resonant frequencies. The amplitude of the vibration was measured by the accelerometers at several points along its length and mode shapes were plotted for its two lowest modes of vibration. Figures 52 and 53 show that these mode shapes are approximately sinusoidal and that there is no significant difference between the behaviour of a spring steel support and a pinned support.

3.2.3 Determination of grid parameters

The weight parameter λ was found by weighing the longitudinal and transverse beams separately. Their fundamental frequencies of vibration were determined

experimentally. The beams were set up between a pin support and a spring steel support. An accelerometer was mounted at the mid point and an electro-mechanical vibrator connected to the same point, as shown in figure 17. The output from the accelerometer was recorded as the frequency applied to the vibrator was varied. Response curves were plotted and figure 18 is an example.

In the case of the transverse tubes, the resonant frequency obtained from the response curve had to be adjusted due to the relatively heavy mass of the accelerometer at the mid-point. The test was repeated to find the resonant frequencies of the tubes carrying various numbers of lead weights. The corrected frequencies are plotted against the reciprocal of the square root of the distributed mass in figure 54.

Due to the eccentricity of the lead masses and the method of attachment to the tubes, the effects of rotatory inertia and damping were considered. The lead weights were clipped to the sides of the tubes to reduce rotatory inertia and resonant frequencies were determined. The damping of the tubes with and without lead weights was measured from the response curves. The results of these tests are given in figure 55.

It was concluded that the influence of these effects is small by comparison with other amplitude-dependent effects which were present. Moreover, the resonant frequencies of the tube when corrected for the concentrated mass, lie on a straight line in figure 54. It was decided that these results should be used and that the accuracy of frequency measurements would be about $\pm$ 0.3 c/second.

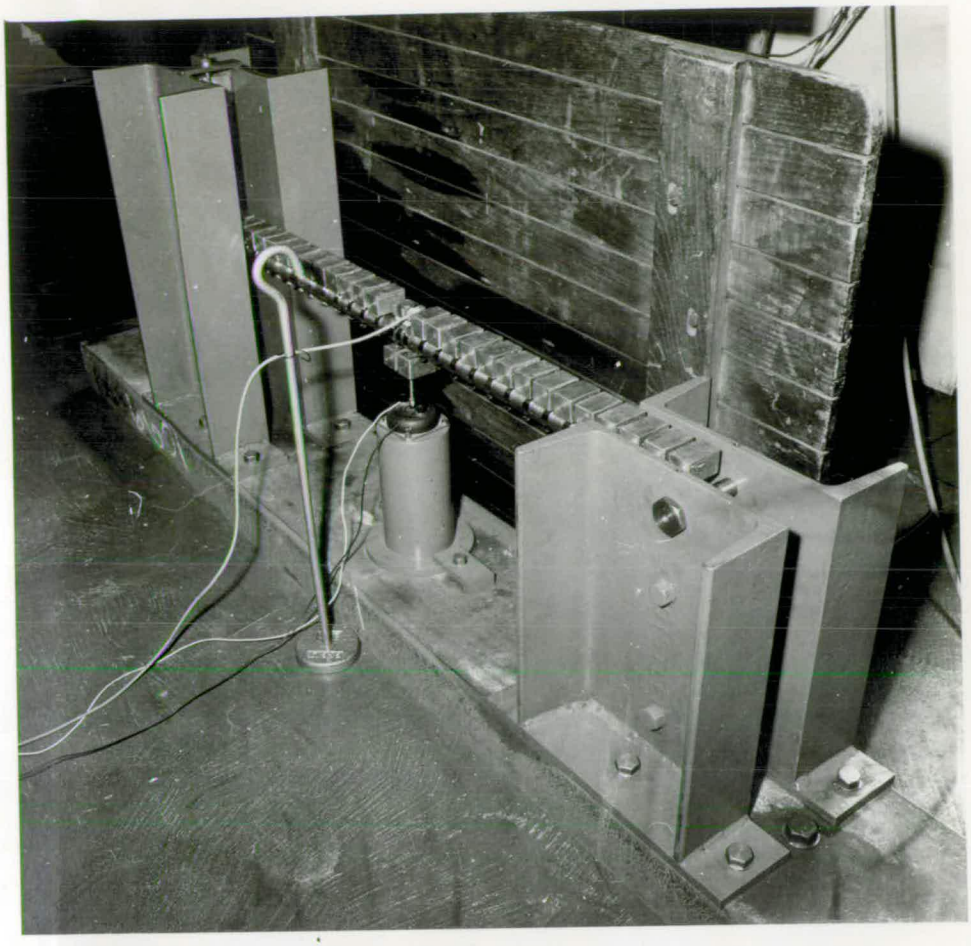

Fig. 17. Determination of the resonant frequency of a single transverse tube.

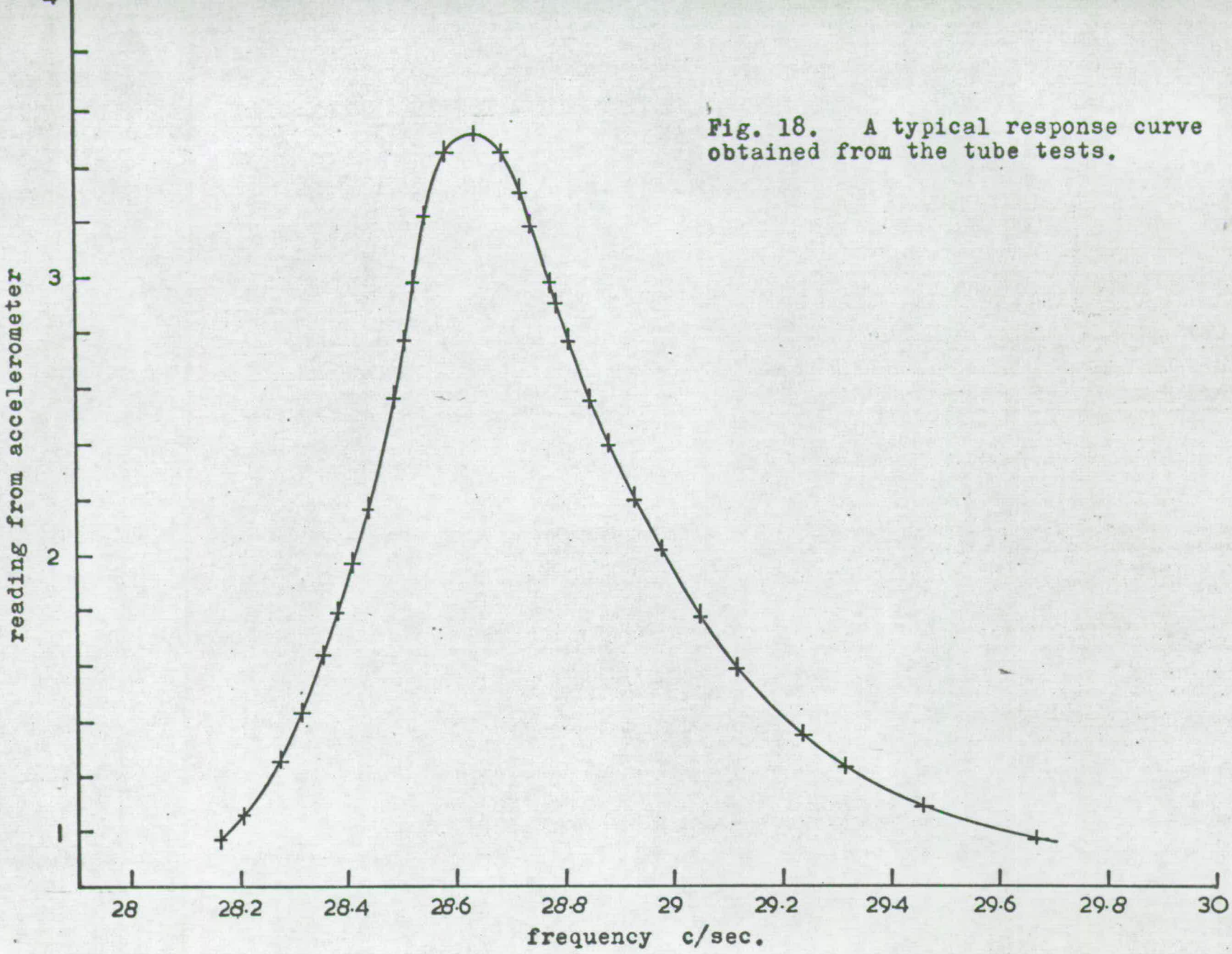

Fig. 18. A typical response curve obtained from the tube tests.

3.2.4 Grid tests

Two and three girder grids were tested, each with nine transverse tubes. In each case the length of the grid was 99" and the total width 36". The parameters of the grids were altered by attaching various numbers of lead masses to the transverse tubes as described in section 3.1.1 above. In all tests, the vibrators were installed under the two outside longitudinal girders; at the mid-points when the odd longitudinal harmonics were being sought and at the quarter points for the even harmonics. The alternating voltages applied to these vibrators by the oscillator were sometimes in phase and sometimes 180° out of phase depending on which transverse mode of vibration was being sought. The vibrators were wired in series and this phase shift was achieved by reversing the connections to one vibrator.

Before the start of each test, the input bridge circuits were balanced by means of the resistive and reactive balancing controls on the equipment. Although absolute measurements were not required, it was necessary to calibrate each channel relative to the other channels. Fortunately, the equipment is provided with a built-in calibration facility which was applied to each channel in turn.

In order to detect resonance, the accelerometers were attached to the longitudinal girders and their outputs recorded while the frequency of the excitation

was varied. Once resonance had been established, the frequency was noted and the mode shape determined by moving the accelerometers to other positions on the grid and comparing the traces on the oscilloscope. The output from each channel was then connected in turn to the digital voltmeter and the reading noted.

3.3 Results

The several resonant frequencies of each grid are compared with the theoretically predicted frequencies in tabular form in figures 56 and 57 and graphically in figures 46-50.

The mode shapes and stresses in modes 1-1 and 1-3 were expressed in terms of the ratios:

$$E = \frac{\text{amplitude at centre of centre transverse beam}}{\text{amplitude at centre of longitudinal beam}}$$

$$F = \frac{\text{maximum stress measured in transversals per unit deflection of outside longitudinal, in mode 1-3}}{\text{maximum stress measured in transversals per unit deflection of outside longitudinal, in mode 1-1}}$$

The experimental and theoretical values of these ratios are tabulated in figure 58 and illustrated in figures 59-62.

CHAPTER 4

Chapter 4.

Application to highway bridges

4.1 Introduction

The modern tendency towards large span-depth ratios has focussed attention on the problem of highway bridge vibrations. Although there now exists a vast literature on the subject, the design criteria remain vague. Newport (15) has concluded that stresses imposed in structural steel beams by vibrations classified as personally unpleasant were less than one-thirtieth of those likely to cause fatigue failure. Steffens (16) considers that reinforced concrete is also unlikely to suffer and that there is little danger of failure due to vibration in bridges unless resonance occurs. CP 117 (1967) recommends that the 25% impact allowance in HA loading (BS 153) is adequate to cover the fluctuation in stress arising from vibrations, although a further restriction is suggested for bridges used by pedestrians. The question of human sensitivity to vibration has been extensively studied, although few investigations have dealt with human tolerance of vibrations over short periods of time. Steffens and Wright and Green (17) give summaries and bibliographies.

Many investigators have attempted to analyse the response of a bridge to moving vehicles (3,9,18-20). They have mostly regarded the bridge as a simple beam, and their conclusions have, in general, been confirmed

by tests (21-24).

Resonance has been found to produce the biggest deflections and stresses. There are two types of resonance in this context. The first occurs when the frequency of the vehicle bouncing on its springs approaches a resonant frequency of the bridge. This is only likely to happen on bridges with very long spans because of the low frequency of most vehicles. It is most important on bridges with a poor approach surface which causes large initial vehicle oscillation. The second type of resonance is caused by vehicles travelling at such a speed that the frequency of application of axle loads at any point on the bridge coincides with a resonant frequency of the bridge. Thus, the most important factors which influence the vibration of a bridge are its resonant frequencies and the condition of the approach surfaces.

Previous investigators have ignored resonant bridge frequencies higher than the fundamental, although these have been observed in tests. The possibility of resonance in these modes and the higher stresses associated with them suggest that they should be considered. The most comprehensive record of the occurence of frequencies higher than the fundamental is given in the report of the Ontario Test Programme (24). Up to four different frequencies are noted for each bridge, the second usually being from three halves to twice the first. No attempt is made to identify higher modes although in some instances they occur more frequently

than the fundamental. Foster and Oehler (23) observed two resonant frequencies of the Fennville Bridge and the higher was identified as the 'third transverse mode' by deflection measurements on all the longitudinal girders.

4.2 Field test set-up

The Touch Burn Bridge is situated on the A 811 road west of Stirling and was chosen for the test because of its reputed 'liveliness'. It is simply supported over a 75ft. effective span and designed with composite action for 45 units of HB load. It is illustrated in figures 19-21 and in figure 68. In order to gain access to the underneath of the bridge, a light staging was hung from the flanges of the universal beams.

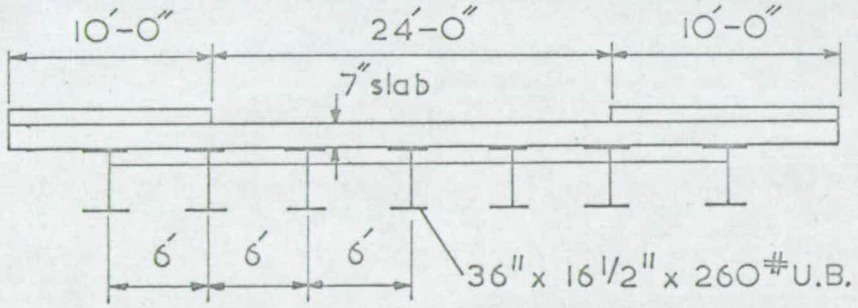

Fig. 19. The Touch Burn Bridge.
(for details see figure 68).

The bridge was vibrated by attaching to it a device consisting of two very unbalanced wheels rotating in opposite directions, and in phase with each other. The wheels were mounted side by side so that the horizontal

Fig. 20. General view of the Touch Burn Bridge.

Fig. 21. Close up view of the Touch Burn Bridge showing the vibrator fitted to a universal beam.

components of the centrifugal forces generated by the unbalance would cancel out, and the vertical components add, to apply a vertical sinusoidal exciting force to the bridge.

Bicycle wheels were used and the unbalance was produced by bolting pieces of lead to the rims. The wheels were rotated in opposite directions by means of a ½ HP DC electric motor and a simple gearbox. The device was constructed on a dexion frame and is illustrated in figures 21-23. The speed of vibration could be varied by changing the pulleys in the drive system and by adjusting the voltage supplied to the motor with a 'Variac' transformer. The power was provided at the site by a 3kva diesel AC generating set and was converted to DC by a full-wave rectifier. The size of the lead masses required to vibrate the bridge was estimated by a preliminary calculation and depended on the frequency of operation. The vibrator was tested and modified before being taken to the bridge. It was found that the maximum speed of rotation with the smallest lead weights was about 15c/sec., although this depends on the damping of the structure to which the device is attached.

Accelerometers were used to detect the vibration of the bridge and the same generator was used to run the instruments.

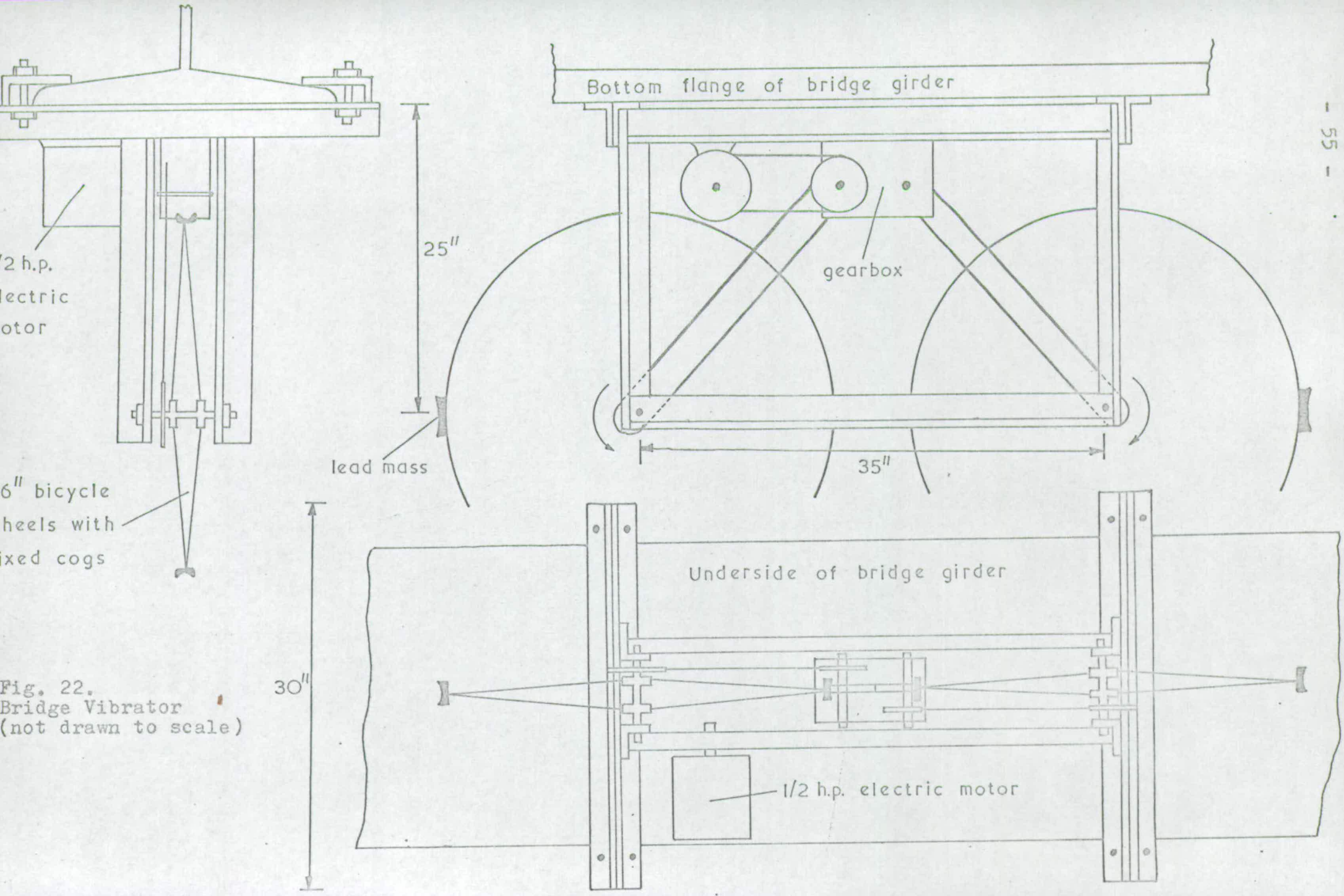

Fig. 22.
Bridge Vibrator
(not drawn to scale)

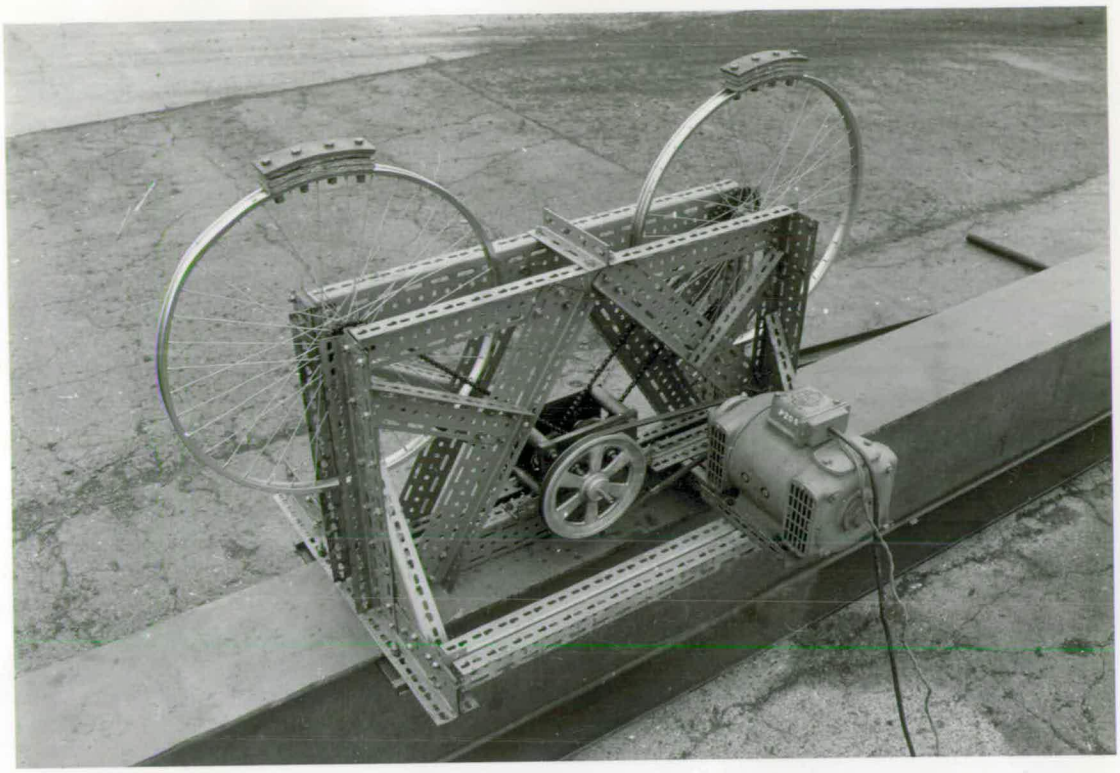

Fig. 23. The vibrating device under test.

4.3 Bridge frequency tests

The vibrating device was clamped onto the bottom flange of a universal beam in one of the four positions marked in figure 24. The position depended on the mode of vibration being investigated. Likewise, the choice of pulley wheels and lead masses depended on the frequency of the mode being sought. The accelerometers were attached to the beams by adhesive tape.

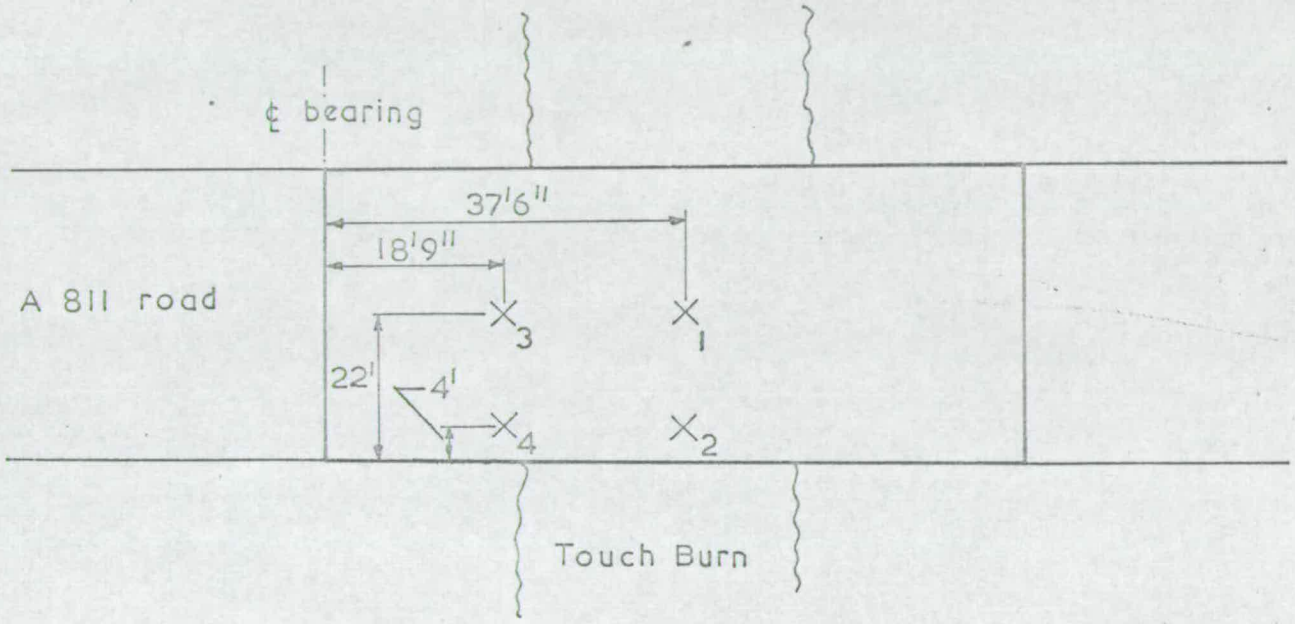

Fig. 24. Positions of the vibrator on the Touch Burn Bridge

A test consisted of slowly varying the voltage supplied to the motor in small steps and recording the response of the accelerometers with the 'Visicorder' ultraviolet recorder. Many recordings were obtained and by measuring the amplitudes and frequencies of the traces, response curves such as figure 25 were drawn. When resonance was established the mode shape was determined

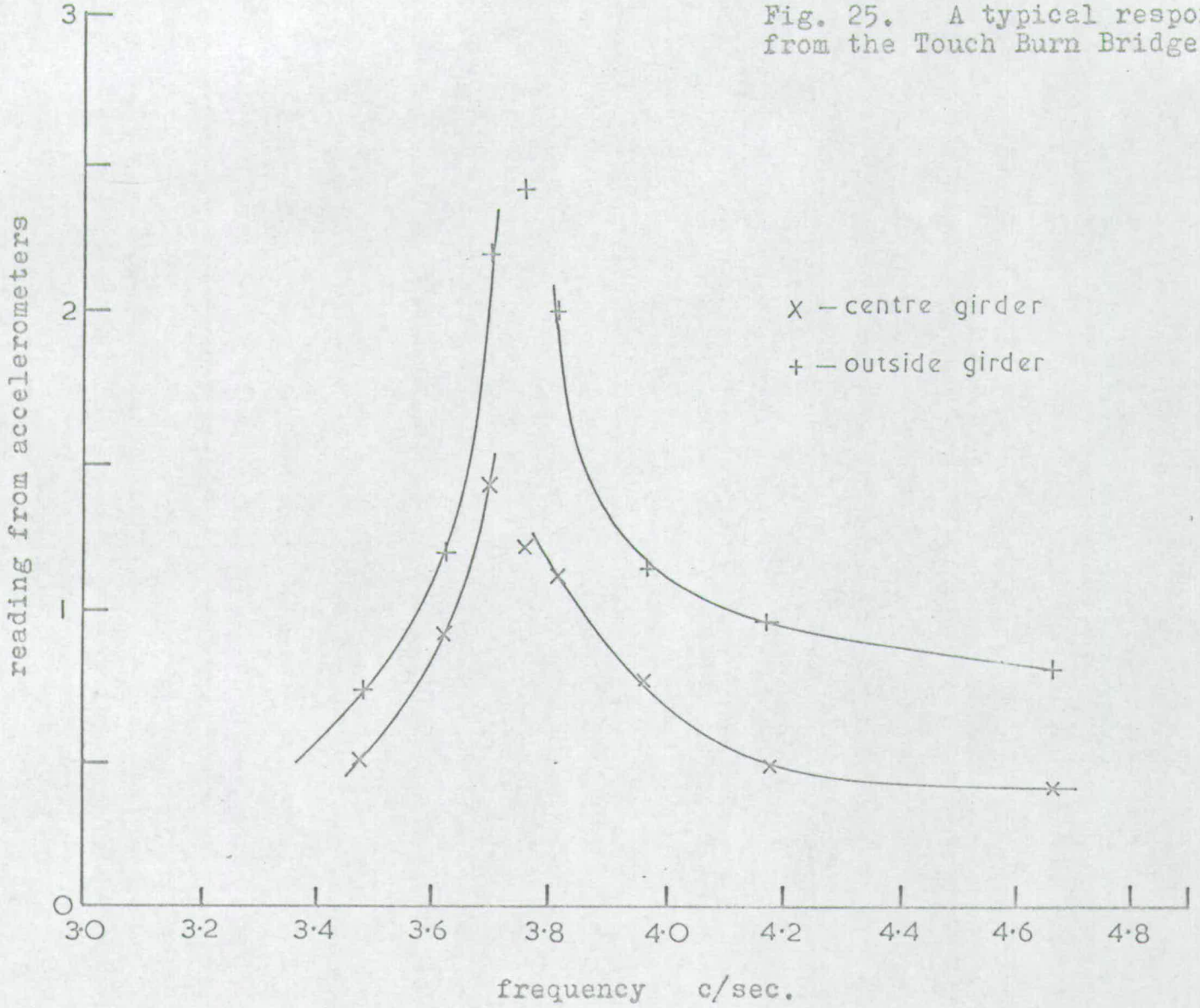

Fig. 25. A typical response curve from the Touch Burn Bridge test.

by comparing the oscilloscope traces from the accelerometers at various positions on the bridge. The observed frequencies are shown in figure 63 alongside the frequencies predicted by the design method suggested in section 2.2 above.

In calculating the grid parameters of the bridge the extra mass due to the pavements and edges was distributed across the whole bridge.

The stiffness of the transverse slab was calculated using the gross concrete section and a modulus of elasticity of 3.75×10^6 lb/sq in. The longitudinal stiffness was calculated using a modular ratio of eight, and assuming that the entire width of the concrete slab contributed. These assumptions are discussed in section 5.3, and the calculation of the grid parameters is given in Appendix 1 below.

4.4 Vehicle observation tests

One day was devoted to recording the response of the bridge to general traffic. Most attention was paid to heavy vehicles. The speeds of the vehicles were measured using a radar traffic-speed analyser and their axle-spacings were estimated. Accelerometers were attached to the bridge at points 1 and 2 on figure 24 and their outputs were recorded on the ultra-violet recorder. By examining the recorded traces the frequencies and modes of vibration of the bridge were deduced.

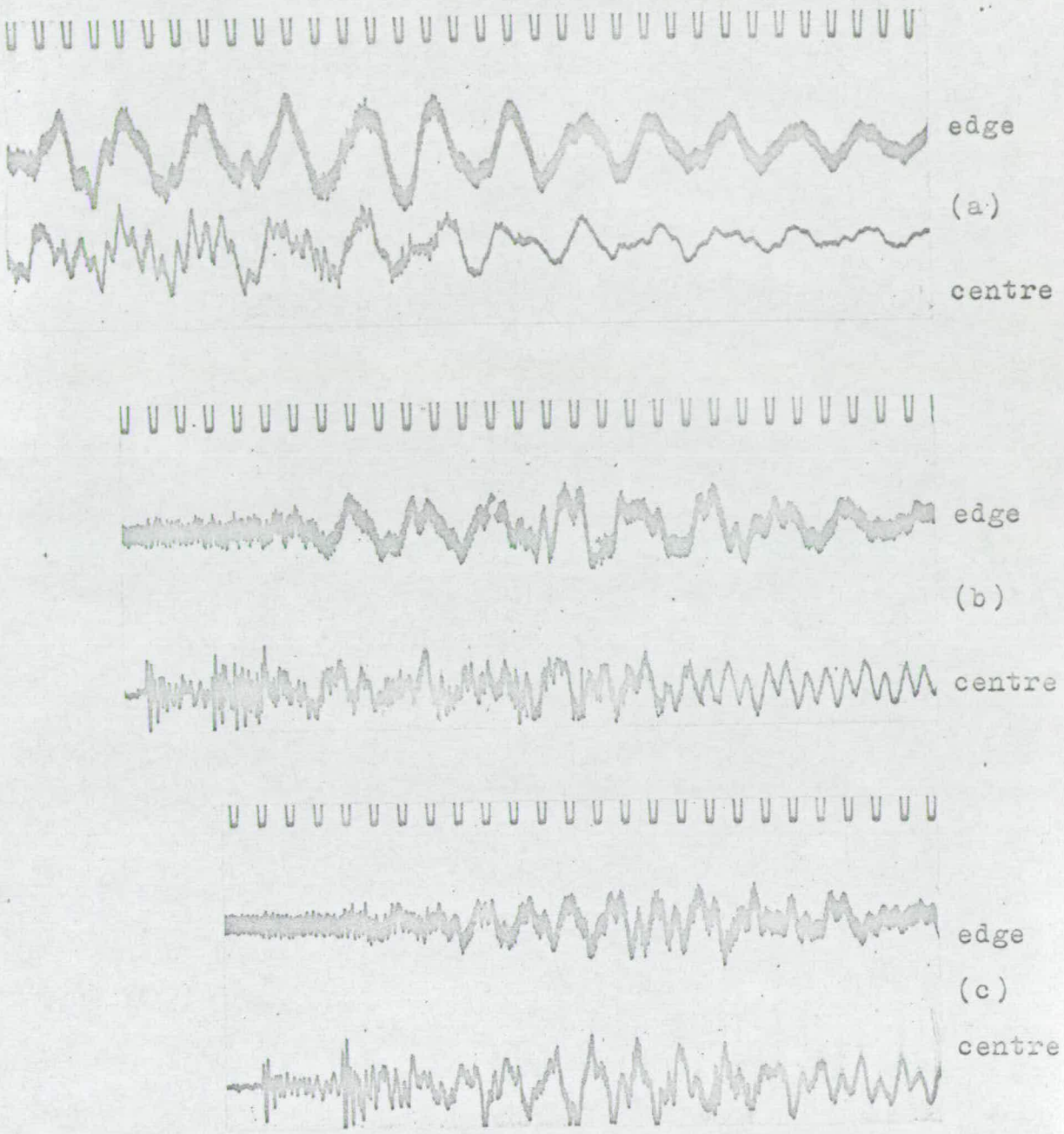

Fig. 26. Response of the Touch Burn Bridge to vehicles. The timer marks are at 0.1 second intervals.

Three typical traces are illustrated in figure 26. Trace (a) shows a strong vibration at approximately 3.8 c/sec. with the edge beam vibrating in phase with the centre beam. This is mode 1-1. Trace (b) shows a fairly strong vibration at about 4.2 c/sec. in the edge girder only, corresponding to mode 1-2, and trace (c) shows an out of phase vibration at about 6.2 c/sec. being mode 1-3. These traces are discussed further in section 5.3.5 below. The number of occurrences of each mode is given in figure 63. In addition, a frequency of about 15 c/sec. was observed on many occasions.

An attempt was made to correlate the period of the vibration provoked by a passing vehicle with the axle-spacing parameter s/v, where s = axle-spacing, and v = vehicle velocity. The condition for this type of resonance is that s/v is a multiple of a natural period of the bridge T, thus,

$$s = vkT \quad \text{where } k = 1,2,3...$$

If s is plotted against v we have a set of straight lines, one for each combination of values of k and T. Each mode was considered separately and lists were compiled of vehicles causing:

1) strong vibration
2) some vibration
3) no vibration in that mode.

Each item of data was plotted as a point on one of the above graphs. If there were a correlation between the axle-spacing parameter of the vehicle and the period of

the vibration caused by it, the points denoting strong vibrations would lie near the lines and the points denoting no vibration would lie elsewhere. This pattern is not evident in figures 64-66.

4.5 Bridge damping

The ultra-violet recorder traces were used to estimate the rate of decay of the bridge vibration after vehicles left the bridge. The damping was expressed as a percentage of the critical damping from measurements of vibration amplitudes, thus:

$$b = \left(\frac{1}{2\pi n}\right) \ln\left(\frac{a_m}{a_{m+n}}\right) \times 100$$

where b is the percentage of critical damping, a_i is the amplitude of the bridge vibration after i cycles and n is the number of cycles between amplitude measurements.

Only those traces with a strongly predominant first mode of vibration were used since otherwise it was not possible to separate the amplitudes of the different modes. As the determination of the damping in an individual trace depends on the comparison between two fairly small quantities, the measured damping varied considerably between 1.6% and 2.8% with a mean of 2.0%.

CHAPTER 5

Chapter 5.

Discussion of Results

5.1 Theoretical results

5.1.1 Summary

The theoretical analysis enables the frequency and the shape of any particular mode of vibration of a grid of any size to be found, together with the bending moments and the energy in that mode. The results from this analysis are compared with the results of the laboratory tests in section 5.2 below. The frequencies of the first three modes of vibration of a wide range of grids are plotted in the design curves (figures 28-45).

5.1.2 Assumptions

The analysis is based on the assumptions that the transverse beams can be replaced by a continuous spread medium without torsional stiffness, and that the torsional stiffness of the longitudinal beams can be neglected. The use of these assumptions is well established in the static analysis of grid frameworks. Leonhardt and Andra (25) hold that any more than five transverse girders have little effect on the distribution of load between the longitudinal girders and they replace five or more transverse beams with the same single cross girder at the middle. Hendry and Jaeger

make the safer assumption of the spread medium and conclude that the effect of torsion of the transverse members is usually unimportant and that for bridges having steel plate girders of I section, the torsion effects can be neglected.

Similar assumptions have been made by Hendry, Zeidan and the present author, when analysing the dynamic behaviour of grids. A preliminary investigation into the effect of torsion of the longitudinals of the models used in this work suggests that it is negligible.

A limitation of the method became apparent when an attempt was made to apply it to model bridges consisting of 1½ inch slabs cast onto 3 x 1½ inch RSJ sections at 12 inch centres with shear connectors. One such model is illustrated in figure 27. Frequency tests were carried out on these models, but the results were not in agreement with the theory. This was probably due to the longitudinal beams being so light and flexible relative to the slab that the assumption of no torsion of the transverse medium was not satisfied.

The theory also assumes continuity of the transverse beams. This was satisfied by the special design of the laboratory models, and also by the composite construction of the Touch Burn Bridge.

5.1.3 Application to other support conditions

Harmonic Analysis is a well established method of expressing unknown or difficult distributions of load in

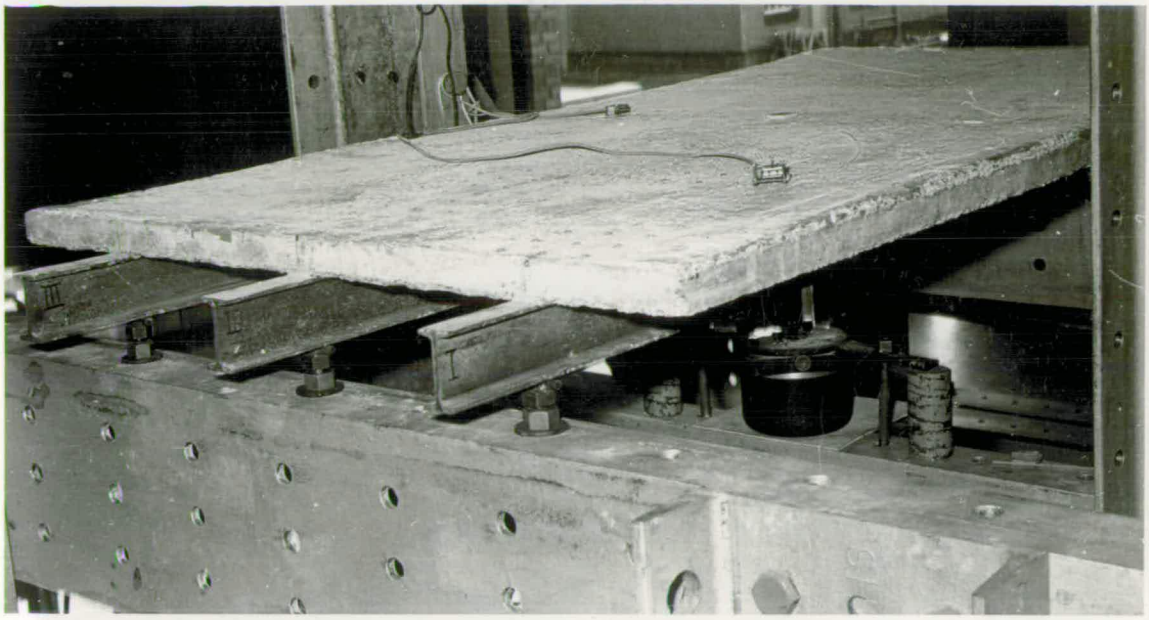

Fig. 27. Three-girder model bridge, showing an electro-mechanical vibrator and accelerometers.

the form of a sine series. Here it has enabled the force between the transverse medium and the longitudinals to be related to the deflection of the longitudinals. The power of the method is due to the fact that, for simply supported structures, a sinusoidal distribution of load produces a similar sinusoidal distribution of deflection.

If other support conditions are considered, more general functions have to be used to describe the load distribution. A method is outlined in Appendix 2, but further tests are called for to assess its accuracy.

5.1.4 Efficiency of the computer programs

The analysis of many grids has been satisfactorily carried out using the computer programs described in section 2.3. The programs were written in Atlas Autocode and the compiling time on an English Electric KDF9 computer is just less than one minute for each program. The running time depends on the size of the grid being analysed and on the choice of the range and increment of the eigenvalue. Typical times taken to calculate and print details of the first four modes of a three-girder and a seven-girder grid are 32 seconds and four minutes respectively.

In all cases the first few eigenvalues lie much closer together than the successive ones, and so smaller increments of the trial eigenvalues are required to find them. The efficiency of these programs could be improved by using a more flexible method of incrementing

the trial eigenvalue. By allowing the program more freedom to choose the appropriate increments, the problem of having to choose the initial increment to include not more than one eigenvalue could probably be avoided.

5.1.5 Stresses

As the lower modes are the ones most likely to occur in practice, the stresses in these modes were examined. The stress in a vibrating beam depends on the shape and amplitude of the vibration and not on the frequency. This means that the stress in the longitudinal beams per unit deflection, is the same in modes 1-1, 1-2, 1-3, etc. The stress in the transverse medium depends on the mode and it is found that the transverse stresses in mode 1-3 are often considerably higher than those in mode 1-1. The transverse stresses in mode 1-2 are always small and have not been considered.

The ratio of the maximum transverse stresses occurring in the model grids, normalised with respect to the deflection amplitudes of the longitudinals, in modes 1-3 and 1-1 are given in figure 58. It can be seen that the transverse stresses in mode 1-3 are several times those in mode 1-1. Of course, the amplitude of the vibration in mode 1-3 will be less than that in mode 1-1 and to take this into account the stress ratio referred to above was calculated again using stresses normalised with respect to the total energy of the grid. This ratio is listed in figure 58 and gives a much better

idea of the magnification of the transverse stresses to be expected in mode 1-3 in practice.

5.2. Laboratory tests

5.2.1. Summary of results

The existence of the mode shapes predicted by the theory was confirmed by the laboratory tests. The shape of the first and third transverse modes (modes 1-1 and 1-3) of the test grids agreed reasonably well with the theory, and the frequencies of the first three modes were within 2½% of the theory. Larger errors were observed in certain of the higher frequencies. For the two-girder grids the frequencies predicted for modes 2-2 and 2-3 were between 6% and 8% too high with an average of 7%. Likewise, the predicted frequencies for modes 2-1, 2-2, 2-3 and 2-4 of the three girder grids were between 4% and 8% too high with an average of 6%.

5.2.2. Source of error

The consistency of the above errors suggests that a simple explanation is likely. The possibility of inaccuracies due to simplification of the theory have been discussed above. The parameters on which the theoretical predictions were made are unlikely to be wrong, because they were based on the results of actual weighings and previous frequency tests.

One possible source of error lies in the spring steel supports, but the control test described in section 3.2.2 above indicates that they behave as simple supports when the longitudinals are vibrating on their own in the first and second harmonics. Moreover, the result given in Appendix 2 suggests that the analysis is independent of the support conditions as long as the appropriate frequency of the longitudinals is used in the calculation of the grid frequency parameter. However, although the longitudinals appear to vibrate as simply-supported beams, the assumption that the frequencies of their second and third modes are four and nine times fundamental frequency respectively may contribute to the error in the estimated frequencies of some of the higher modes of the grid. Further control tests are required to define the behaviour of the spring steel supports.

5.2.3 Stresses

The stresses were measured by strain gauges attached at the quarter points and mid-point of the centre transverse tube. The maximum stresses occurred at the mid-point of the tube except in the case of mode 1-1 of the three girder grid, when the theoretical maximum position was about six tenths of the way from an outer longitudinal to the centre longitudinal. Thus the stress measured in this mode is slightly less than the maximum

and the stress magnification ratio is consequently too large. The difference should be between 4% and 5%.

The comparison of normalised transverse stresses in modes 1-1 and 1-3 shows a disagreement between the theory and experiment. Stresses are very sensitive to mode shapes, and the disparity may be due to the relatively small number of lead masses on the tubes affecting the transverse mode shape. In all cases, the stress in the third mode relative to that in the first is greater than expected. This experimental result emphasises the importance of considering stresses in higher modes. Although the frequencies of the first three modes of vibration lie fairly close together, the normalised stress in the third mode is much higher than that in the first mode.

5.2.4 Suggestions for future tests

In order to determine mode shapes and stresses in higher modes, a more sophisticated measuring and recording system would be required. The system would have to be more sensitive and include a rapid data-logging device to overcome the effect of the drift of the instrument readings.

Further tests are called for to investigate the application of the theory to grids with four and more longitudinal girders, and with different support conditions. The effect of torsion in structures consisting of a reinforced concrete slab cast onto longitudinal

beams could also be investigated by comparing the behaviour of model grids constructed with and without torsion, but having the same grid parameters.

5.3 Field test

5.3.1 Application of the design method

The test has shown that the first two resonant frequencies of the composite-construction bridge can be accurately predicted, and several others predicted with reasonable precision using the proposed design method.

The analysis does not consider the torsion of the longitudinal beams or the transverse medium. In this case, however, the transverse medium takes the form of a reinforced concrete slab which also contributes to the longitudinal stiffness, and this neglect of the torsion effects may be a source of inaccuracy.

5.3.2 Extra mass of edges and pavements

The main effect of spreading the extra mass due to the edges and pavements was to increase the mass of the transverse medium used in the evaluation of the grid parameters. This will have introduced some error, particularly in the calculation of the higher frequencies where the properties of the transverse slab are more important.

The contribution of this inaccuracy to the total error in the predicted frequencies should be assessed by further control tests. It is suggested that two model grids should be constructed, one with extra mass at the edges and one without, but both having the same grid parameters when the extra mass of the first grid has been spread. By comparing the dynamic behaviour of each, some idea of the effect of the mass concentration at the edges could be gained.

5.3.3 Transverse stiffness

The stiffness of the transverse slab was calculated on the basis of the recommendations of the Structural Bureau of the Portland Cement Association (26). To calculate the deflection of a reinforced concrete member caused by an instantaneous load, the uncracked gross section is used together with a modulus of elasticity of concrete of one thousand times the twenty eight day cylinder strength. In the absence of records of the actual concrete strength, a typical cylinder strength of 3750 lb/sq in. was assumed, which corresponds to a cube strength of 4400 lb/sq in. This value seems reasonable as the specified cube strength was 3750 lb/sq in. It is in agreement with Reynolds (27) who recommends an E value for concrete of 3.75×10^6 lb/sq in. for live loads.

5.3.4 Longitudinal Stiffness

The longitudinal stiffness was calculated using a modular ratio of eight, corresponding to a concrete strength of 3.75×10^6 lb/sq.in. The entire width of the concrete slab was assumed to contribute, as recommended for static analysis by C.P. 117 (Composite Construction in Structural Steel and Concrete). The longitudinal stiffness of the theoretical model is concentrated in the longitudinal beams and this difference may introduce error into the calculation of the frequencies. Again, the higher frequencies will probably be more sensitive to this error.

Further control tests are called for to estimate the importance of this discrepancy. However, any attempt to compare the behaviour of a model grid having a longitudinally stiff transverse slab with a conventional model grid would also involve a comparison of the torsion of the transverse medium in each case.

5.3.5 Response to vehicles

The three lowest frequencies are close together and occur often under normal traffic conditions. The second mode of vibration (mode 1-2) does not occur so often because the vehicles mostly travel very near the centre line of the bridge which is a node. In this respect, the Touch Burn Bridge may not be typical due to its wide pavements and freedom from traffic.

The small discrepancies between the frequencies of vibration of the bridge during the passage of vehicles and the natural frequencies measured previously reflect the forced-motion nature of these vibrations.

The lack of correlation between the axle-spacing parameter and the period of vibration of the bridge may be due to inaccurate estimates of the axle-spacings and in particular to the small axle-spacings of articulated units and tandem axles having been neglected. Moreover, if all the points representing vehicles are plotted on the same sheet as all the lines of resonance, it is evident that the two sets do coincide (figure 67). This would not be the case if the bridge vibrated at a higher frequency, say 5.5 c/sec., which is the average frequency of similar bridges in Ontario.

5.3.6 Damping

The damping in the Touch Burn Bridge was 2% of the critical damping and this is the same as in similar bridges in Ontario.

5.3.7 Suggestions for future field tests

Further tests on other bridges in Britain are called for to see whether the low natural frequency of the Touch Burn Bridge is the cause of its 'liveliness',

and to confirm the accuracy of the design method in predicting natural frequencies.

Now that the vibration characteristics of the Touch Burn Bridge are known, a more detailed attempt to correlate its response with the movement of vehicles could be carried out. Accelerometers are not the best instruments to use for this purpose since they confuse the traces by exaggerating the higher frequencies. A recording system measuring displacements and having a better signal to noise ratio would be desirable. The axle-spacings of vehicles would have to be measured, possibly using pneumatic tubes across the road connected to a recorder. An attempt to measure stresses occuring in each mode of vibration would also be useful.

5.4 Conclusion

The laboratory tests have shown that the proposed design method can predict several frequencies and mode shapes of vibration of two and three girder grids without torsion with reasonable accuracy. The design curves provide designers with a very convenient means of doing this.

The Touch Burn Bridge test suggests that the method can be reliably used for multi-girder composite construction bridges, where the concrete slab is thin relative to the dimensions of the longitudinal girders. The frequency of the third mode (mode 1-3) of the bridge

lies very near the first, and occurs often under normal traffic conditions. The transverse stresses associated with mode 1-3 of the laboratory models were very much higher than those associated with mode 1-1, although the ratio of these stresses was underestimated by the theoretical analysis.

It is suggested that these results are significant because, although previous investigators have all agreed that the natural frequency of a bridge is the most important parameter in the problem, they have mostly treated a bridge as a simple beam and have ignored all frequencies higher than the first.

APPENDIX 1

Appendix 1.

Calculation of the Touch Burn Bridge parameters

Weight of longitudinal beam, $m_L g = 260$ lb/ft.

Composite section

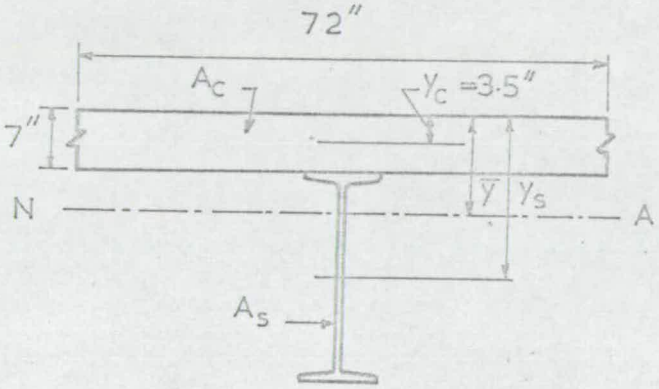

Fig. A.1. Composite section.

7" slab 2" surface

36" x 16½" x 260lb. U.B.

$A_s = 76.56 \text{in.}^2$

$\frac{A_c}{m} = \frac{7 \times 72}{8} = 63 \text{in.}^2$

Depth of neutral axis, $\bar{y} = \frac{A_s y_s + \frac{A_c}{m} y_c}{A_s + A_c/m}$

$$= \frac{76.56 \times 25.12 + 63 \times 3.5}{76.56 + 63}$$

$$= 15.36 \text{in.}$$

Second Moment,

$$I_L = I_s + A_s(y_s - \bar{y})^2 + \frac{I_c}{m} + \frac{A_c}{m}(\bar{y} - y_c)^2$$

$$= 17234 + 76.56 \times (9.76)^2 + \frac{72 \times 7^3}{12 \times 8} + 63 \times (11.86)^2$$

$$= 33,646 \text{ in.}^4 \qquad \text{steel units}$$

Frequency,

$$\omega_L = \frac{\pi}{2 \times L^2}\sqrt{\frac{EI_L}{m_L}}$$

$$= \frac{\pi}{2 \times (75 \times 12)^2}\sqrt{\frac{30 \times 10^6 \times 33646 \times 32.2 \times 12^2}{260}}$$

$$= 8.23 \text{ c/sec.}$$

Transverse slab

weight/ft.^{2} of 7" slab $= \frac{7}{12} \times 150 = 87.5$

weight/ft.^{2} of 2" surface $= \frac{2}{12} \times 144 = 24.0$

Extra weight due to pavements, etc. (distributed)

edges $\frac{7}{12} \times 3 \times 150 = 263$

$2 \times 1 \times 150 = 300$

sand fill $\frac{7\frac{1}{2}}{12} \times 9 \times 110 = 619$

parapet $= 50$

$1232 \times \frac{2}{42} = 58.7$

diaphragm at mid-span $= \frac{31}{75} \times \frac{36}{42} \times \frac{35}{17} = 0.7$

$mg = 170.9$ lb/sq.ft.

Second Moment $I_T = \frac{1}{12} \times 12 \times 7^3 = 343$ in.^{4}/ft. width

Frequency $\omega_T = \frac{\pi}{2h^2} \sqrt{\frac{EI_T}{m_T}}$

$$= \frac{\pi}{2 \times (6 \times 12)^2} \sqrt{\frac{3.75 \times 10^6 \times 343 \times 32.2 \times 12^2}{170.9}}$$

$= 56.6$ c/sec.

Grid parameters

$$\lambda = \frac{mh}{m_L} = \frac{170.9 \times 6}{260} = 3.944$$

$$K = \frac{\omega_L}{\omega_T} = \frac{8.23}{56.6} = 0.145$$

APPENDIX 2

Appendix 2.

Analysis of grids with other support conditions

The equation of free vibration of a longitudinal girder is:

$$EI_L \frac{\partial^4 y}{\partial x^4} + m_L \frac{\partial^2 y}{\partial t^2} = 0$$

and we can investigate solutions of the form:

$$y(x,t) = X(x).\sin \omega t$$

Hence:

$$EI_L \frac{d^4 X}{dx^4} - m_L \omega^2 X = 0$$

The general solution of this equation is:

$$X = A\sin\theta x + B\cos\theta x + C\sinh\theta x + D\cosh\theta x$$

where: A,B,C,D are constants depending on the end conditions of the beam, and,

$$\theta^4 = \frac{m_L \omega^2}{EI_L}$$

From the end conditions we can obtain the ratios of the constants and the frequency equation. The deflection of the beam when it is vibrating in the n'th mode is:

$$y = X_n \sin \omega_n t$$

The mode shape is given by the 'normal function' X_n, which

has the property of othogonality, i.e.

$$\int_0^L X_i \, X_j \, dx = 0 \quad \text{when } i \neq j$$

This enables any arbitrary function to be expanded as a series of normal functions. Inglis (7) has shown that if a non-uniform load on a vibrating beam is represented by a series of the normal functions of that beam, the deflection is given by another, rapidly-convergent series of the normal functions.

Consider now a longitudinal girder as part of a grid which is vibrating freely. The force between the transverse medium and the longitudinal girder can be given by a sum of the normal functions of the beam, thus:

$$P(x,t) = \sum_n (P_n X_n).\sin\omega t$$

The equation of motion of the longitudinal beam is:

$$EI_L \frac{\partial^4 y}{\partial x^4} + m_L \frac{\partial^2 y}{\partial t^2} = P(x,t)$$

The particular solution will be:

$$y = \sum_n (a_n X_n).\sin\omega t$$

Substituting in the differential equation and equating coefficients, we have:

$$EI_L a_n \Theta_n^4 - m_L \omega^2 a_n = P_n$$

Therefore:

$$a_n = \frac{P_n}{m_L\left[\frac{EI_L}{m_L}\theta_n^4 - \omega^2\right]} = \frac{P_n}{m_L\left[(\omega_L)_n^2 - \omega^2\right]}$$

Thus we have a relation between the force and the deflection, which is independant of the end conditions. $(W_L)_n$ is the frequency of the n'th mode of the longitudinal girder vibrating on its own, with the appropriate end conditions.

Comparison of this relation with that obtained for a simply supported grid shows that grids with any support conditions can be analysed using the method described in section 2.4 with:

$$K = \frac{\text{freq. of a longitudinal beam vibrating on its own supported as it is in the grid.}}{\text{freq. of a simply supported transverse beam vibrating on its own.}}$$

The unknown quantities in the normal functions can be determined from the end conditions.

For a simply supported grid, the end conditions are:

$$y = \frac{d^2y}{dx^2} = 0 \qquad \text{at } x = 0 \text{ and } x = L$$

The normal functions become:

$$X_n = \sin\frac{n\pi x}{L}$$

and the method reduces to harmonic analysis.

For a grid with built-in supports:

$$y = \frac{dy}{dx} = 0 \qquad \text{at } x = 0 \text{ and } x = L$$

and the normal functions become:

$$X_n = D_n (\cosh \theta_n x - \cos \theta_n x) - (\sinh \theta_n x - \sin \theta_n x)$$

where:

$D_1 = 1.0178$ $\qquad \theta_1 L = 4.73004$

$D_2 = 0.99922$ $\qquad \theta_2 L = 7.8540$

$D_3 = 1.000034$ $\qquad \theta_3 L = 10.9956$

APPENDIX 3

Appendix 3.

Bibliography

1. ROGERS, G.L. Dynamics of Framed Structures, Wiley, 1959.

2. HENDRY, A.W. and JAEGER, L.G. The Analysis of Grid Frameworks and Related Structures. Chatto and Windus, 1958.

3. INGLIS, C.E. A Mathematical Treatise on Vibrations in Railway Bridges. Cambridge University Press, 1934.

4. HENDRY, A.W. The Structural Behaviour of Grid Frameworks, Taylor Woodrow Lectures, University of Nottingham, 1963.

5. ZEIDAN, M.A. The Dynamic Response of Certain Grid Frameworks, M.Eng. thesis, University of Liverpool, 1963.

6. AUSTIN, C.W. The Response of Grid Frameworks to Impact Loads, B.Sc. thesis, University of Edinburgh, 1965.

7. INGLIS, C.E. The Determination of Critical Speeds, Natural Frequencies and Modes of Vibration by

Means of Basic Functions. Parsons Memorial Lecture, N.E. Coast Institution of Engineers and Shipbuilders, Newcastle, 1945.

8. NORRIS, C.H. et al. Structural Design for Dynamic Loading, McGraw Hill, 1959.

9. TIMOSHENKO, S. Vibration Problems in Engineering, Van Nostrand, third edition, 1955.

10. BLEICH, H.H. Frequency Analysis of Beam and Girder Floors, Trans. A.S.C.E., Vol. 115, 1950, pp. 1023-1064.

11. HURTY, W.C. and RUBINSTEIN, M.F. Dynamics of Structures, Prentice Hall, 1965.

12. OSBORNE, M.R. A New Method for the Solution of Eigenvalue Problems, The Computer Journal, Vol. 7, No. 3, October 1964.

13. FODDEN, E.J. Hybrid Computer Solution of Two Point Boundary Value Problems, Applied Dynamics Inc. Application Report.

14. MORSE, P.M. and FESHBACH, H. Methods of Theoretical Physics, Part 1, pp. 719-724, McGraw Hill, 1953.

15. NEWPORT, A.J. The Possibility of Fatigue

Failure in Welded Connections of Steel Floor Beams as a Result of Vibration and Shock. Welding Panels Steel Struct. Res. Comm. Rep., pp. 196-213, H.M.S.O., London, 1939.

16. STEFFENS, R.J. Some Aspects of Structural Vibration, Proc. of a Symposium "Vibration in Civil Engineering", British National Section of the International Association for Earthquake Engineering, 1965.

17. WRIGHT, D.T. and GREEN, R. Human Sensitivity to Vibration, Report No. 7, Queens University, Kingston, Ontario, February 1959.

18. WALKER, W.H and VELETSOS, A.S. Response of Simple-span Highway Bridges to Moving Vehicles, Civil Eng. Studies, Struct. Res. Ser. No. 272, 134th Progress Rep. of the Highway Bridge Impact Investigation, University of Illinois, Urbana, Illinois, September 1963.

19. SCHEFFEY, C.F. Dynamic Load Analysis and Design of Highway Bridges, Highway Res. Board Bull. No. 124, 1950.

20. TUNG, T.P., GOODMAN, L.E., CHEN, T.Y. and NEWMARK, N.M. Highway Bridge Impact Problems, Highway Res. Board Bull. No. 124, 1950.

21. BIGGS, J.M. and SUER, H.S. Vibration

Measurements on Simply Supported Bridges, Highway Res. Board Bull. No. 124, 1950.

22. HAYES, J.M. and SBAROUNIS, J.S. Vibration Study of a Three-span Continuous I Beam Bridge, Highway Res. Board Bull. No. 124, 1950.

23. FOSTER, G.M. and OEHLER, L.T. Vibration and Deflection of Rolled Beam and Plate-girder Bridges, Highway Res. Board Bull. No. 124, 1950.

24. WRIGHT, D.T. and GREEN, R. Highway Bridge Vibrations, Part 2, Ontario Test Programme, Report No. 5, Queens University, Kingston, Ontario, September 1963.

25. LEONHARDT, F. and ANDRA, W. Die Vereinfachte Trägerostberechnung, Stuttgart, 1950.

26. PORTLAND CEMENT ASSOCIATION. Deflection of Reinforced Concrete Members, Structural Bureau, S.T. 70.

27. REYNOLDS, C.E. Reinforced Concrete Designer's Handbook, Concrete Publications, 1964.

28. LECKIE, F.A. and LINDBERG, G.M. The Effect of Lumped Parameters on Beam Frequencies. Aeronautical Quarterly, Vol. 14, 1963.

APPENDIX 4

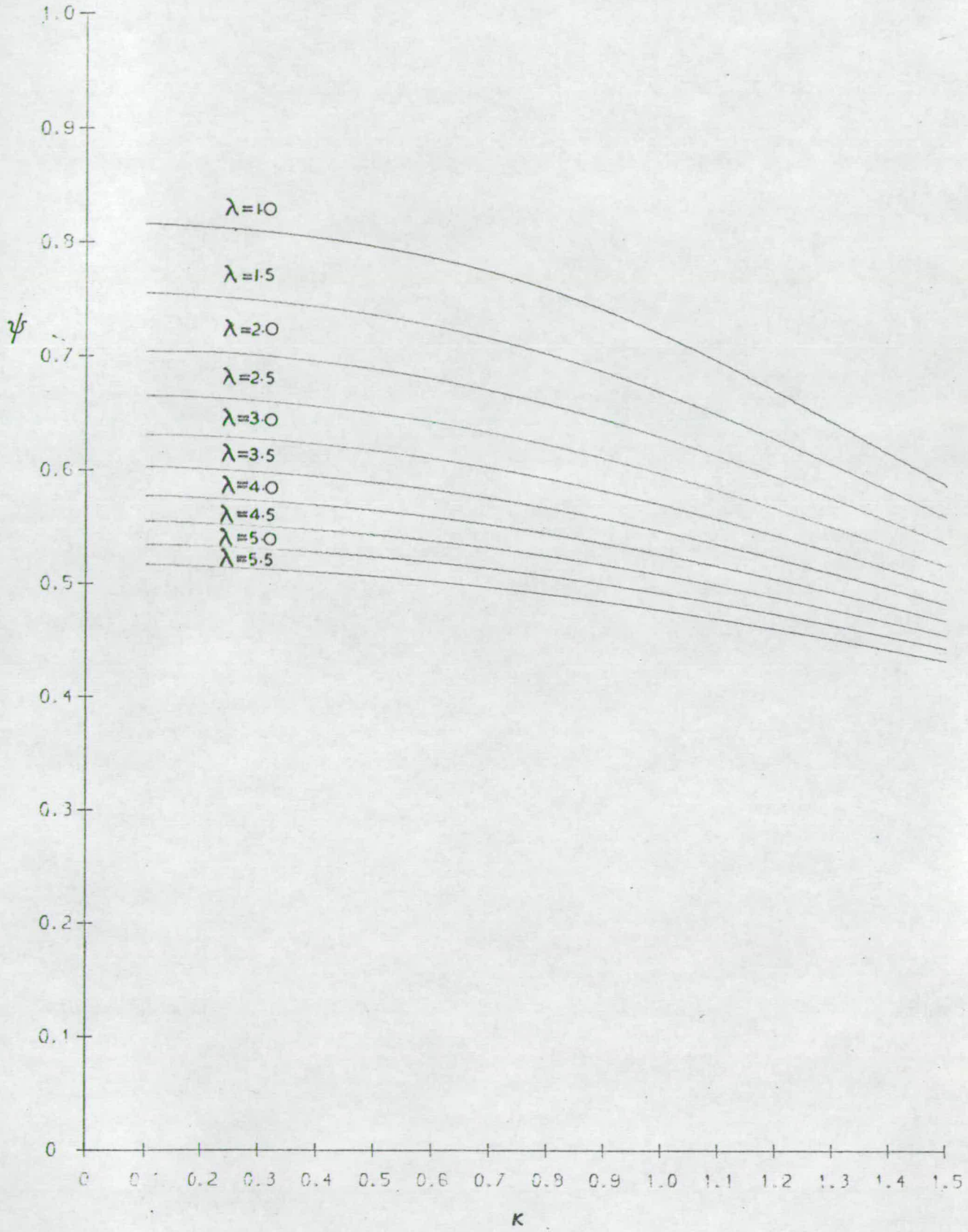

Fig. 28. Design curves, 2 girder grid. Transverse mode 1.

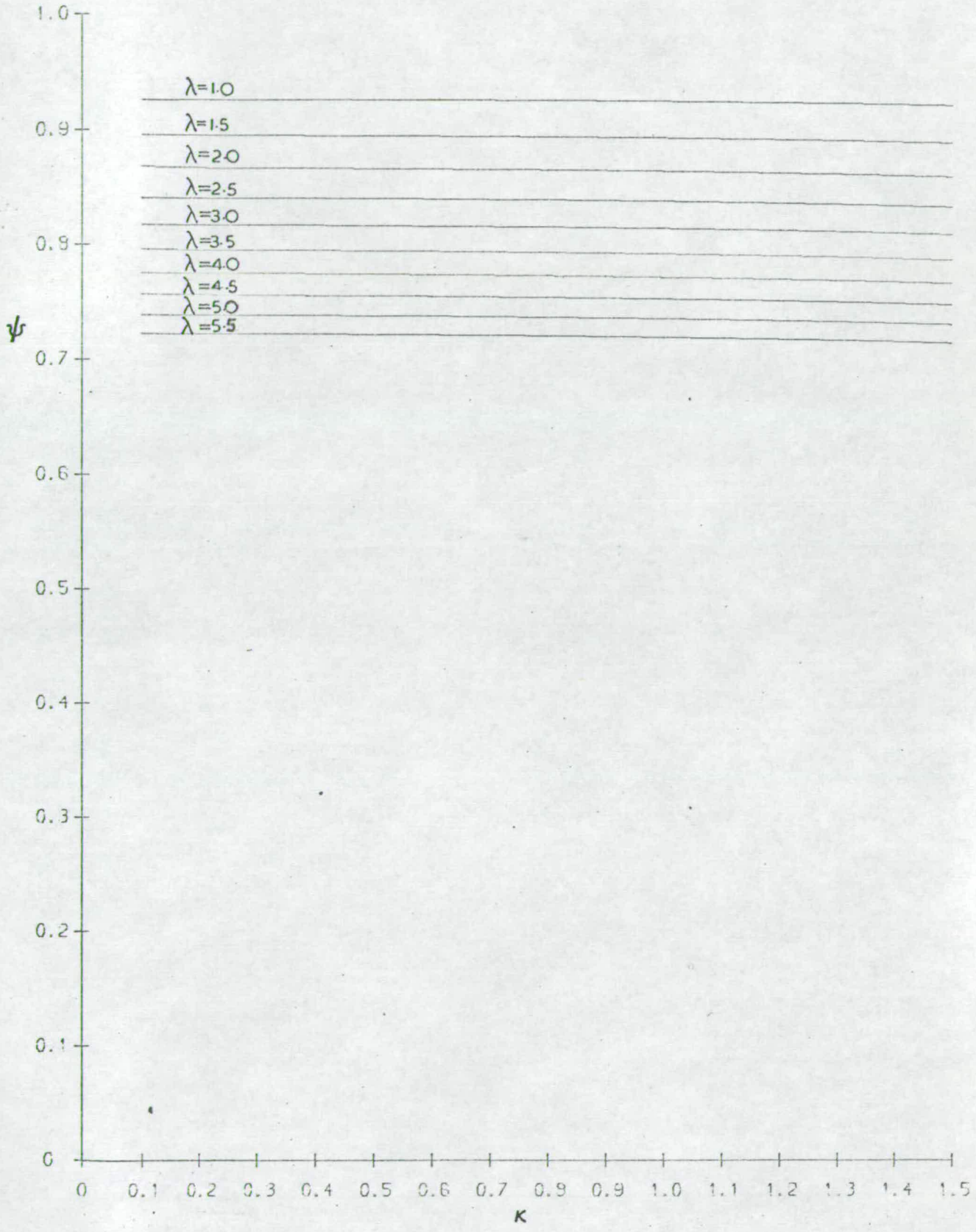

Fig. 29. Design curves, 2 girder grid. Transverse mode 2.

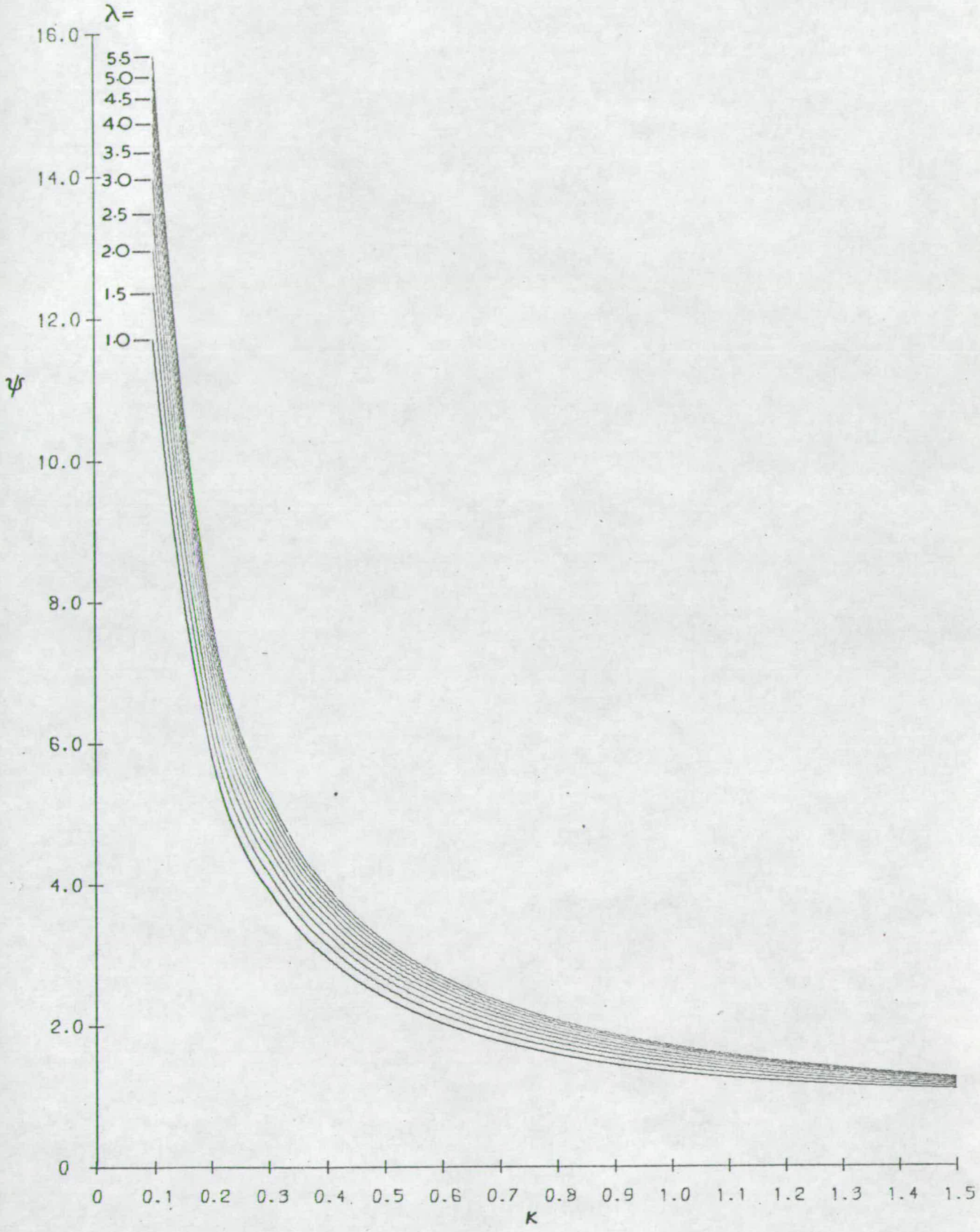

Fig. 30. Design curves, 2 girder grid. Transverse mode 3.

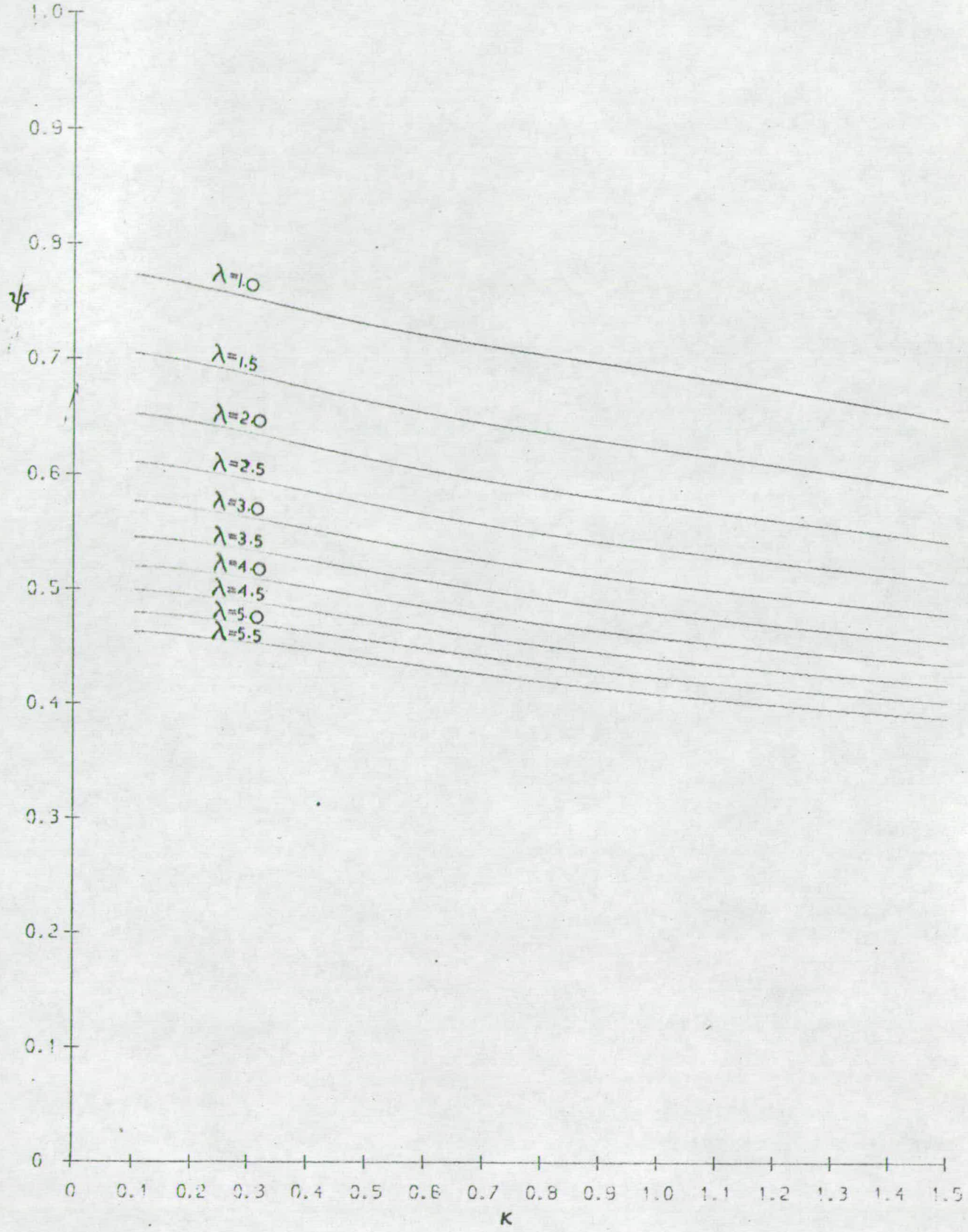

Fig. 31. Design curves, 3 girder grid. Transverse mode 1.

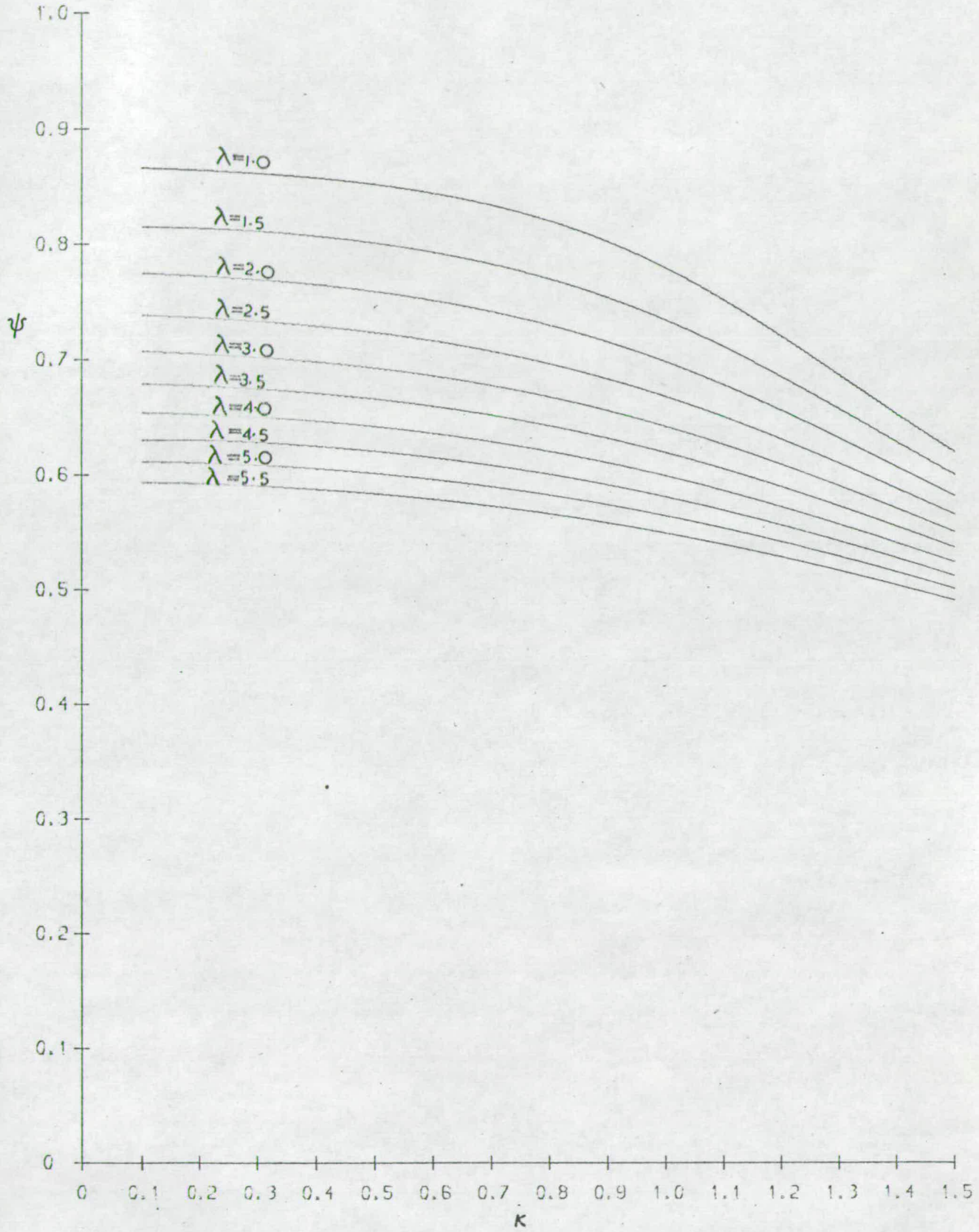

Fig. 32. Design curves, 3 girder grid. Transverse mode 2.

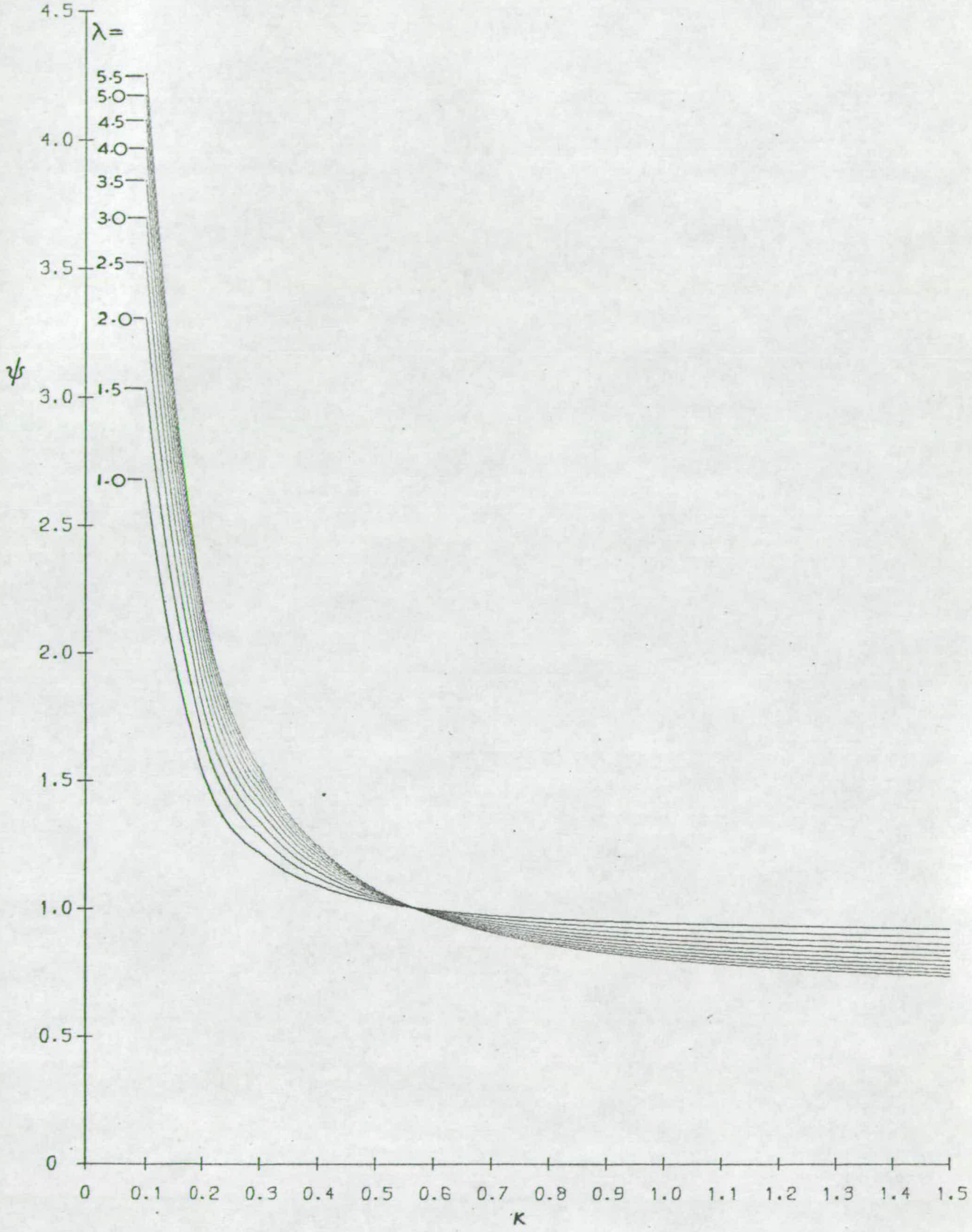

Fig. 33. Design curves, 3 girder grid. Transverse mode 3.

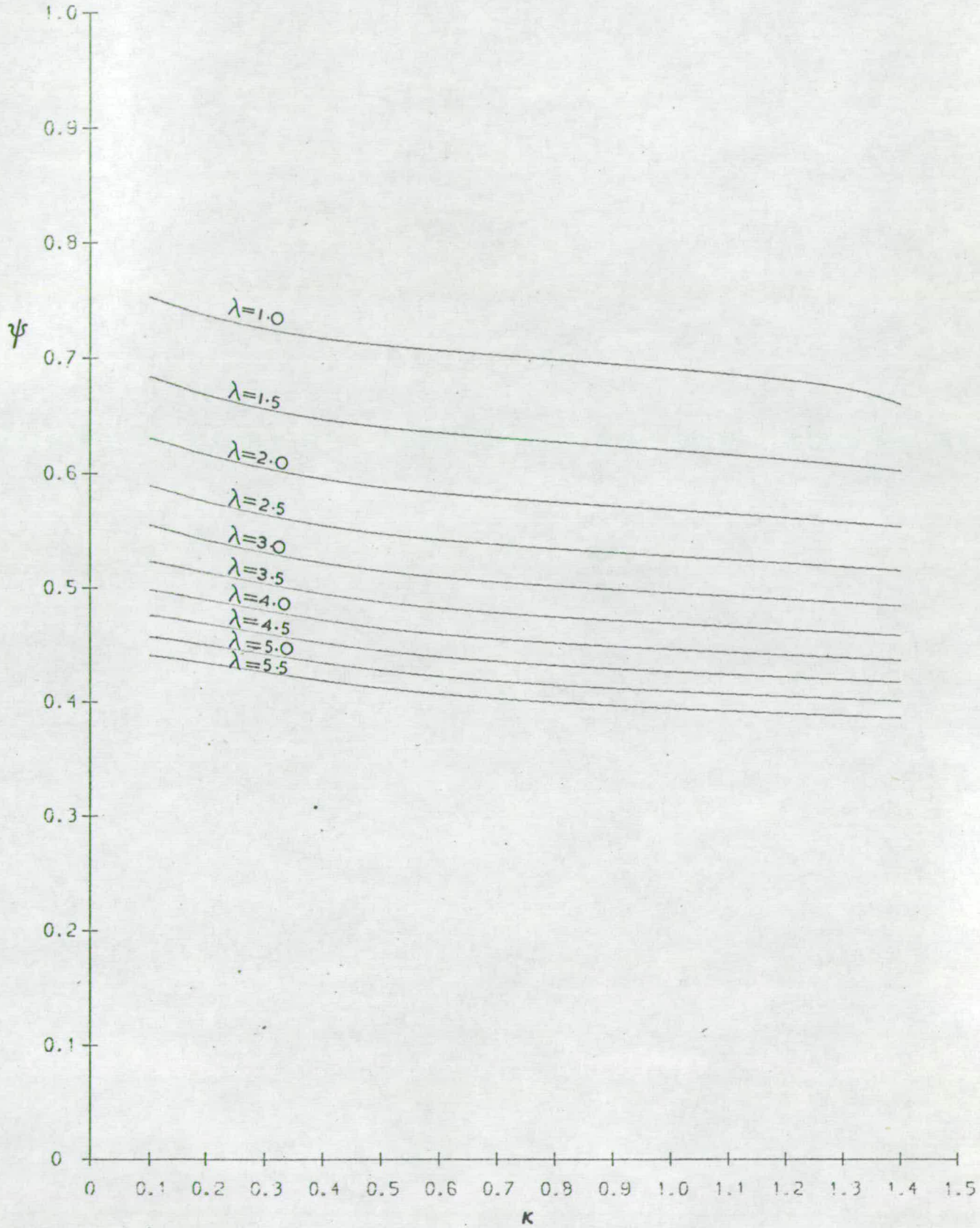

Fig. 34. Design curves, 4 girder grid. Transverse mode 1.

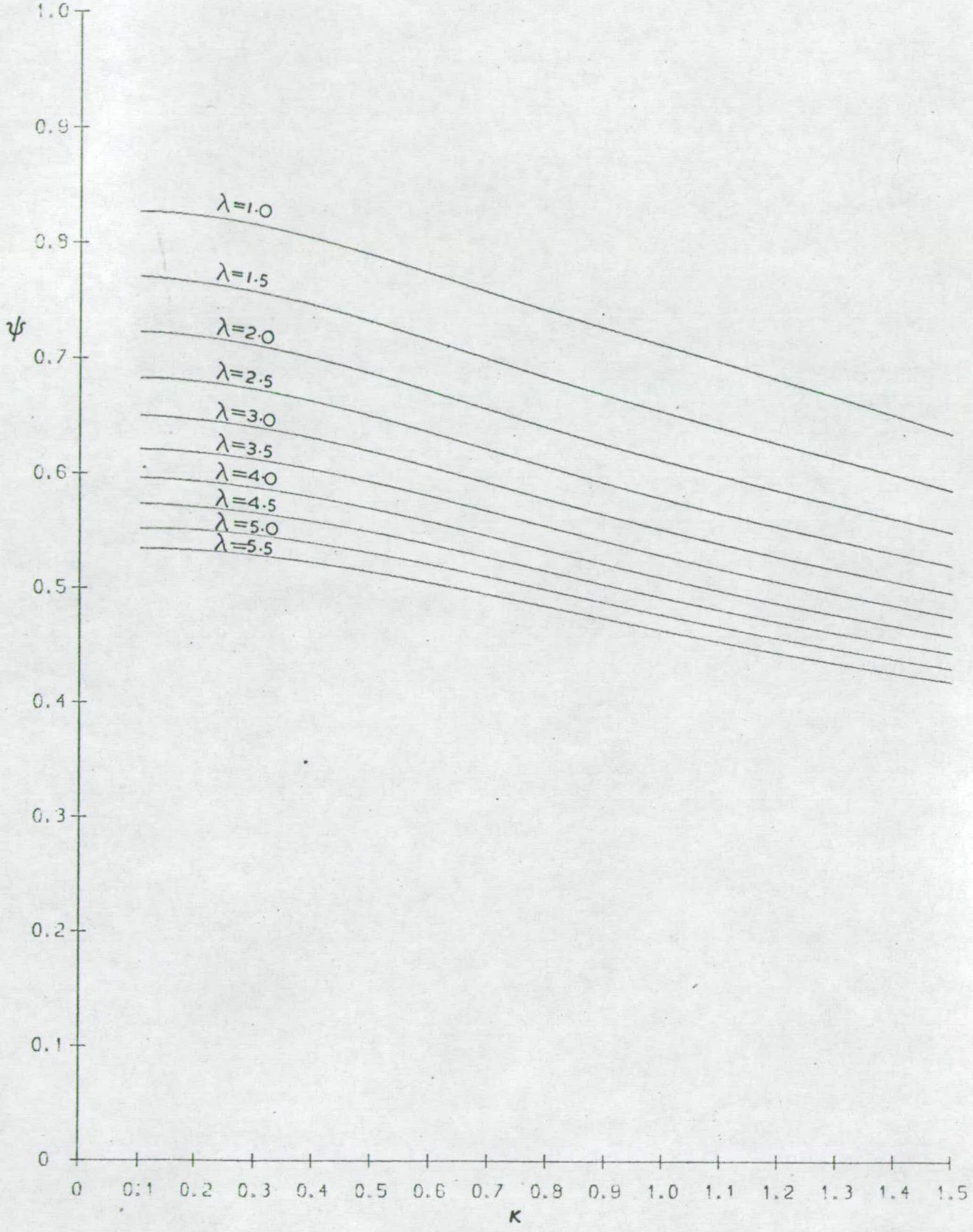

Fig. 35. Design curves, 4 girder grid. Transverse mode 2.

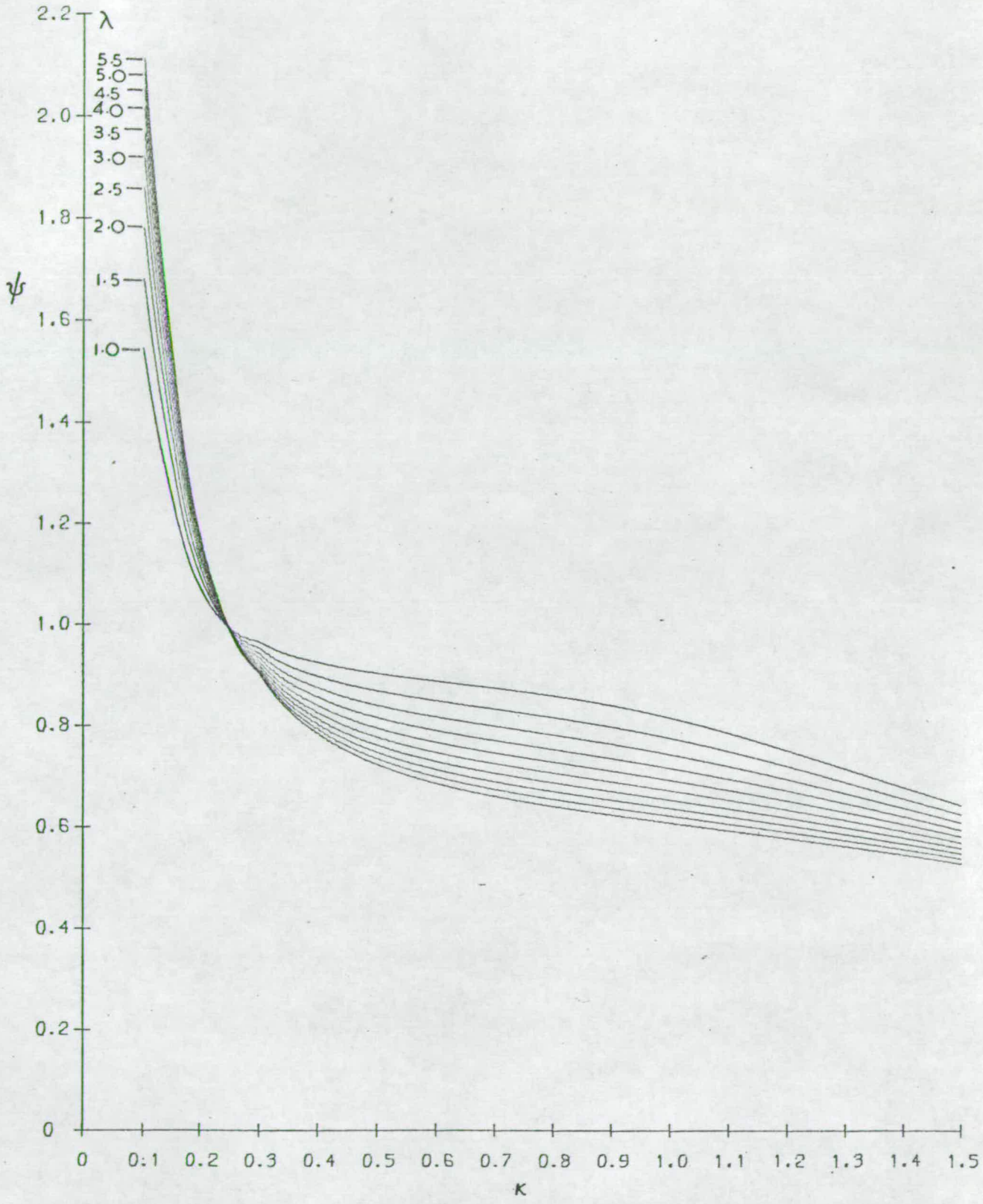

Fig. 36. Design curves, 4 girder grid. Transverse mode 3.

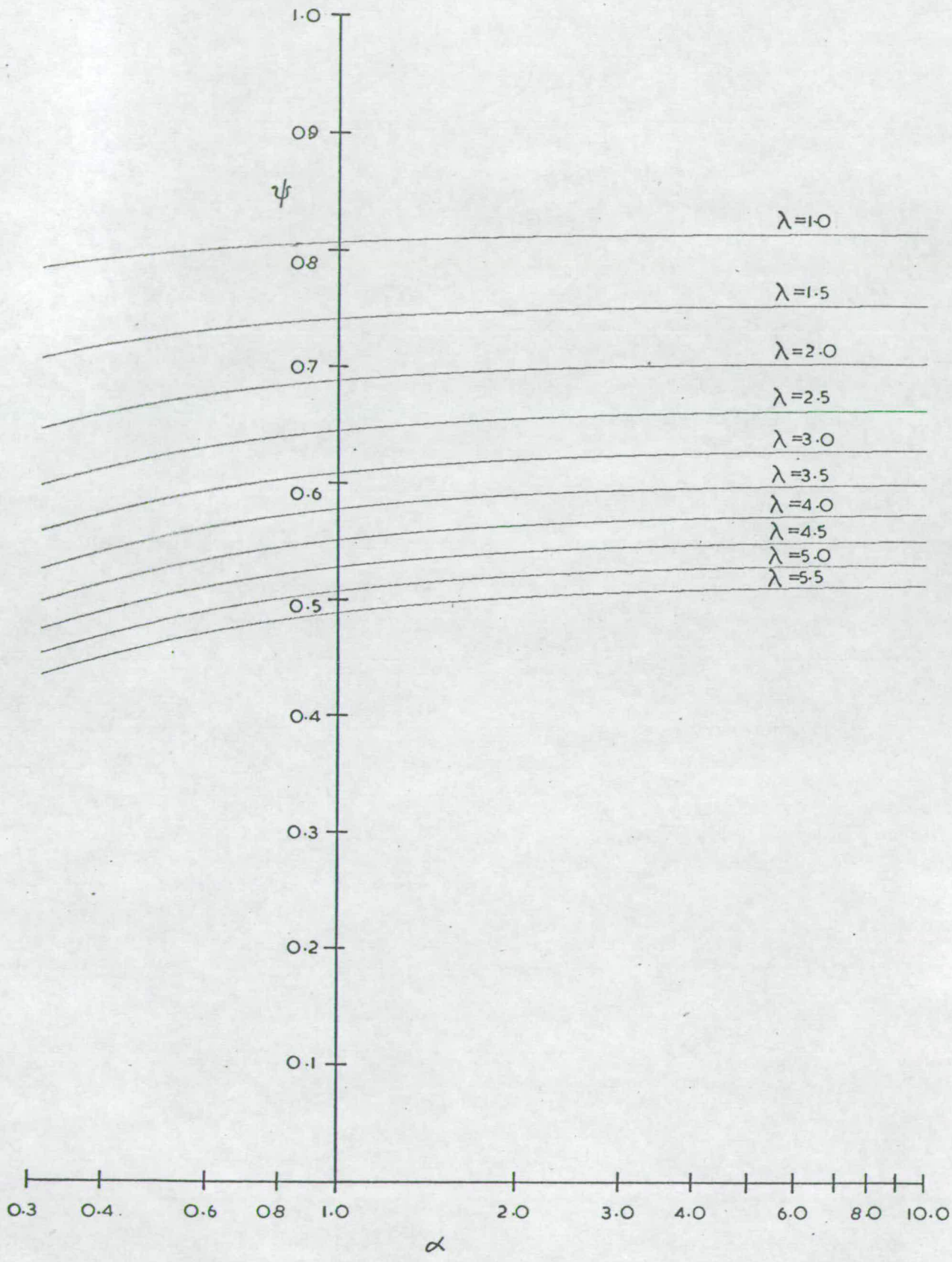

Fig. 37. Design curves, 2 girder grid. Transverse mode 1.

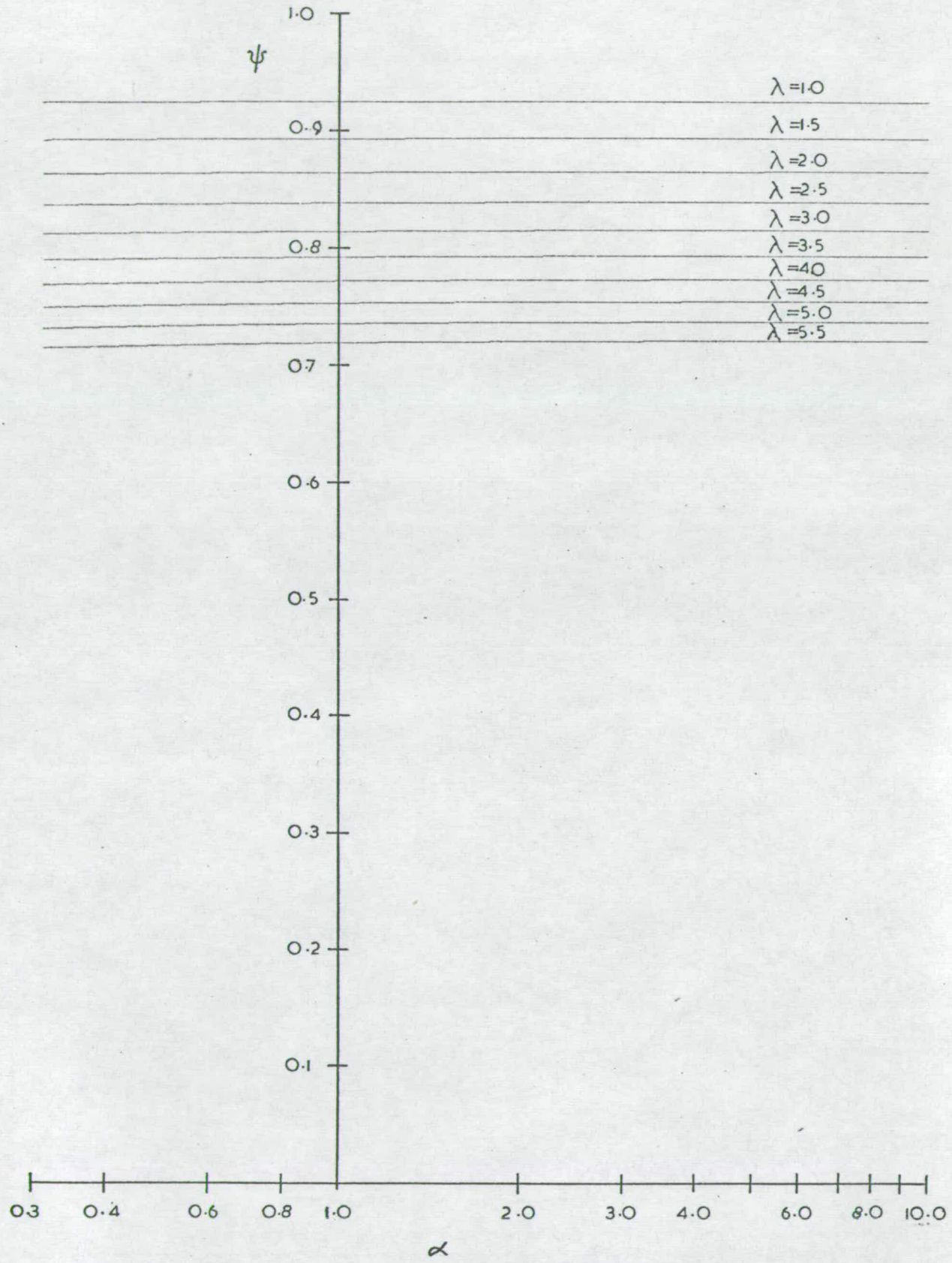

Fig. 38. Design curves, 2 girder grid. Transverse mode 2.

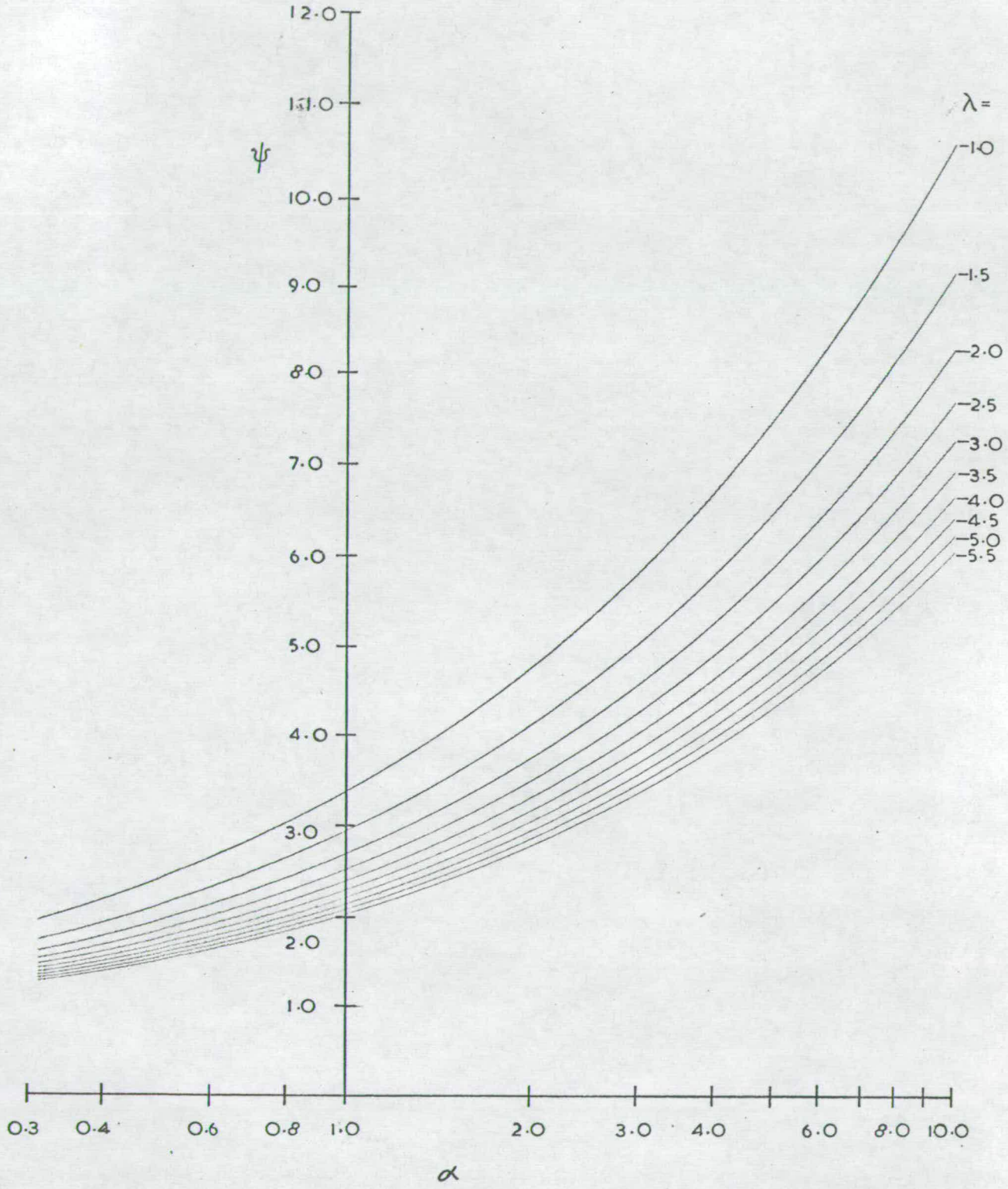

Fig. 39. Design curves, 2 girder grid. Transverse mode 3.

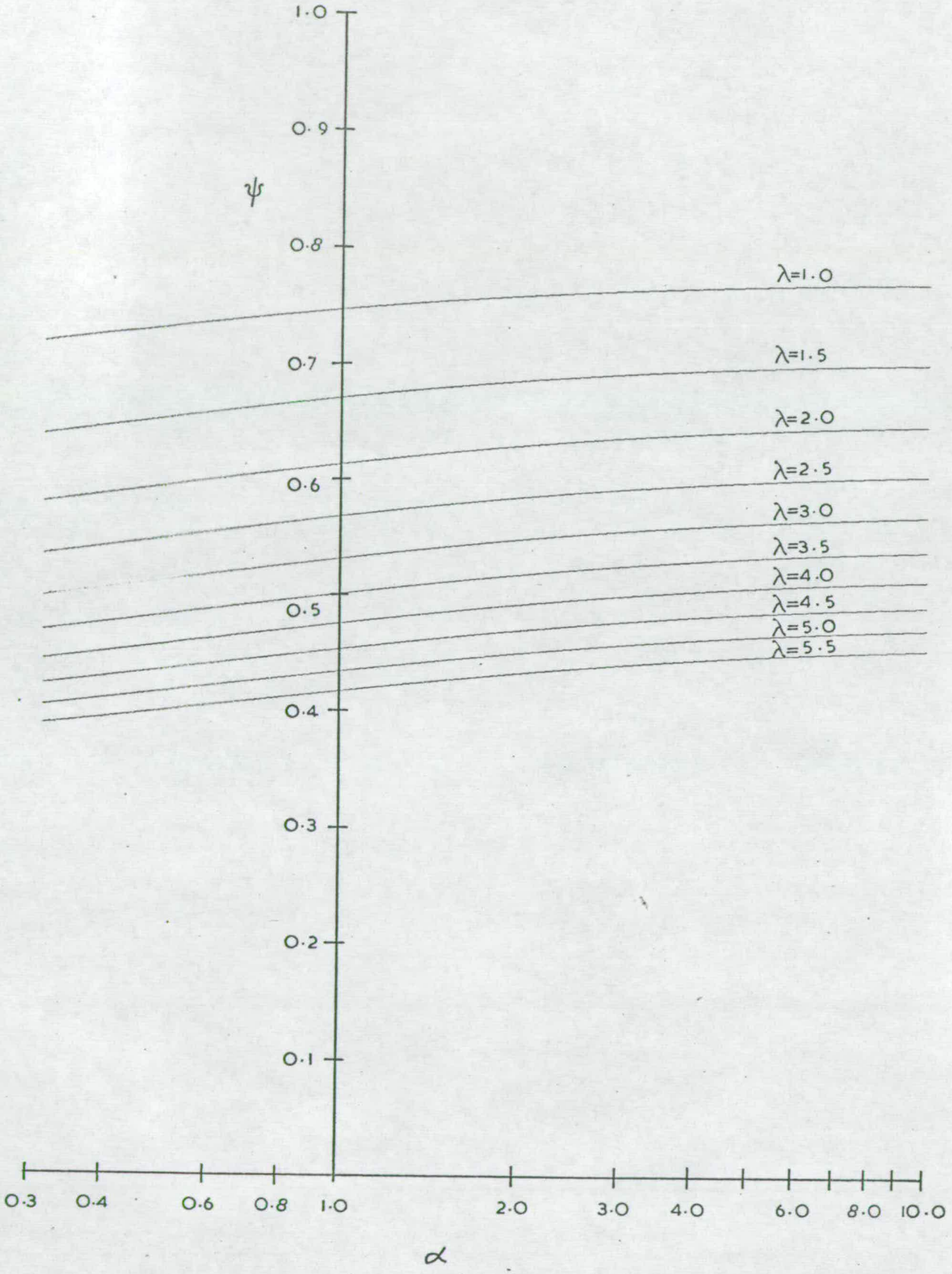

Fig. 40. Design curves, 3 girder grid. Transverse mode 1.

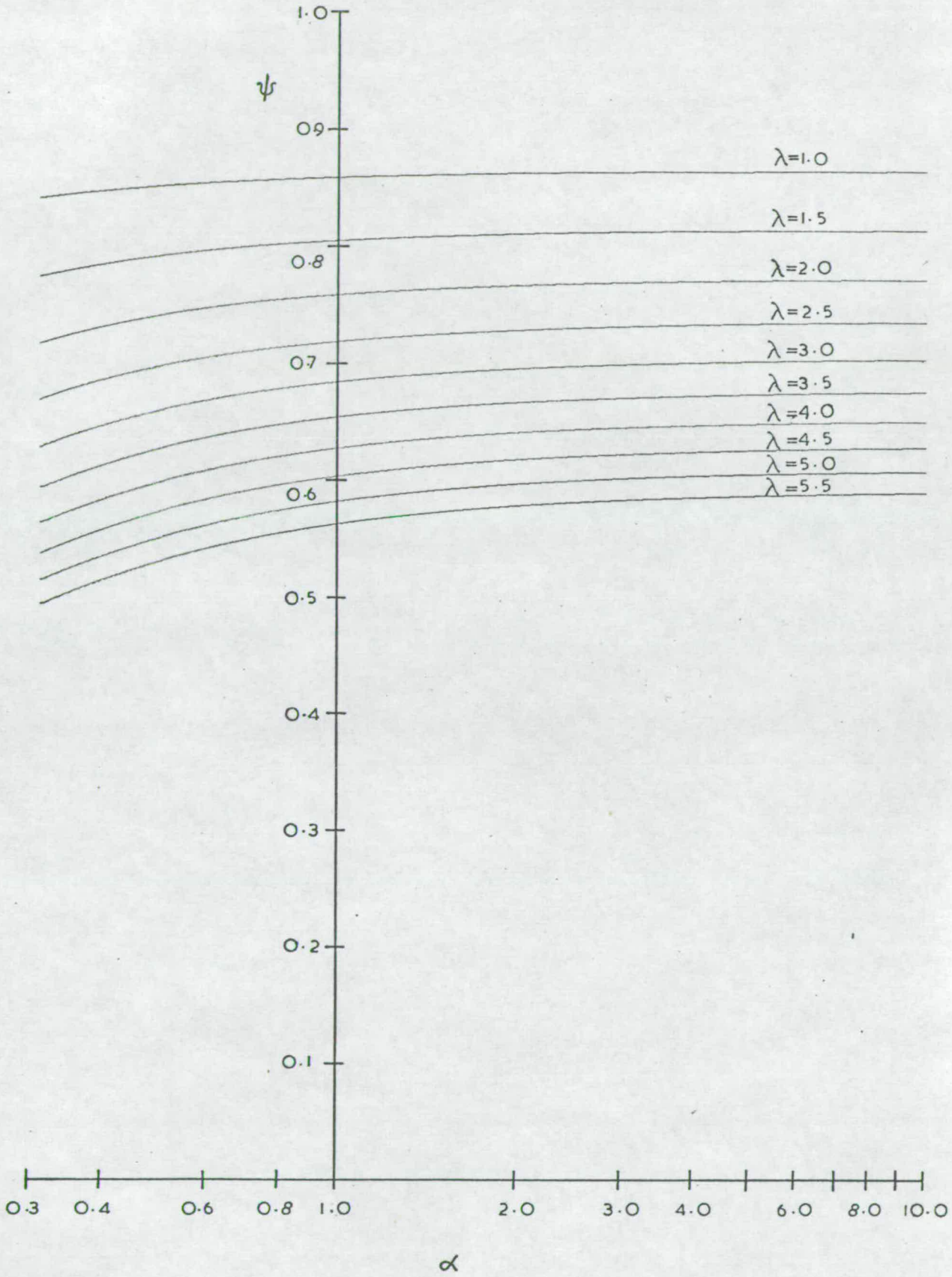

Fig. 41. Design curves, 3 girder grid. Transverse mode 2.

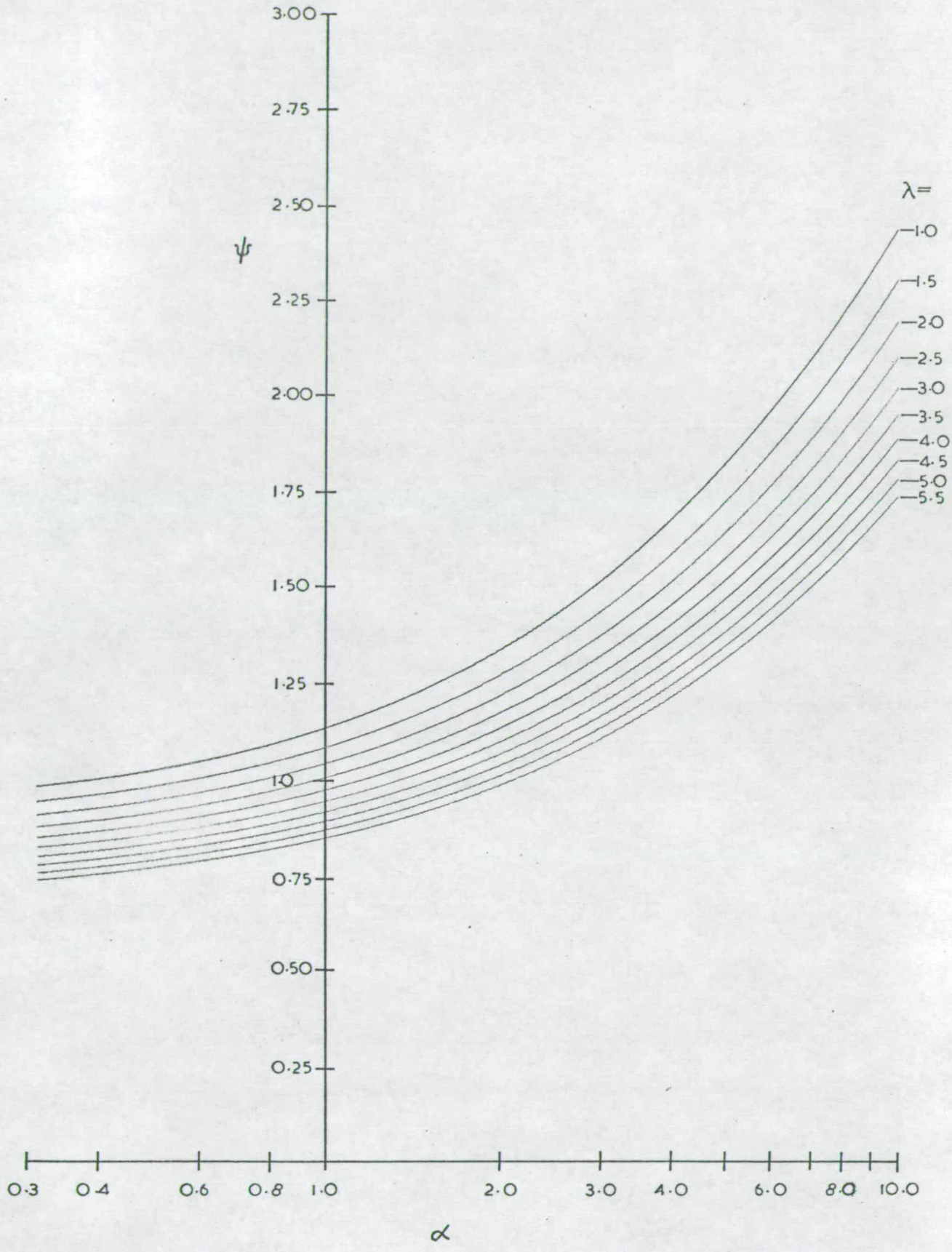

Fig. 42. Design curves, 3 girder grid. Transverse mode 3.

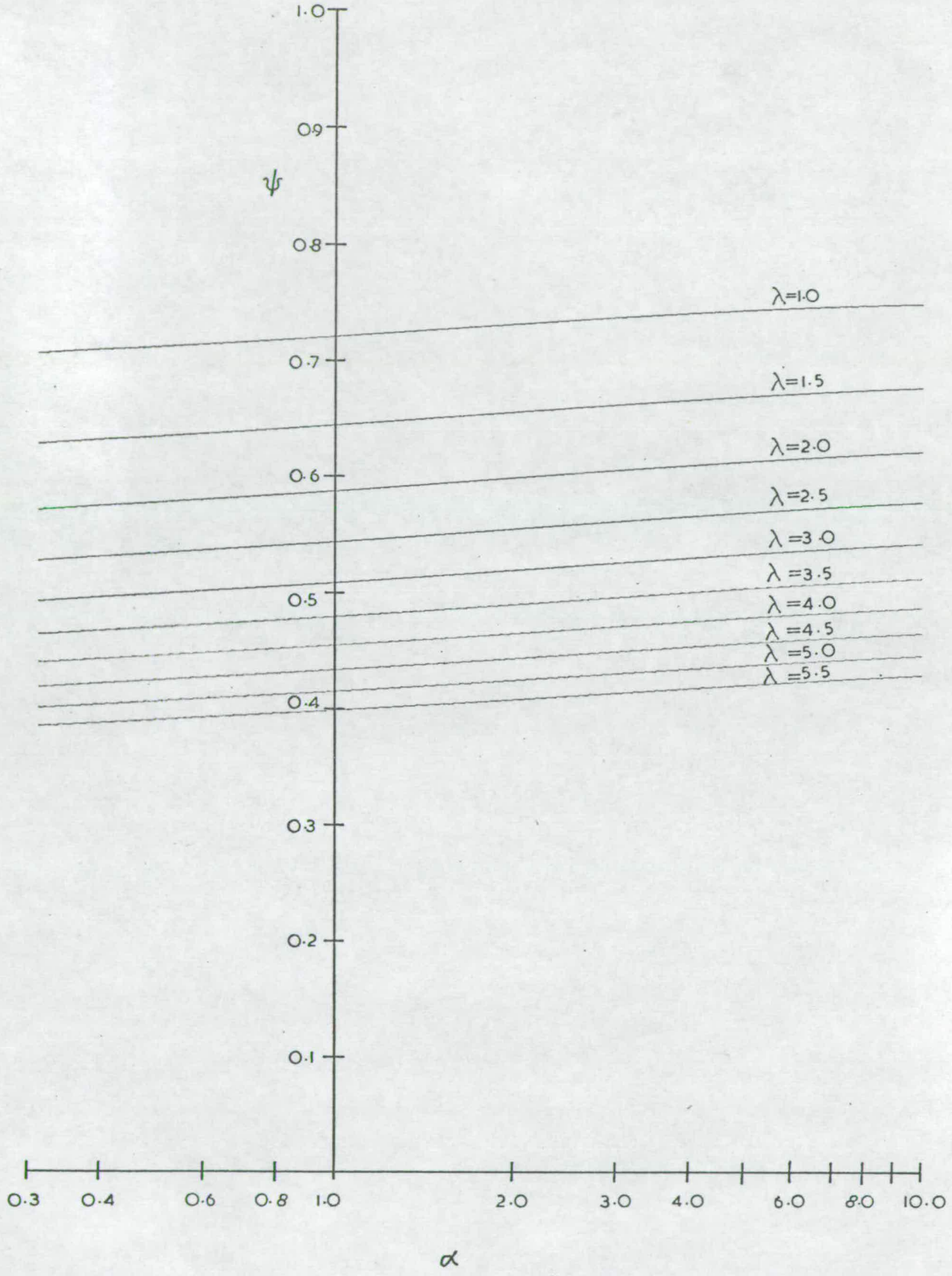

Fig. 43. Design curves, 4 girder grid. Transverse mode 1.

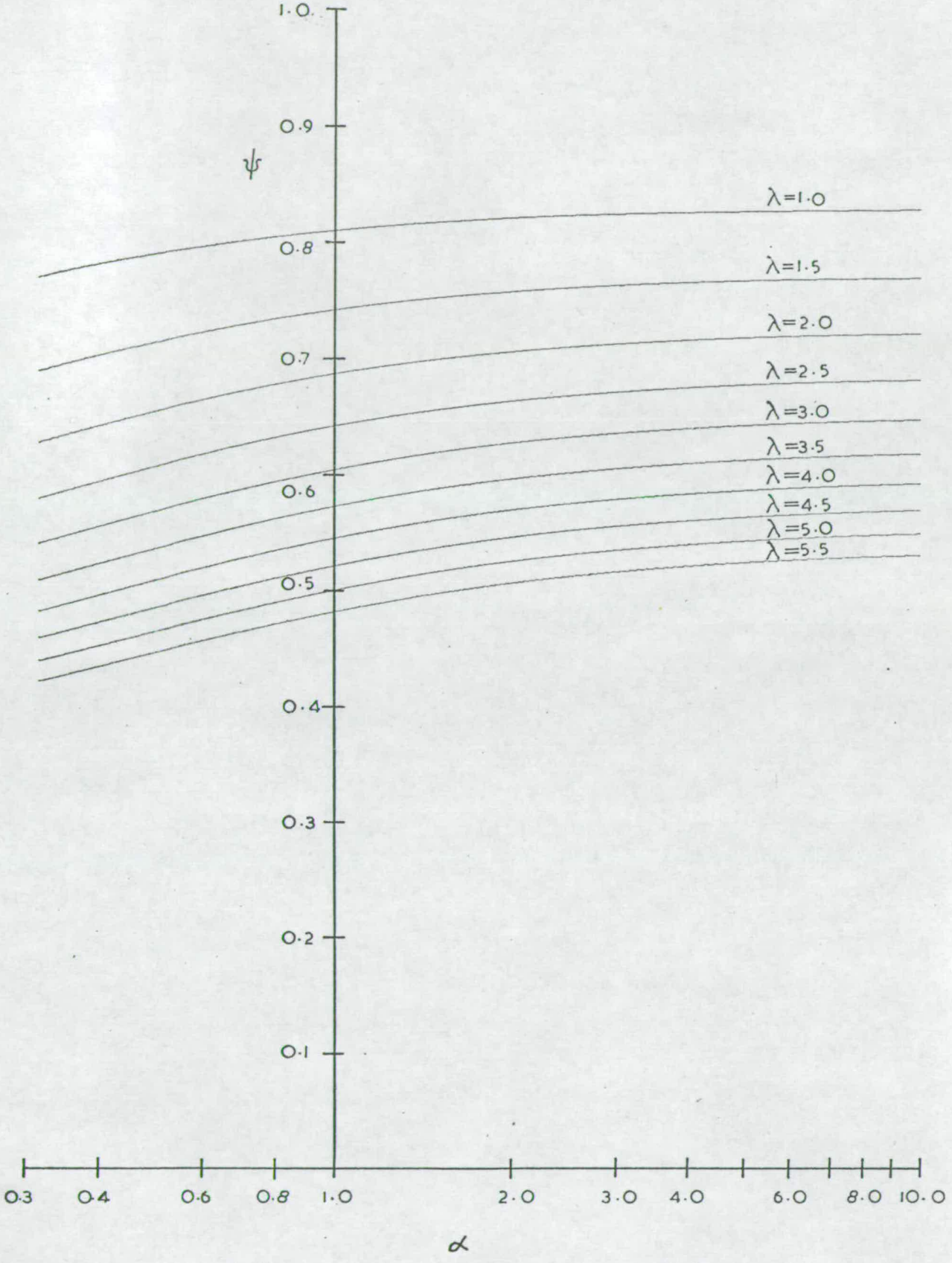

Fig. 44. Design curves, 4 girder grid. Transverse mode 2.

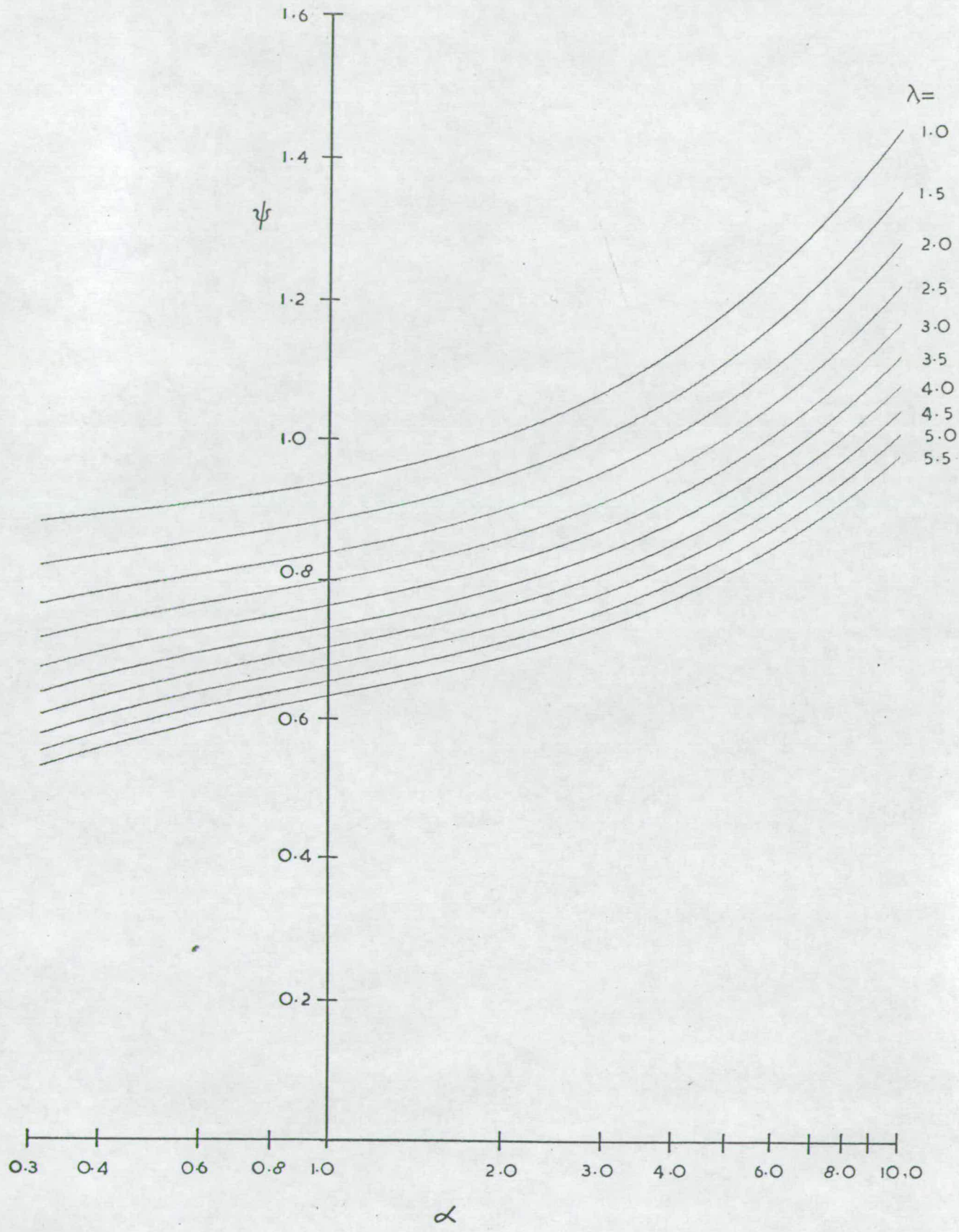

Fig. 45. Design curves, 4 girder grid. Transverse mode 3.

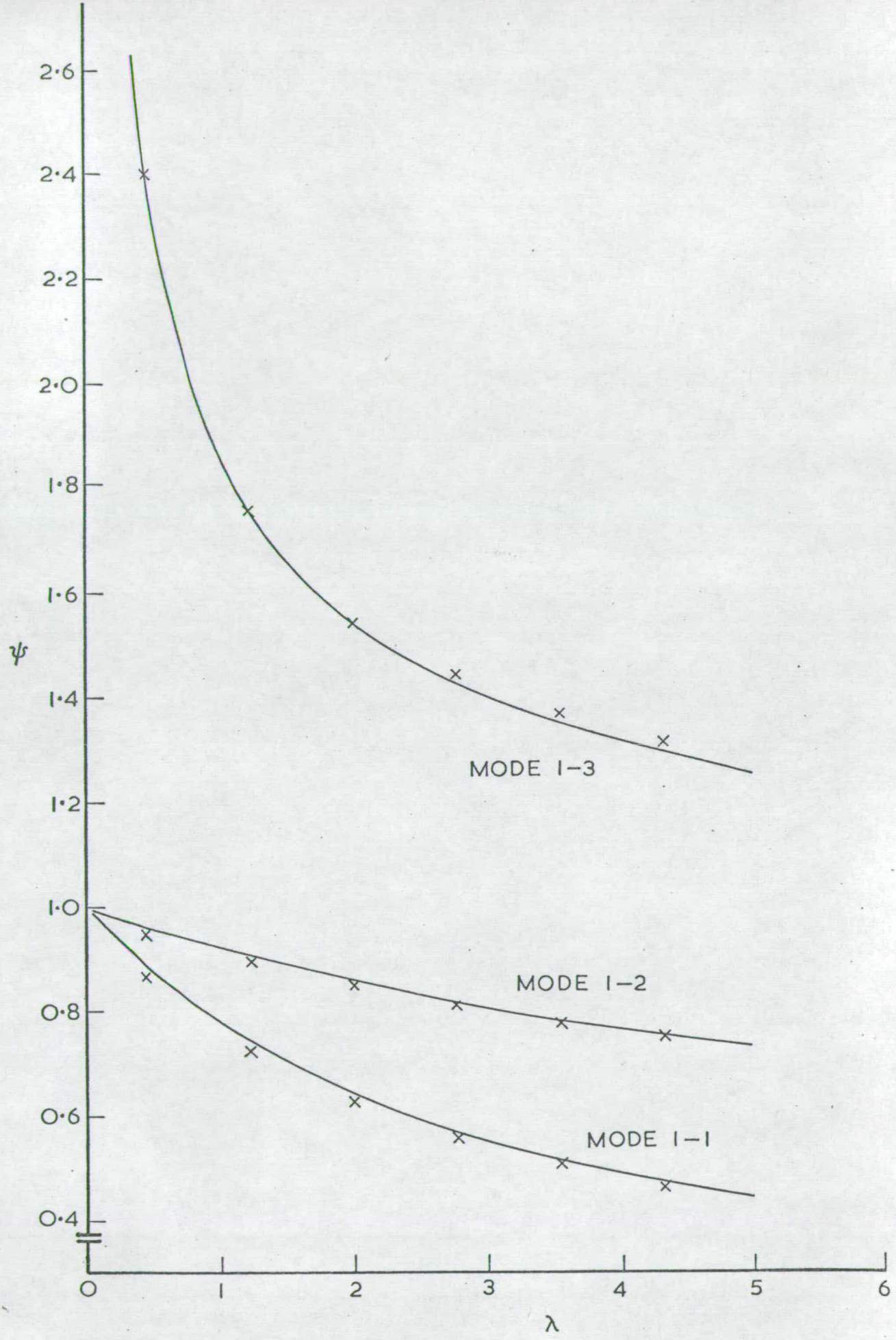

Fig. 46. Two girder grid - frequency results.

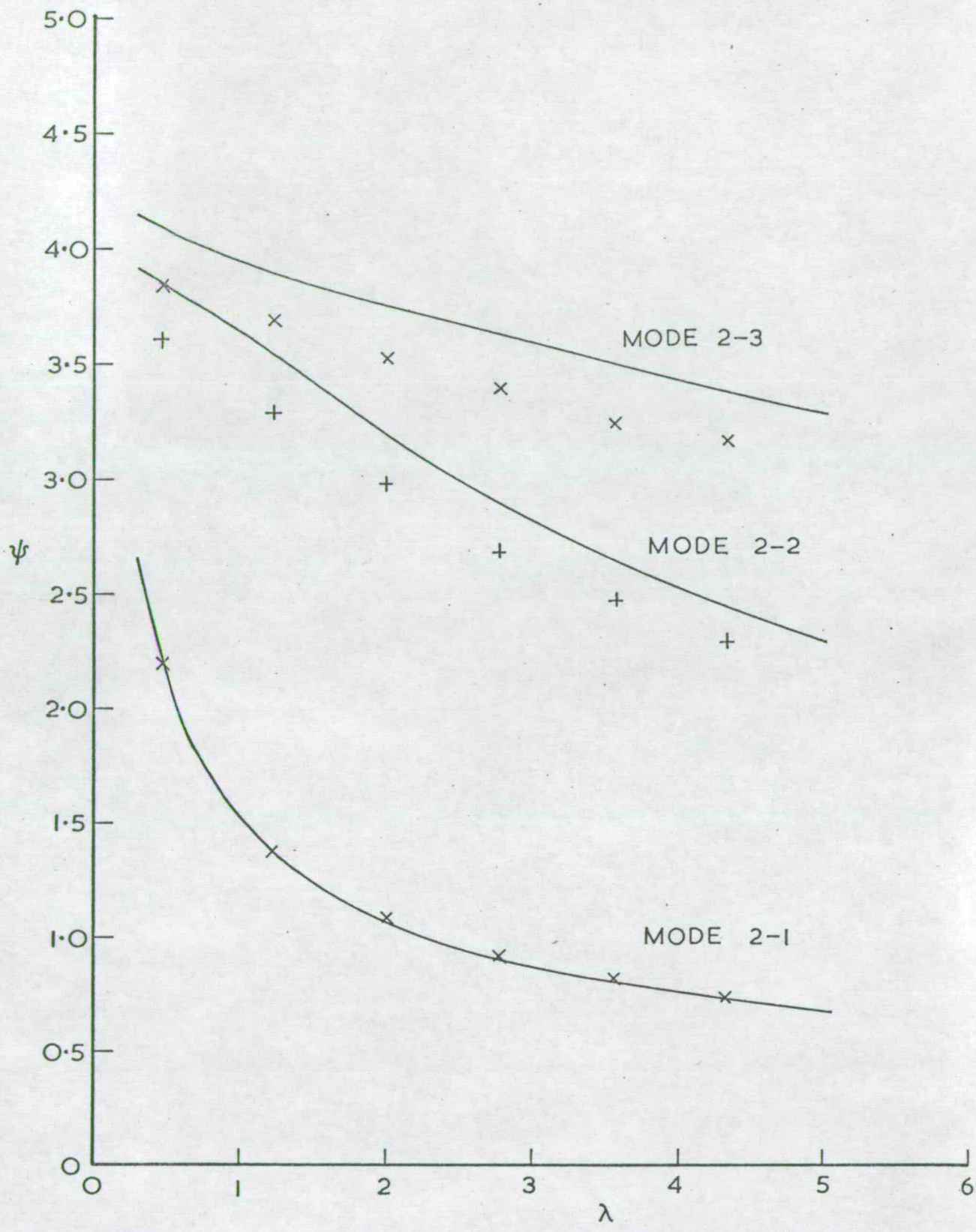

Fig. 47. Two girder grid - frequency results (continued).

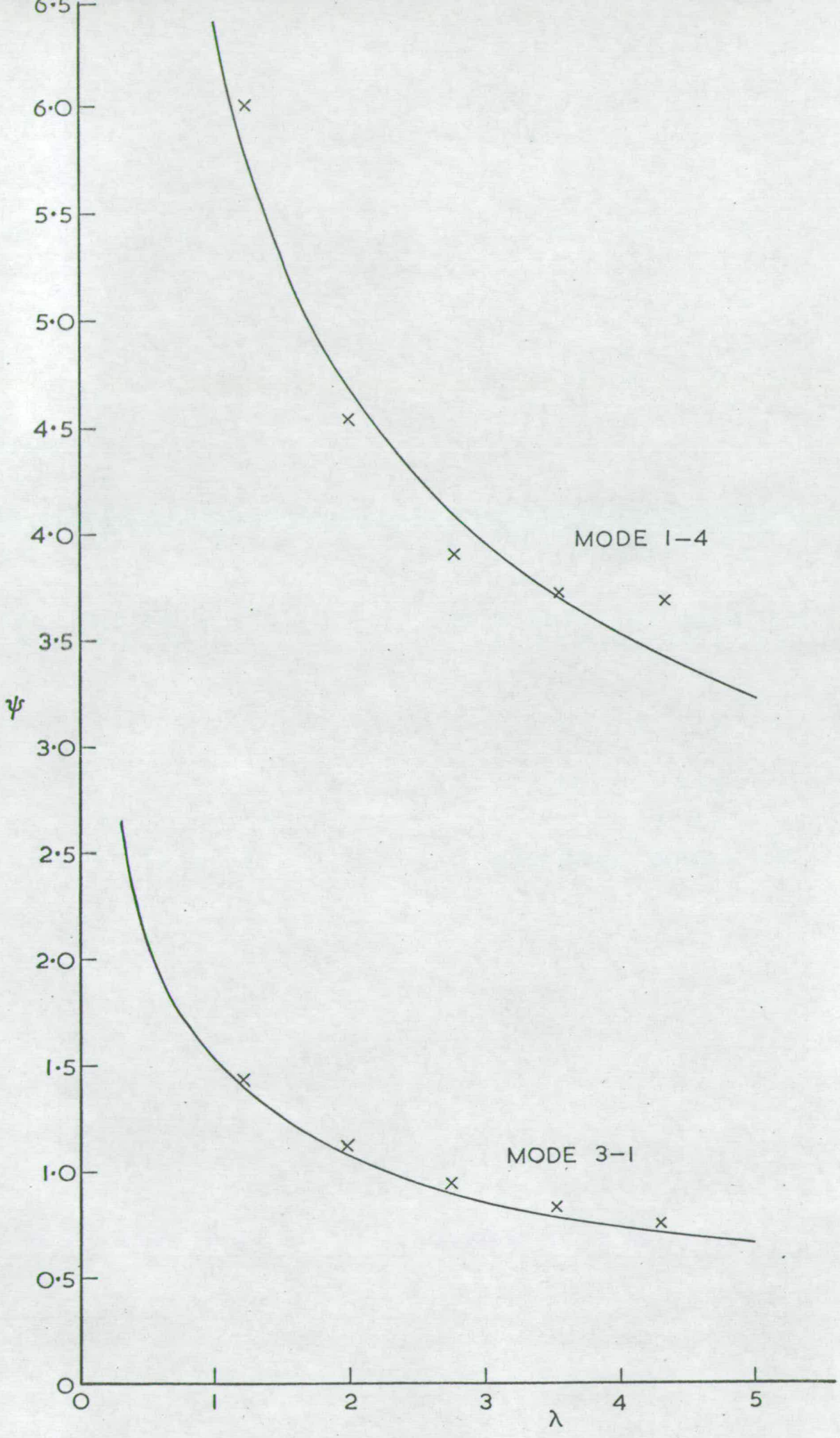

Fig. 48. Two girder grid - frequency results (contd.).

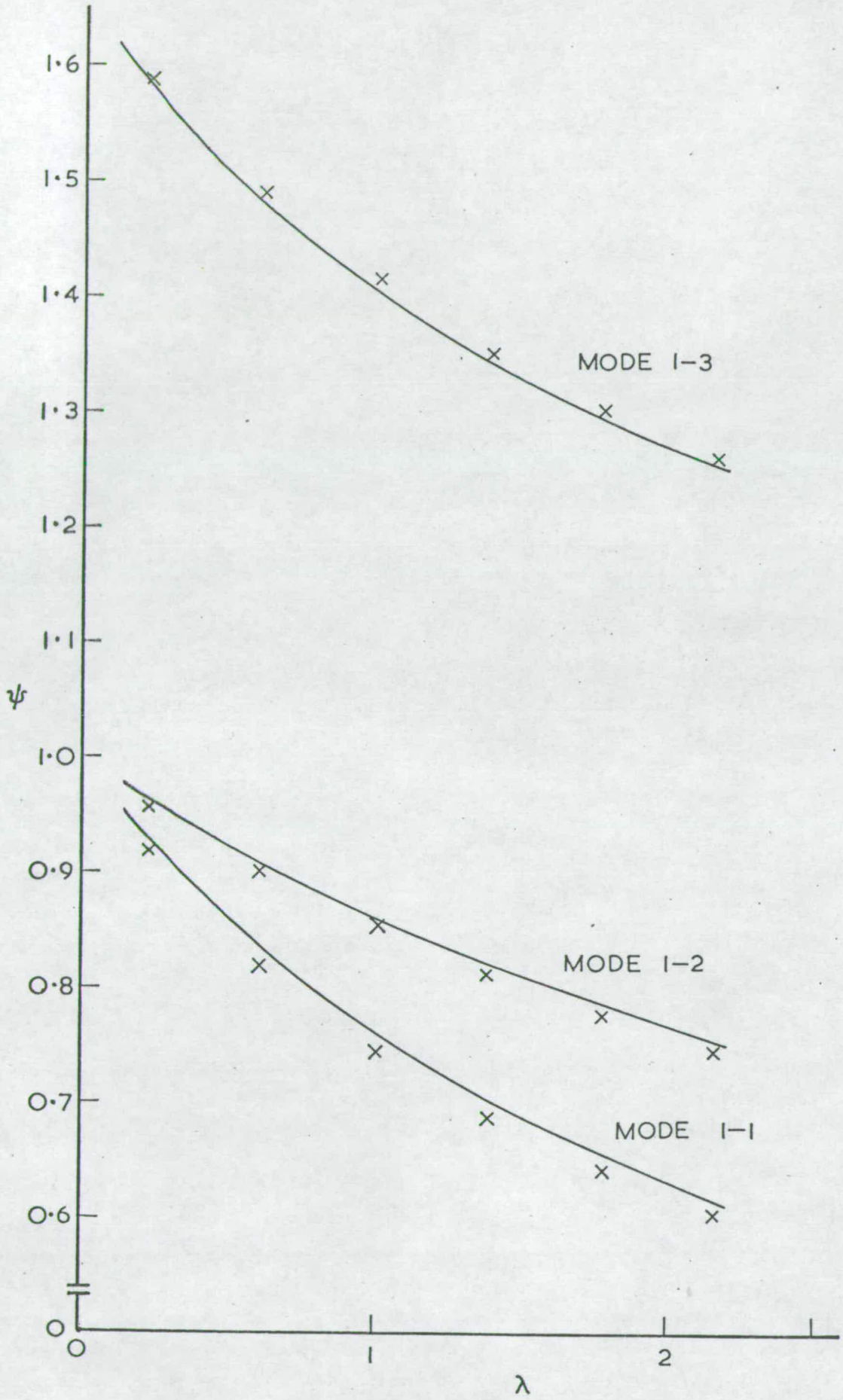

Fig. 49. Three girder grid - frequency results.

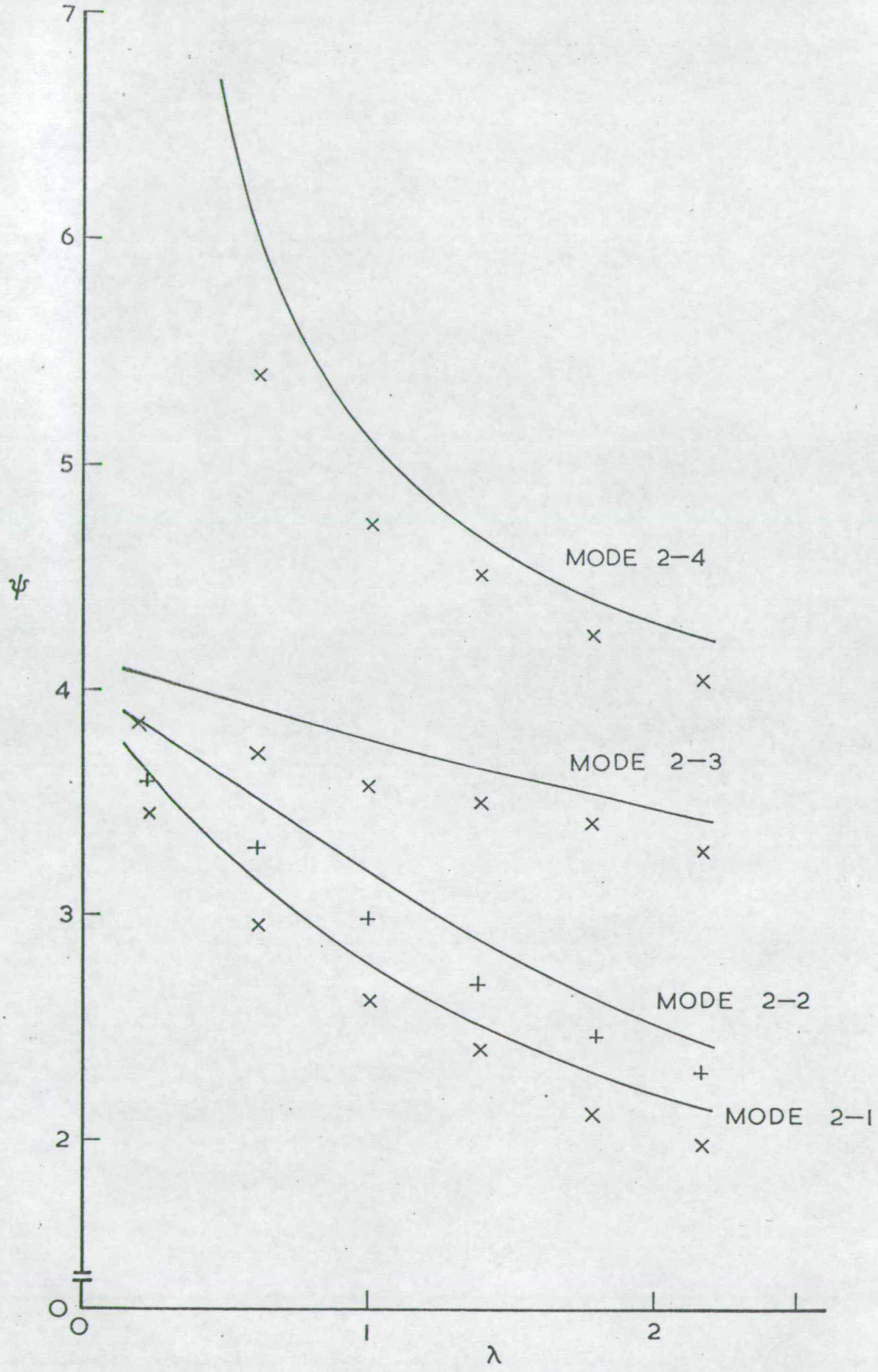

Fig. 50. Three girder grid - frequency results (contd.).

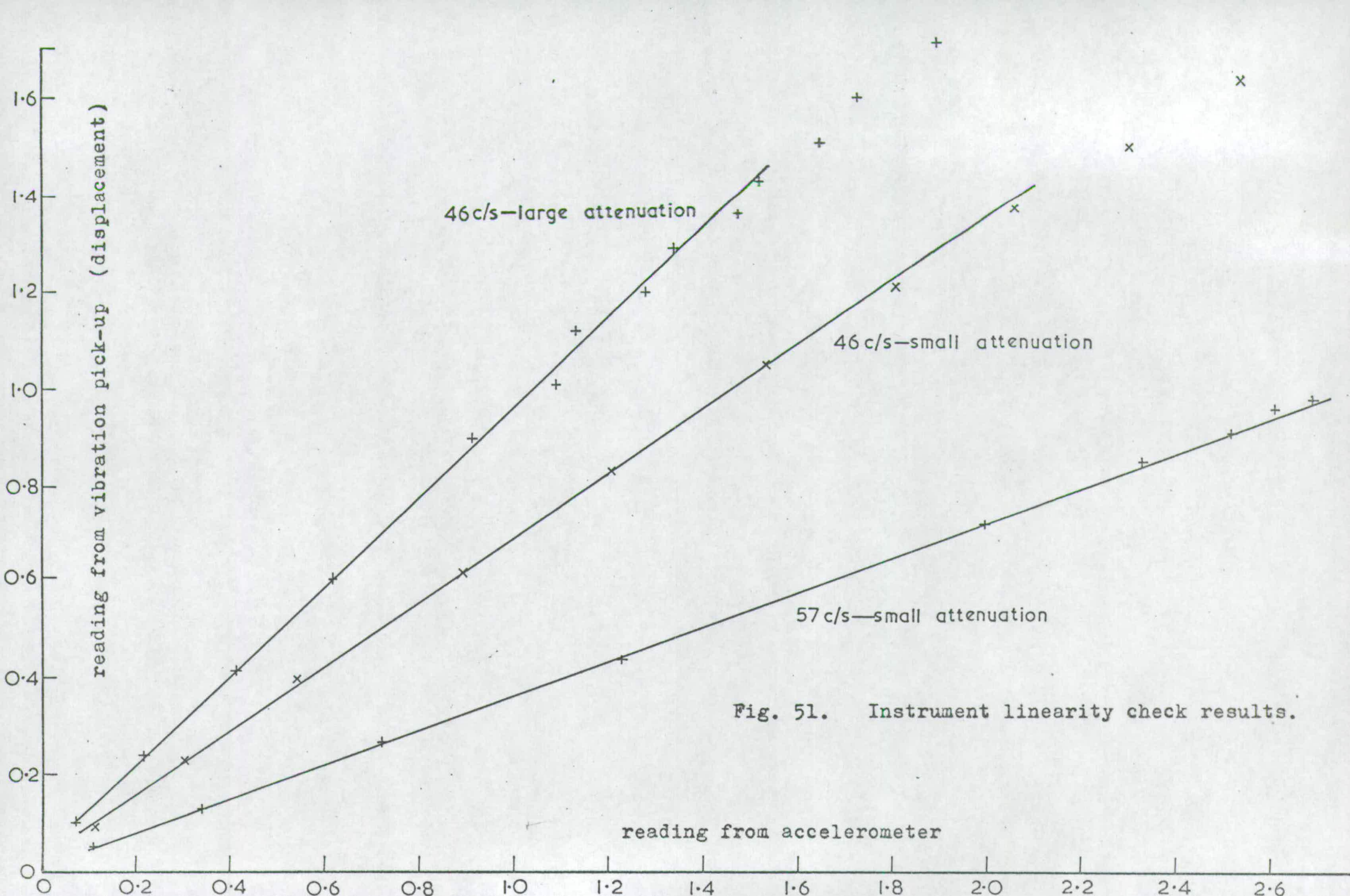

Fig. 51. Instrument linearity check results.

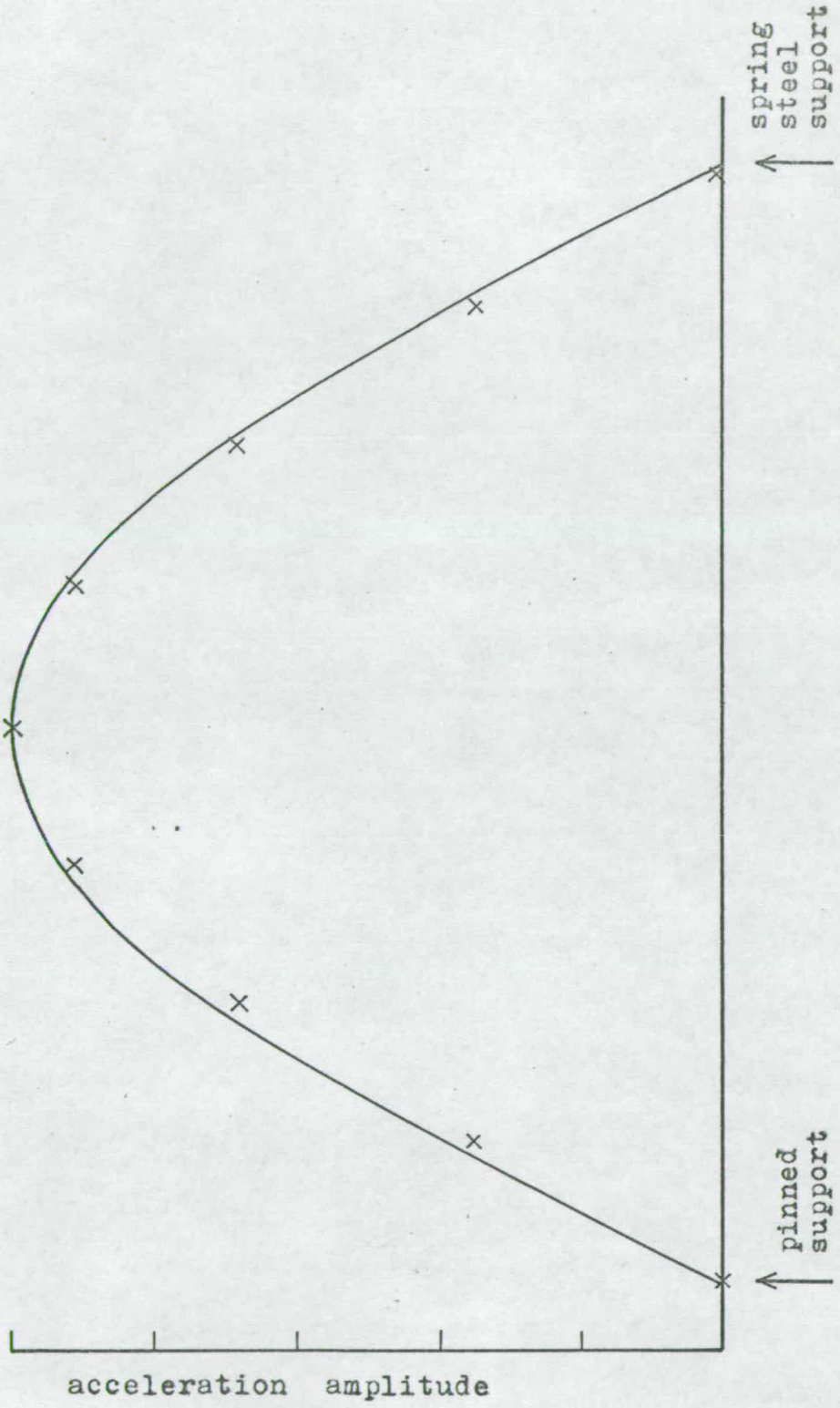

Fig. 52. Spring steel support check.

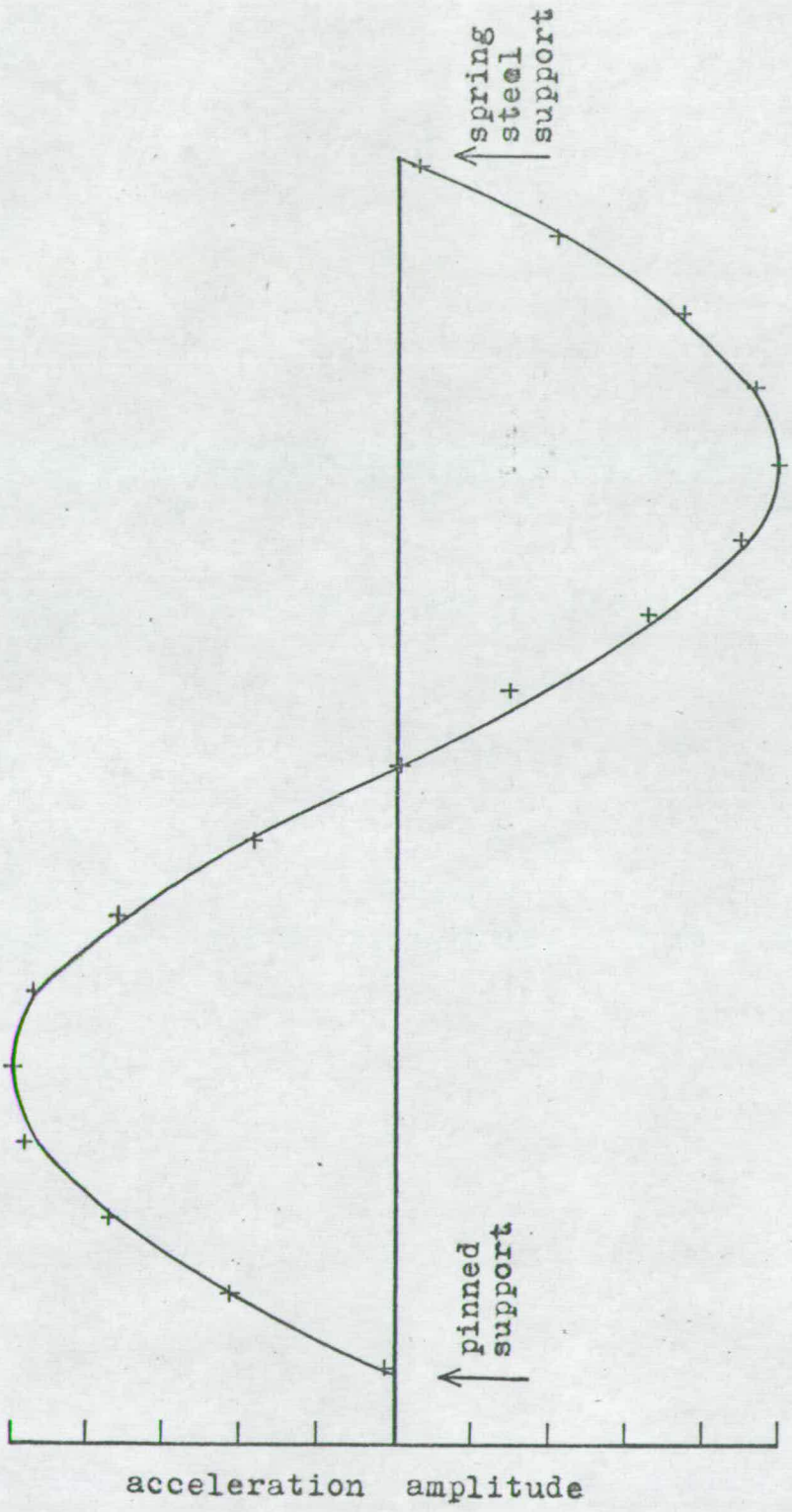

Fig. 53. Spring steel support check.

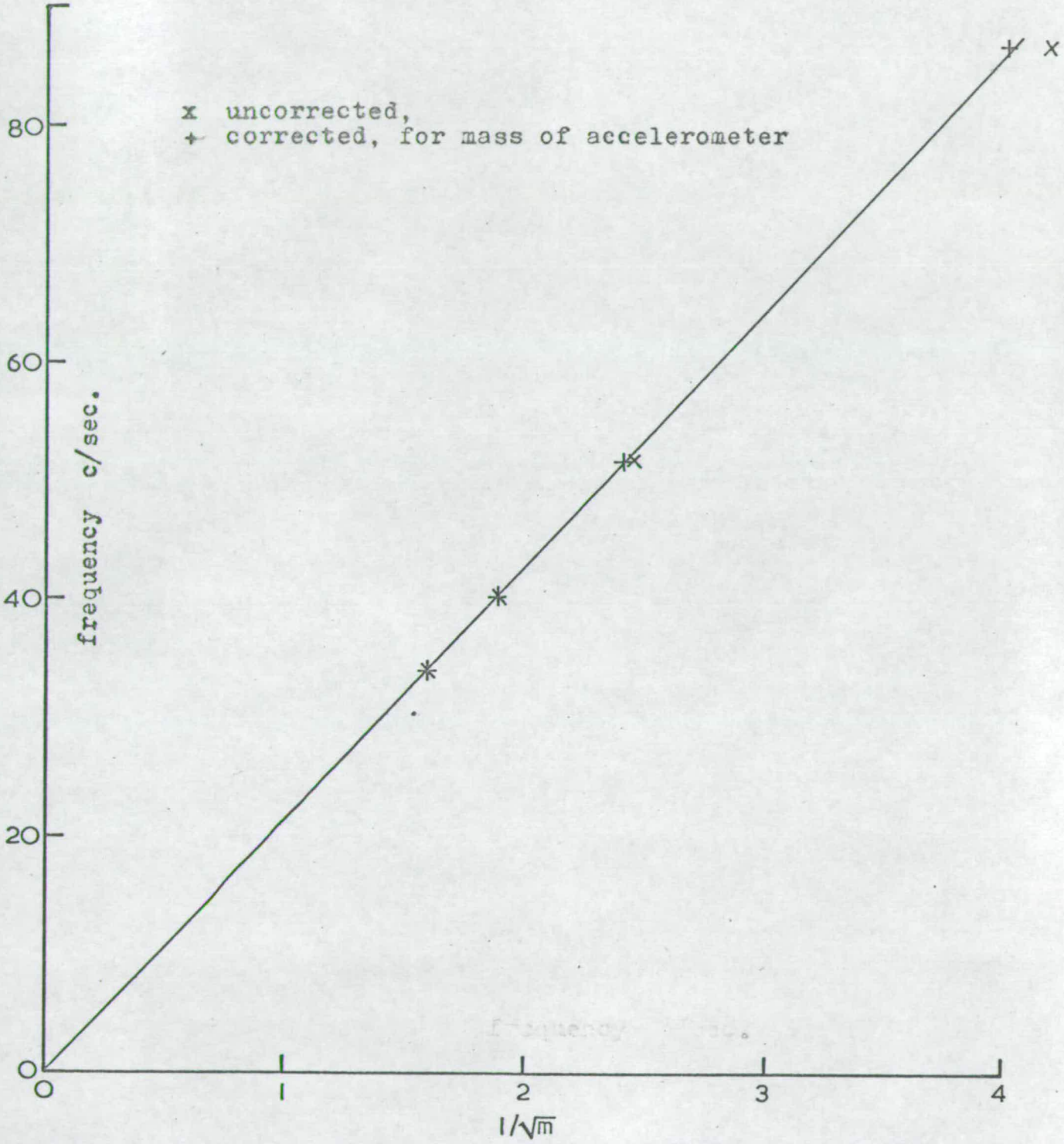

Fig. 54. Tube frequency test results

	amplitude of vibration		difference due to amplitude dependent effects
	small	large	
	Frequency (c/sec.)		
30 lead masses on top	29.22	28.72	-0.50
8 on top, 22 on side	29.01	28.40	-0.61
diff. due to rotatory inertia	-0.21	-0.32	
	Damping Factor		
No extra lead masses	0.16	–	–
30 lead masses on top	0.20	0.12	-0.08
difference due to lead masses	+0.04	–	

Fig. 55. Effects of extra lead masses on resonant frequencies and damping of the tubes.

No. of extra masses	ω_T	K	λ	mode	ψ	frequency	
						theory	observed
30	28.0	1.358	4.330	1-1	0.476	18.1	17.6
				1-2	0.755	28.7	28.7
				1-3	1.301	49.5	50.0
				1-4	3.438	130.8	140.1
				2-1	0.714	27.2	27.8
				2-2	2.440	92.8	86.5
				2-3	3.386	128.8	120.2
				3-1	0.732	27.8	29.0
24	31.0	1.226	3.556	1-1	0.517	19.6	19.3
				1-2	0.787	29.9	29.4
				1-3	1.363	51.8	51.9
				1-4	3.732	141.8	141.4
				2-1	0.791	30.1	30.8
				2-2	2.645	100.5	93.8
				2-3	3.504	133.1	123.1
				3-1	0.811	30.8	32.2
18	35.2	1.080	2.782	1-1	0.570	21.7	21.2
				1-2	0.822	31.2	30.8
				1-3	1.444	54.9	54.8
				1-4	4.140	157.0	148.6
				2-1	0.897	34.1	34.7
				2-2	2.895	110.1	101.8
				2-3	3.628	137.9	128.7
				3-1	0.920	35.0	36.3

Fig. 56. Frequency results from the 2-girder model grid tests

No. of extra masses	ω_T	K	λ	mode	ψ	frequency	
						theory	observed
12	41.2	0.923	2.007	1-1	0.640	24.4	23.9
				1-2	0.863	32.8	32.3
				1-3	1.550	59.0	58.6
				1-4	4.720	179.4	172.4
				2-1	1.050	39.9	40.9
				2-2	3.187	121.1	113.0
				2-3	3.758	142.8	133.8
				3-1	1.077	40.9	42.9
6	52.8	0.719	1.233	1-1	0.742	28.2	27.6
				1-2	0.909	34.5	34.1
				1-3	1.773	67.3	66.8
				1-4	5.884	223.6	228.2
				2-1	1.345	51.1	52.0
				2-2	3.522	133.8	124.7
				2-3	3.903	148.3	140.0
				3-1	1.382	52.5	54.4
0	86.8	0.438	0.459	1-1	0.890	33.8	33.1
				1-2	0.964	36.6	36.1
				1-3	2.512	95.5	91.2
				2-1	2.188	83.2	83.2
				2-2	3.833	145.7	136.9
				2-3	4.079	154.9	145.6

Fig. 56(contd.). Frequency results from the 2-girder model grid tests.

No. of extra masses	ω_T	K	λ	mode	ψ	frequency	
						theory	observed
30	112.0	0.339	2.165	1-1	0.617	23.4	22.9
				1-2	0.755	28.7	28.3
				1-3	1.258	47.8	47.9
				2-1	2.151	81.7	75.7
				2-2	2.442	92.8	87.6
				2-3	3.438	130.6	125.1
				2-4	4.240	161.1	153.6
24	124.0	0.306	1.778	1-1	0.656	24.9	24.4
				1-2	0.787	29.9	29.5
				1-3	1.302	49.5	49.5
				2-1	2.313	87.9	80.5
				2-2	2.647	100.6	93.5
				2-3	3.545	134.7	129.2
				2-4	4.430	168.3	161.4
18	140.8	0.270	1.391	1-1	0.703	26.7	26.1
				1-2	0.822	31.2	30.8
				1-3	1.350	51.3	51.3
				2-1	2.516	95.6	91.2
				2-2	2.895	110.0	102.4
				2-3	3.659	139.0	132.8
				2-4	4.695	178.4	171.4

Fig. 57. Frequency results from the 3-girder model grid tests.

No. of extra masses	ω_T	K	λ	mode	ψ	frequency theory	frequency observed
12	164.8	0.231	1.004	1-1	0.760	28.9	28.3
				1-2	0.863	32.8	32.5
				1-3	1.400	53.2	53.8
				2-1	2.777	105.5	99.6
				2-2	3.186	121.1	113.3
				2-3	3.779	143.6	135.5
				2-4	5.103	193.9	180.2
6	211.2	0.180	0.616	1-1	0.834	31.7	31.1
				1-2	0.909	34.5	34.2
				1-3	1.476	56.1	56.7
				2-1	3.135	119.1	112.5
				2-2	3.521	133.8	125.3
				2-3	3.913	148.7	141.1
				2-4	6.067	230.5	204.9
0	347.2	0.109	0.230	1-1	0.929	35.2	34.9
				1-2	0.964	36.6	36.3
				1-3	1.582	60.1	60.4
				2-1	3.641	138.3	131.4
				2-2	3.837	145.8	136.8
				2-3	4.044	154.5	146.2

Fig. 57(contd.). Frequency results from the 3-girder model grid tests.

No. of extra masses	mode shape ratio, E				stress ratio, F normalised w.r.t.:		
	mode 1-1		mode 1-3		longitudinal deflection		total energy
	theory	observed	theory	observed	theory	observed	theory
Two-girder grid							
30	1.91	1.81	-0.89	-0.76	2.24	6.13	1.09
24	1.85	1.64	-1.00	-0.91	2.51	7.36	1.07
18	1.77	1.56	-1.18	-1.04	2.97	10.2	1.06
12	1.68	1.60	-1.50	-1.59	3.85	17.3	1.05
6	1.51	1.49	-2.39	-2.57	6.81	33.0	1.04
0	1.23	1.17	-6.34	-34.0	33.3	45.3	1.04
Three-girder grid							
30	1.438	1.32	-0.763	-0.86	4.78	8.97	3.33
24	1.402	1.21	-0.812	-0.90	5.41	8.80	3.48
18	1.358	1.23	-0.882	-0.93	6.38	14.06	3.66
12	1.306	1.05	-0.986	-1.06	8.01	20.40	4.05
6	1.221	1.00	-1.171	-1.34	12.43	76.79	4.95
0	1.099	1.03	-1.545	-2.36	34.21	116.2	9.10

Fig. 58. Results from laboratory model grid tests.

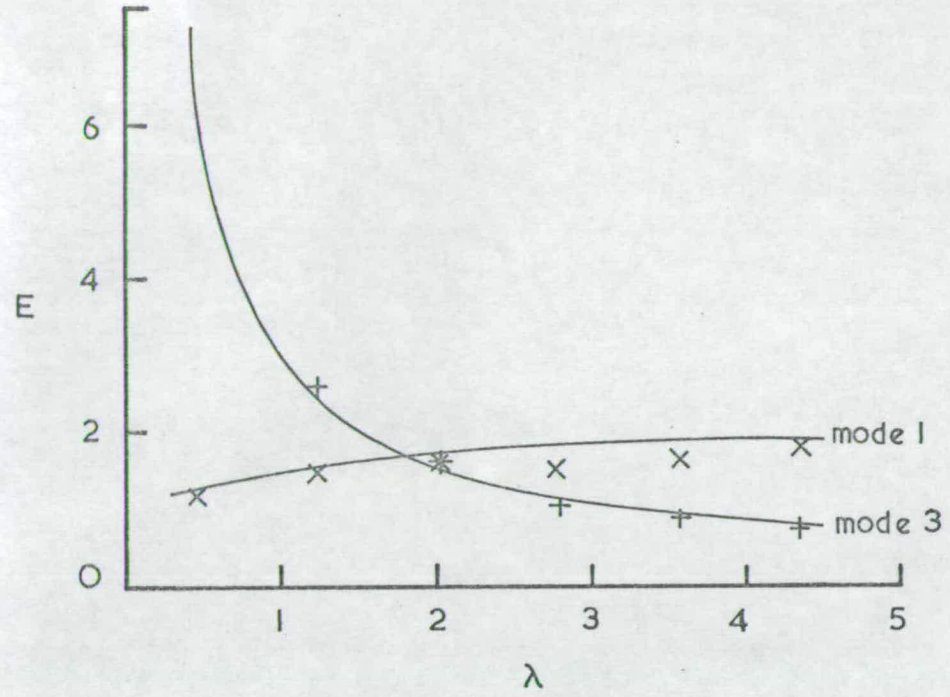

Fig. 59. Two girder grid - mode shape results.

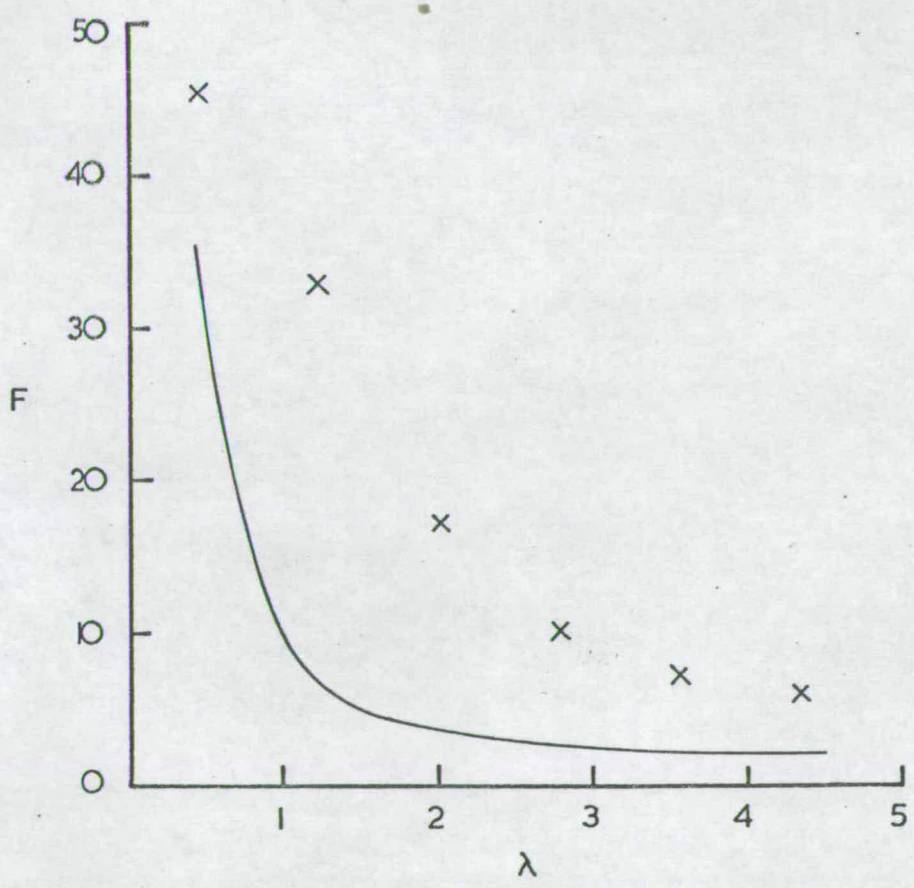

Fig. 60. Two girder grid - stress results.

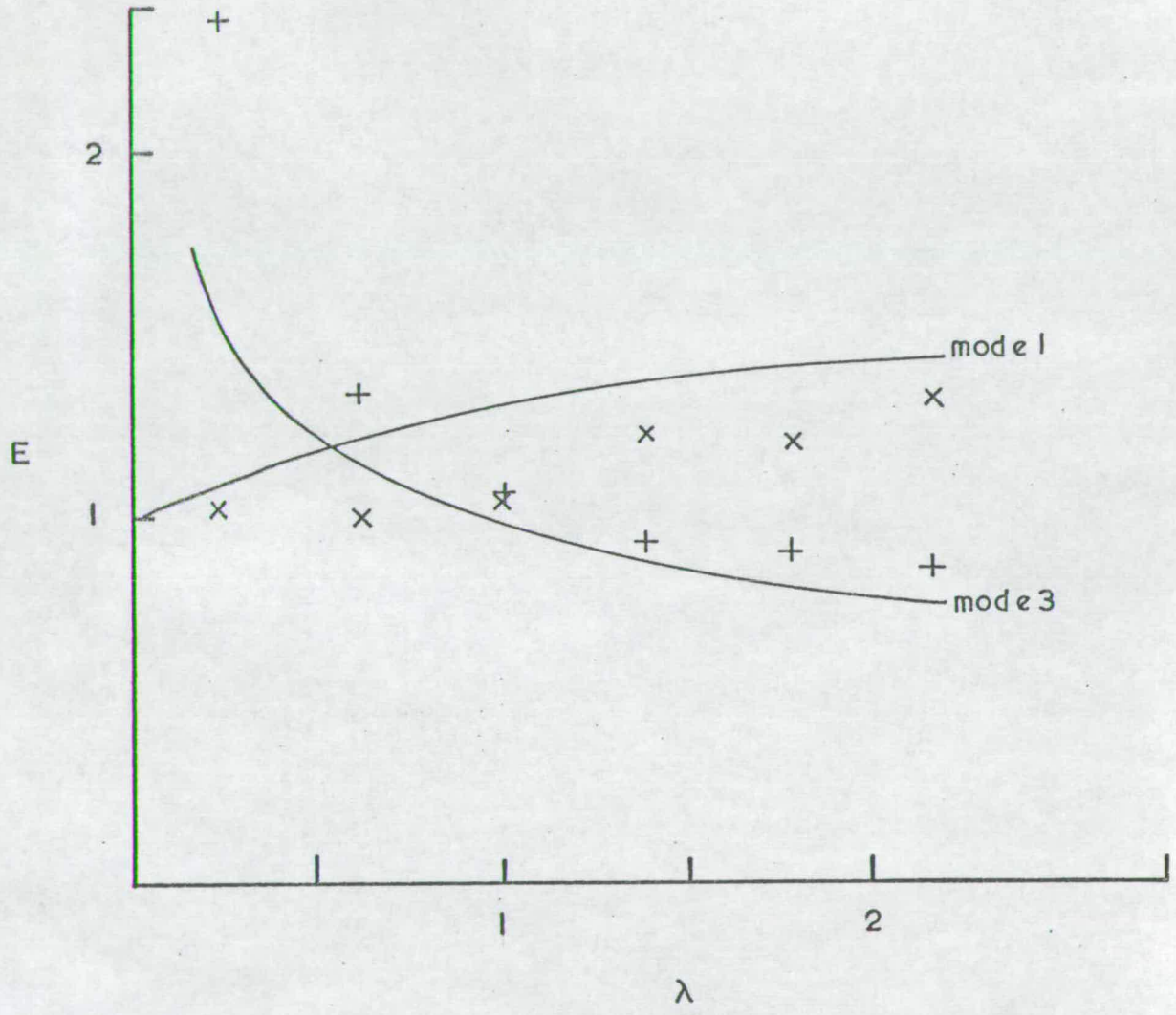

Fig. 61. Three girder grid - mode shape results.

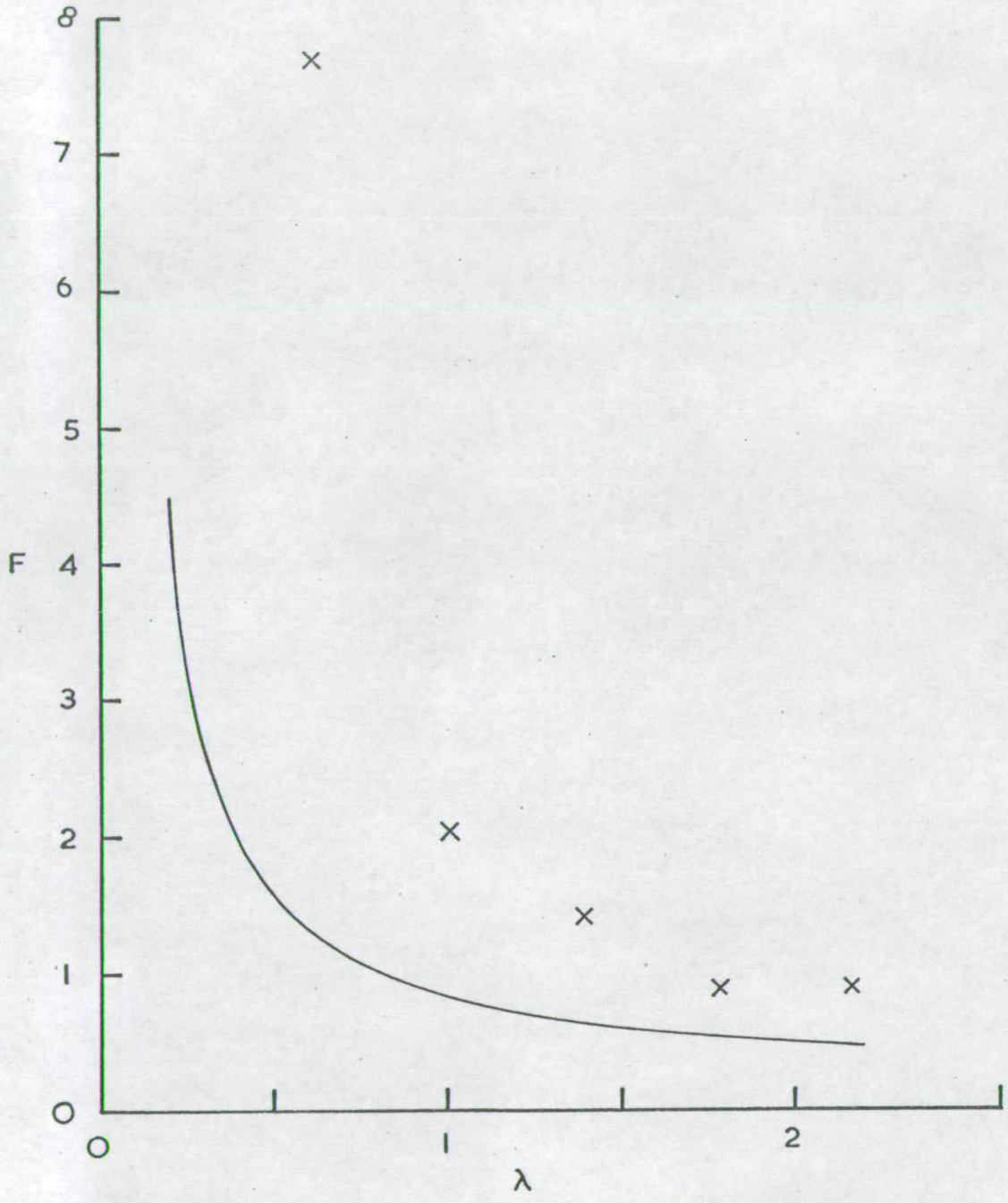

Fig. 62. Three girder grid - stress results.

mode	frequency c/sec. theory	observed	no. of occurences in 74 vehicles
1-1	3.81	3.8	51
1-2	4.29	4.3	6
1-3	5.50	6.1	37
1-4	9.32	10.2	-
1-5	16.41	13.2	-
2-1	14.75	13.3	-
2-2	15.37	13.7	-
2-3	17.32	14.6	-

Fig. 63. Touch Burn Bridge test results.

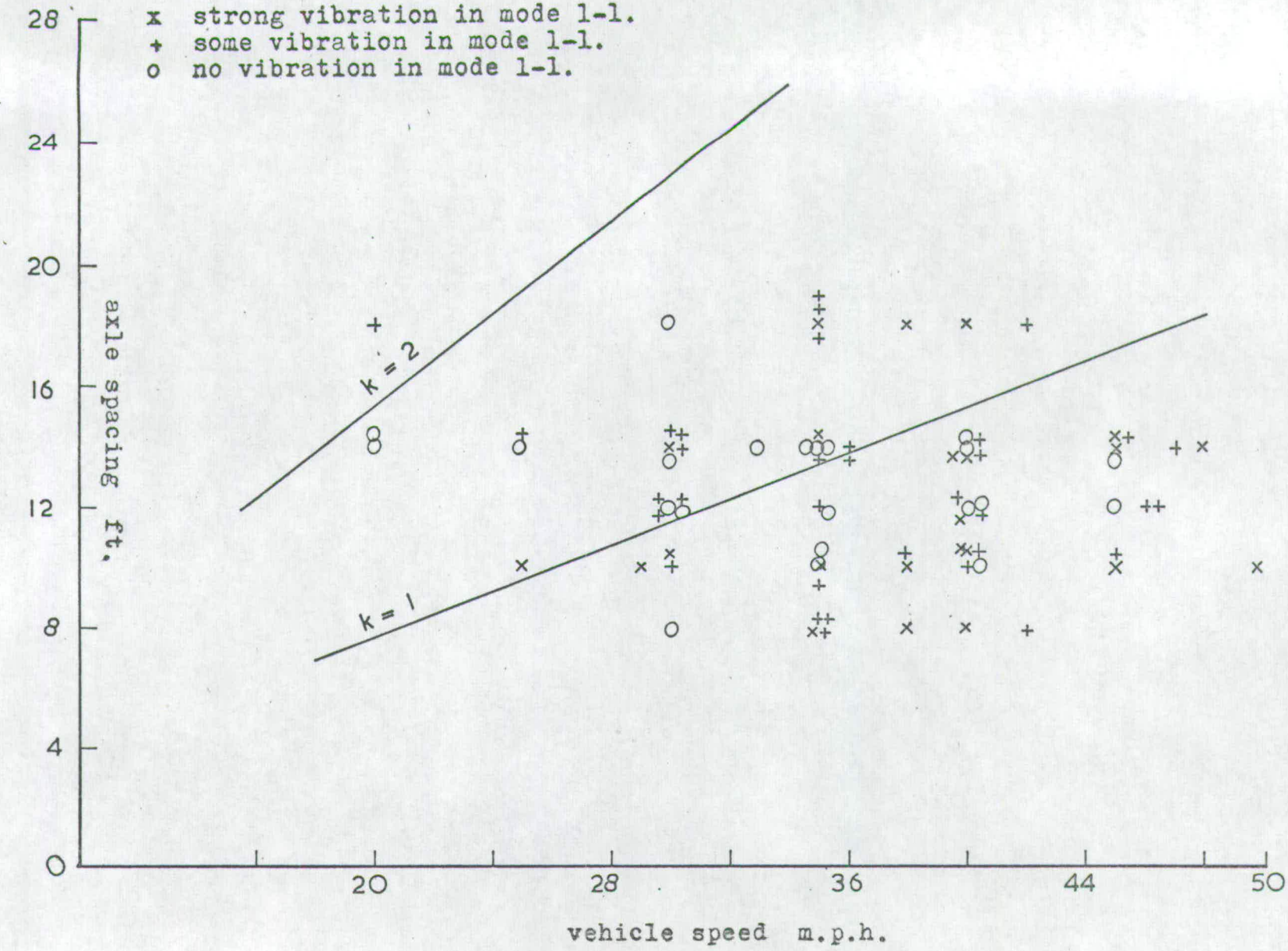

Fig. 64. Touch Burn Bridge test - response to vehicles

Fig. 65. Touch Burn Bridge test - response to vehicles (contd.).

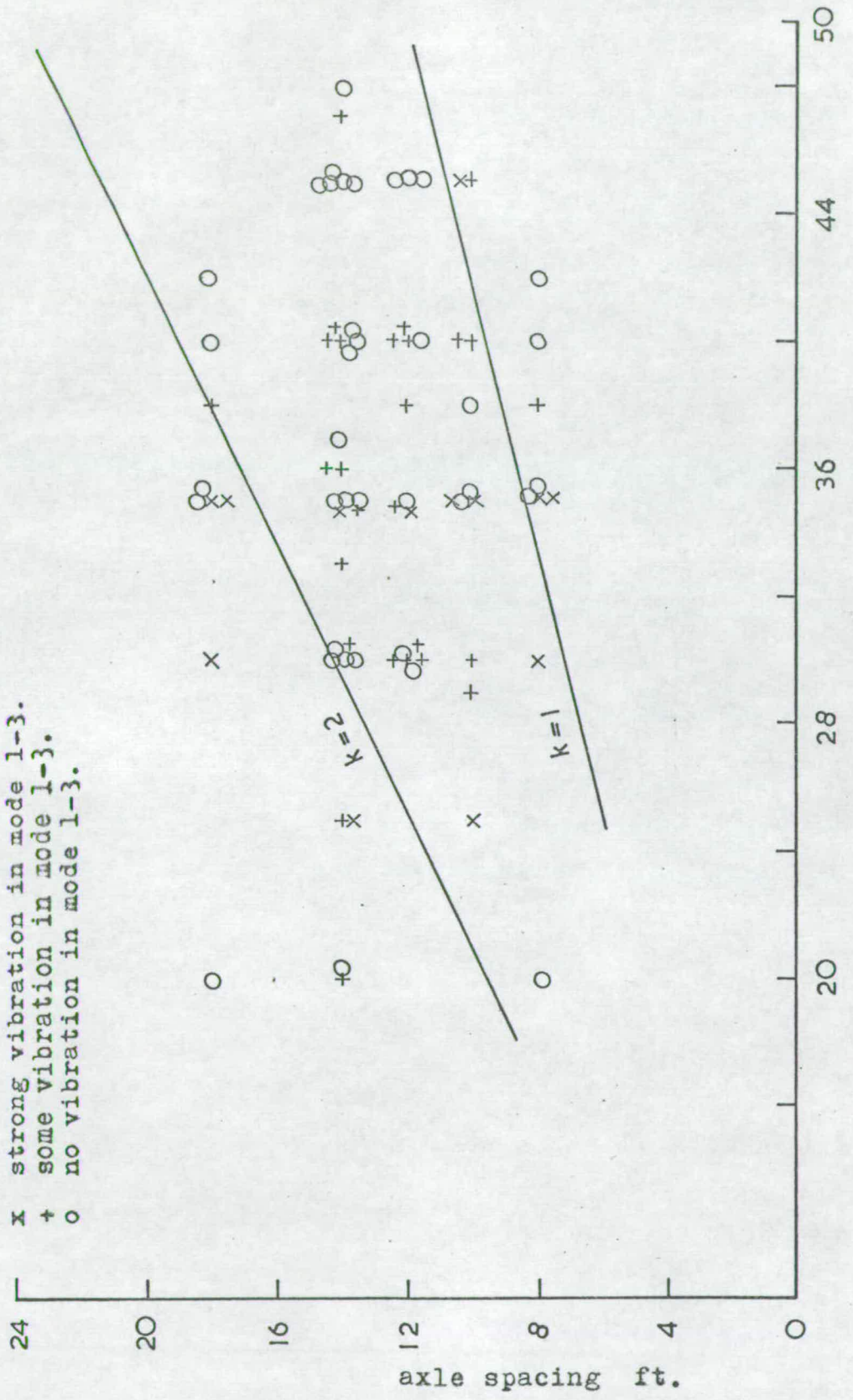

Fig. 66. Touch Burn Bridge test - response to vehicles (contd.).

Fig. 67. Touch Burn Bridge test--response to vehicles (continued).

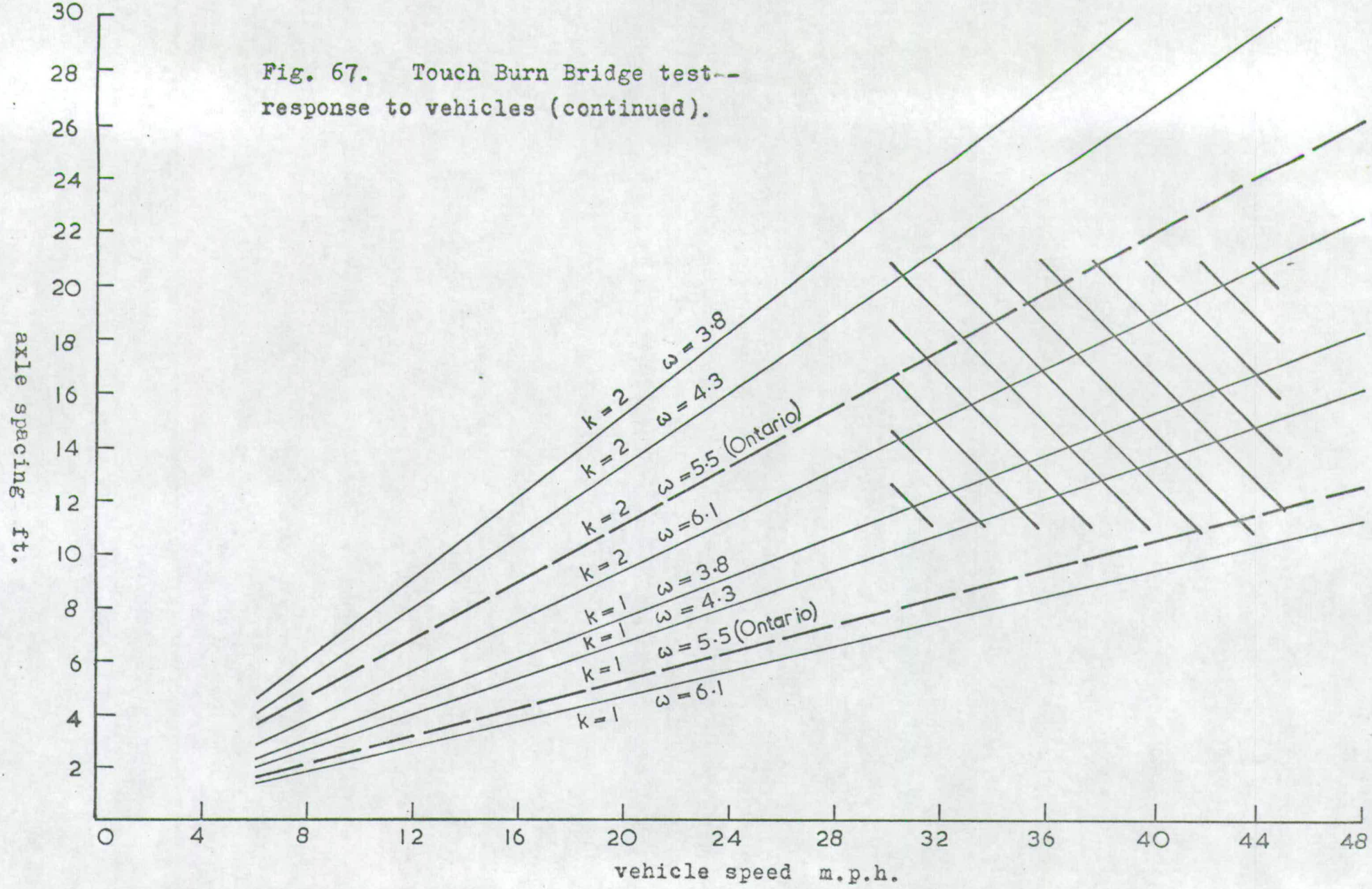

Road ℄ approx. 37·0 O.D

22·5 ft O.D

Flood level 24·9 ft O.D.

22·5 ft. O.D

1 in 2

1 in 2

Herkules Type H420 piles driven to rock at -93·5 ft. O.D. approx.

12·5 ft O.D.

For details of bearings see separate drg.
"Pinned" type bearings requd. at east abutment
"Roller" type bearings requd. at west abutment

UPSTREAM ELEVATION

Scale :- ½ in to 1 ft

Setting-out note :-
Carriageway to have 1° curve,
Bridge not curved,
Bearings of central U.B. on curve

75'-0" c/c bearings

72'-6" clear span

West Abutment

East Abutment

X

36" x 16½" x 260# U.B's

Tail slab

Tail slab

To Dumbarton

From Stirling

1° Curve
Rad. 5729·6 ft.

6'-0"

6'-0"

6'-0"

12'-0" lane

9'-0" verge

1'-0"

Ch. 1780

'Trinasco'

Kerb line

Pockets 4"x4"x10" deep at 6'-2" crs.

2'-0"

72'-4"

76'-6"

2'-0"

1"

1"

N

X

PLAN ON DECK

Scale :- ⅛ in to 1 ft.

3"

3"

24'-0"
Carriageway
1 in 36 crossfall

1'-0"

9'-0"
Verge

9'-0"
Verge

1'-0"

2" p/c concrete flags on sand infill

5"x5" conc fillet

6"x7" p/c kerb 3" chamfer beaded on ½" mortar (dry)

2" Wearing course — Hot rolled asphalt ½" p/c. chippings

Single layer copper lined bituminous sheeting returned into parapets

7" R.C. deck slab

2½" fall

6½" fall

3'-6"

1'-3"

9"

6"

36

36

36

North side

South side

18" deep x 24" wide R.C. transverse ena beam

1'-0"

2'-0"
3'-0"

6'-0"

6'-0"

6'-0"

6'-0"

6'-0"

2'-0"
3'-0"

1'-0"

Sand infill drains —
2" ϕ asbestos pipes with ⅜" no fines conc filter,
One each side at each end of deck

Carriageway drains —
2" ϕ asbestos pipes, kerb notched
One each end of deck

SECTION XX

Scale :- ⅜ in to 1 ft

Handrail :- 3"x3"x Guage 8 R.H.S - welded joints.
Sleeve expansion joints each end of deck
Stanchions :- 3"x3" solid M.S. 4'-3" long set 9" into 4"x4"x10" deep pockets in concete

STIRLING COUNTY COUNCIL

A 811 STIRLING - DUMBARTON ROAD

RECONSTRUCTION OF TOUCH AND POLROGAN BRIDGES

TOUCH BRIDGE — LAYOUT AND DIMENSIONS